



HAL
open science

The toxicokinetics of bisphenol A and its metabolites in fish elucidated by a PBTK model

Corentin Mit, Anne Bado-Nilles, Gaëlle Daniele, Barbara Giroud, Emmanuelle Vulliet, Rémy Beaudouin

► **To cite this version:**

Corentin Mit, Anne Bado-Nilles, Gaëlle Daniele, Barbara Giroud, Emmanuelle Vulliet, et al.. The toxicokinetics of bisphenol A and its metabolites in fish elucidated by a PBTK model. *Aquatic Toxicology*, 2022, 247, pp.106174. 10.1016/j.aquatox.2022.106174 . hal-03702730

HAL Id: hal-03702730

<https://hal.science/hal-03702730v1>

Submitted on 8 Nov 2022

HAL is a multi-disciplinary open access archive for the deposit and dissemination of scientific research documents, whether they are published or not. The documents may come from teaching and research institutions in France or abroad, or from public or private research centers.

L'archive ouverte pluridisciplinaire **HAL**, est destinée au dépôt et à la diffusion de documents scientifiques de niveau recherche, publiés ou non, émanant des établissements d'enseignement et de recherche français ou étrangers, des laboratoires publics ou privés.

The toxicokinetics of bisphenol A and its metabolites in fish elucidated by a PBTK model

Corentin Mit ^{1,2} Anne Bado-Nilles ², Gaëlle Daniele ³, Barbara Giroud ³, Emmanuelle Vulliet ³ and Rémy Beaudouin^{1*}

1 Experimental Toxicology and Modelling Unit, INERIS, UMR-I 02 SEBIO, Verneuil en Halatte, 65550, France. Tel: +33344618238

2 Ecotoxicology of substances and fields Unit, INERIS, UMR-I 02 SEBIO, Verneuil en Halatte, 65550, France

3 Univ Lyon, CNRS, Université Claude Bernard Lyon 1, Institut des Sciences Analytiques, UMR 5280, 5 rue de la Doua, F-69100, Villeurbanne, France

*Corresponding author, e-mail: remy.beaudouin@ineris.fr

Abstract

Bisphenol A (BPA) is a chemical of major concern due to its endocrine disrupting function, high production volume, and persistence in the aquatic environment. Consequently, organisms such as fish are subject to chronic exposure to BPA. However, physiologically-based toxicokinetic (PBTK) models, which are valuable tools to improve the understanding of a chemical's fate in an organism, have never been specifically adapted to model BPA toxicokinetics (TK) in fish. In our work, an existing PBTK developed for four different fish species was modified to model BPA ADME processes (absorption, distribution, metabolization and excretion). The metabolization of BPA into BPA-mono-glucuronide (BPA gluc) and BPA-mono-sulfate (BPA sulf) and their TK in various organs was taken into account in the model. Experiments were performed to generate BPA TK data in a model species commonly used in ecotoxicology, the stickleback. The model structure had to include two sites of metabolization to simulate BPA TK accurately in stickleback organs. Thus, the fish liver may not be the only site of the metabolization of BPA: plasma or gills could also play a role in BPA metabolization. The PBTK model predictive performance evaluated on literature data in zebrafish and rainbow trout concurs with this conclusion. Finally, a calibration mixing data from the three species was compared to the calibration on stickleback data only.

Keywords: PBTK model, fish, BPA, Metabolites, three-spined stickleback, LC-MS/MS

Abbreviation

BPA gluc: BPA monoglucuronide

BPA sulf: BPA monosulfate

BPA: bisphenol A

EDC: endocrine-disrupting compound

ER: estrogen receptor

GIT: gastrointestinal tract

IVIVE: in vitro-in vivo extrapolation

LC: liquid chromatography

MS: mass spectrometry

PBPK: physiologically based pharmacokinetic model

PBTK: physiologically based toxicokinetic model

PC: partition coefficient

PP: poorly perfused tissue

QSAR: quantitative structure-activity relationship

SA: sensitivity analysis

ST: sulfotransferase

TD: toxicodynamic

TK: toxicokinetics

UF: unbound fraction

UGT: UDP-glucuronosyltransferase

1. Introduction

During the first decade of the 21st century, bisphenol A (BPA) has raised serious concern among the scientific community. BPA was first synthesized in 1891 and its use became widespread in the 1950s; its production exceeded six billion pounds in 2000 (Vandenberg *et al.* 2007). BPA was first developed as a synthetic estrogen because it can bind to estrogen receptors (ERs). However, because its binding capacity is 5 to 6 orders of magnitude smaller than that of estradiol, its use as a synthetic estrogen was abandoned (Dodds *et al.* 1938). Nevertheless, its use as a plastic monomer and plasticizer in various everyday products has led to ubiquitous environmental contamination. Over the last decade, BPA has been detected in freshwater courses, usually below 1 µg/L, but downstream from wastewater discharge levels reached 100 µg/L (Faheem & Bhandari 2021). Consequently, Flint *et al.* (2012) determined the typical environmental BPA contamination level to be 12 µg/L or less.

Several studies have focused on the effects of BPA on aquatic communities and, in particular, its endocrine disrupting effects on reproduction and growth process in fish. Moreover, recent papers have demonstrated that exposure to BPA triggers a variety of effects that are not only related to reproduction but also innate immunity, cardiac response, and oxidative stress (Wu *et al.* 2011; Little & Seebacher 2015; Qiu *et al.* 2016; Pandey *et al.* 2018; Gu *et al.* 2020). In the context of environmental risk assessment, effects at higher levels of organization are extrapolated from individual-level data. However, extrapolations generally fail because the link between each level is mostly empirical (Forbes *et al.* 2008). The first step in building a mechanistic framework to assess the environmental risk of BPA is to describe the relationship between environmental levels and internal levels in the organism, i.e. the toxicokinetics. On this basis, physiologically-based toxicokinetic (PBTK) models have been proven to be valuable tools to predict how fish accumulate chemicals based on ADME (Absorption, Distribution, Metabolization, and Excretion) processes (Gerlowski & Jain 1983; Brinkmann *et al.* 2016; Grech *et al.* 2017; Tebby *et al.* 2019; Mit *et al.* 2021). PBTK models have the advantage of simulating the time-course of toxicant concentrations over time and can also provide a mechanistic framework to improve the understanding of the contribution of each ADME process.

Two PBTK models have already been used to simulate the TK of BPA in fish. Both models were generic, meaning that they were not specific to BPA but initially applied to various substances. Pery *et al.* (2014) developed a PBTK for zebrafish (*Danio rerio*) with eight compartments, and Grech *et al.* (2019) extended the PBTK to three more species used in ecotoxicology, fathead minnow (*Pimephales promelas*), rainbow trout (*Oncorhynchus mykiss*), and three-spined stickleback (*Gasterosteus aculeatus*). The model proposed by Pery *et al.*

(2014) was successfully evaluated on only one study reporting BPA zebrafish whole-body concentrations (Lindholst *et al.* 2003). The model presented by Grech *et al.* (2019) was evaluated on both BPA whole-body and organ concentrations in zebrafish and trout (Lindholst *et al.* 2000; Lindholst *et al.* 2001; Lindholst *et al.* 2003; Fang *et al.* 2016). However, in those models, metabolism was extremely simplified since it was treated as a way of excretion, many parameters were retrieved from publications related to mammals (Shin *et al.* 2004; Edginton & Ritter 2009) and, since no calibration was performed on the model parameters, ten-fold overpredictions compared to data from the literature were sometimes observed (Grech *et al.* 2019).

Few data are available regarding the ADME processes of BPA in fish. As in mammals, BPA undergoes phase II metabolism, which is assumed to occur mainly in the liver (Lindholst *et al.* 2001; Lindholst *et al.* 2003). Interestingly, the enzymes involved in metabolite synthesis have been characterized since zebrafish cells are commonly used as human metabolism models. The activity of UDP glucuronosyltransferases (UGTs) and sulfotransferases (STs) in the presence of BPA result in the fast production of BPA monoglucuronide (BPA gluc) and BPA monosulfate (BPA sulf) (Lindholst *et al.* 2001; Lindholst *et al.* 2003; Ohkimoto *et al.* 2003; Wang *et al.* 2014). BPA gluc was shown to be the main metabolism product in mammals and fish, with BPA sulf production being a minor pathway (Lindholst *et al.* 2003; Gramec Skledar & Peterlin Mašič 2016). Thus, BPA gluc levels reached 22 times the steady-state whole body BPA concentration in zebrafish, whereas BPA sulf only represented less than a tenth of the BPA level (Lindholst *et al.* 2003). Nevertheless, it has been shown that BPA gluc cannot bind to ERs and cannot be considered an EDC (Matthews *et al.* 2001). Yet, as pointed out in Karrer *et al.* (2018), some mechanisms of action of BPA metabolites may still be unknown. For example, Boucher *et al.* (2015) showed that BPA gluc induced adipocyte differentiation when it was supposed to be inactive. In addition, BPA metabolites could be subject to deconjugation that could increase the actual concentration in fish organs, as shown in rats (Kawamoto *et al.* 2007).

This study aimed to propose a new PBTK explicitly developed for BPA in the three-spined stickleback. To this purpose, we modified the PBTK of Grech *et al.* (2019) to describe the kinetics of the two primary BPA metabolites, BPA gluc, and BPA sulf, in fish organs. New kinetic data in stickleback was obtained and used to calibrate the model. PBTK predictions were then compared to observed data found in the literature for zebrafish and trout. The inter-species variability of BPA kinetics was then studied using the PBTK model and discussed to improve the mechanistic understanding of BPA TK.

2. Materials and methods

2.1. Literature experimental data

Five publications were identified in the literature to provide TK data for the calibration of the model (Lindholst *et al.* 2000; Lindholst *et al.* 2001; Lindholst *et al.* 2003; Fang *et al.* 2016; Eser *et al.* 2021). A description of each experimentation can be found in Table 1 and an extended description can be found in SI section 7. Experiments had been carried out on rainbow trout and zebrafish with various exposure scenarios. BPA levels were measured at 1, 5, 12, and 21 days (Lindholst *et al.* 2000; Fang *et al.* 2016; Eser *et al.* 2021) or sampled at multiple times during a seven-day exposure and a seven-day depuration (Lindholst *et al.* 2001; Lindholst *et al.* 2003). Fish were only waterborne exposed to BPA ranging from 2 to 900 µg/L. In most experiments, no information was given about the sex of the fish. Trout weight was ranging from 90 to 130 g and zebrafish weight was not informed. Water temperature for trout and zebrafish was set to 15°C and 27°C, respectively. In addition, Lindholst *et al.* (2001) measured BPA gluc content in trout plasma, and Lindholst *et al.* (2003) BPA gluc and BPA sulf contents in whole body zebrafish homogenates. As described in Table 1, BPA levels and bile metabolites were also provided in Lindholst *et al.* (2003). However, it was hypothesized in this work that the BPA levels in bile could result from metabolite deconjugation. For this reason, BPA excretion via bile was not added to the model. In Lindholst *et al.* (2001), juvenile trout were exposed to BPA by intraperitoneal injection. Since this type of exposure was not modeled and the diffusion processes in the peritoneal cavity are poorly understood in fish, this data was not used for model validation.

2.2. Stickleback experimental data

Experimental protocols were conducted following the European directive 2010/63/UE for the protection of animals used for scientific purposes at INERIS, registration number E60–769–02. The experimental protocols were submitted and reviewed by a French nationally recognized ethical committee, CREMEAPS, registration number 96.

During this study, the 380 mature three-spined sticklebacks (48.8 ± 4.36 mm; 1.66 ± 0.44 g; sex ratio 1:1) used were obtained from the INERIS husbandry (Verneuil-en-Halatte, France). At the beginning of the experiment, males and females were separated to avoid stress and each was randomly distributed into 8 L tanks with ten fish per tank, 12 tanks per condition ($\pm 1^\circ\text{C}$, 350 µS/cm, photoperiod of 12:12 h) in a continuous flow system. After five days of acclimation, fish were exposed for seven days to BPA (99%, 0, 10, and 100 µg/L, CAS number 80-05-7, Sigma). BPA was dissolved in dimethyl sulfoxide (Sigma) as it has low water solubility. Fish were fed daily with frozen blood worms, except the day before removal from aquarium.

Water was randomly sampled from one tank at 2, 4, 8, 24, 48, 72, and 168 h for each condition and stored at -20°C. BPA water concentration was monitored at each sampling time to measure the actual exposure concentrations in the aquarium. Samples were analyzed by LC-MS/MS. During exposure, 20 fish (ten females and ten males) were sampled at 5, 24, 48, 96, and 168 h for each condition to evaluate BPA, BPA sulf, and BPA gluc internal concentrations in organs. After exposure was ceased, ten remaining male and female fish were taken for 24 h and ten other males and females for 168 h. When sampled, fish were anesthetized in MS222 (tricaine methanesulfonate, 100 mg/L, Sigma-Aldrich), sacrificed by cervical dislocation, measured, and weighed. Blood, liver, and carcass, which consisted of fish bodies free from the gastrointestinal tract (GIT), kidney, and spleen, were used to quantify BPA, BPA sulf, and BPA gluc concentrations by LC-MS/MS on pools of two individuals (see SI section 1 for more details). In addition, liver, kidney, gonads, and carcass were weighed. During this experiment, various biomarkers were measured in all sacrificed fish and will be presented in future work. The duration of the exposure was based on the review of previous BPA TK data. Indeed, steady state was showed to be quickly reached (about one day). In addition, to increase the certainty of metabolism and excretion parameters, the internal concentrations during depuration were also monitored.

2.3. Model structure

2.3.1. General structure

The model structure is based on the fish model developed by Grech *et al.* (2019). The structure was extended to model BPA metabolization into BPA gluc and BPA sulf, as well as the kinetics of both metabolites (Figure 1). All model equations are available in SI (section 7. Model code).

BPA is distributed in twelve well-mixed compartments. Absorption is assumed to be mainly branchial in the absence of data regarding gastro-intestinal or dermal absorption. As modeled by Nichols *et al.* (1990) and Erickson and McKim (1990), absorption by the gills was assumed to be proportional to the effective respiratory volume. In terms of distribution, BPA has a high affinity to plasmatic proteins in mammals, around 90-95% in rats (Kurebayashi *et al.* 2003; Teeguarden *et al.* 2005). As proposed by Vidal *et al.* (2019) for PFOS, arterial volumes entering organs were reduced to describe only the unbound fraction of chemicals (considered the active fraction) in plasma. Equation 1 describes BPA quantities in organs without considering either elimination or absorption.

$$\frac{d(Q_i)}{dt} = F_i \times UF \times (C_{art} - \frac{C_i}{PC_i}) \quad (\text{Equation 1})$$

where Q_i is the quantity of chemical (μg of BPA, BPA gluc or BPA sulf) in the compartment i , F_i is the arterial plasma flow (mL/d) to the compartment i , UF is the unbound fraction of chemical, C_{art} is the chemical concentration in arterial plasma, C_i is the chemical concentration in venous plasma ($\mu\text{g}/\text{mL}$) leaving the compartment i . F_i was calculated by multiplying the relative fraction of plasma flow to each organ ($Frac_i$) by the cardiac output.

In terms of metabolization, observations in rats demonstrated that BPA undergoes an extensive and rapid phase II metabolization in both the intestine and the liver (Inoue *et al.* 2003; Inoue *et al.* 2005; Mazur *et al.* 2010). In fish, metabolization into BPA gluc and BPA sulf was supposed to occur mainly in the liver. We also test the hypothesis of a second metabolization site modeled by default in the plasma.

Hepatic metabolization was described with the saturable metabolism equation of Michaelis-Menten (Equation 2):

$$\frac{d(Q_{met})}{dt} = \frac{Vmax_j \times C_{liver}/PC_{liver}}{Km_j + C_{liver}/PC_{liver}} \quad (\text{Equation 2})$$

where $Vmax$ is the maximum rate ($\mu\text{g}/\text{d}/\text{g}$) and Km ($\mu\text{g}/\text{mL}$) the substrate concentration at which the rate is equal to half $Vmax$. In the absence of information regarding plasmatic metabolization, a first-order kinetics was chosen with a plasmatic *in vivo* clearance.

BPA gluc and BPA sulf were assumed to be distributed in five compartments (Figure 1). This choice was driven by the available data in the literature and the different purposes of the model. The original dataset described previously (see part 2.2) allowed us to compare model predictions with measured concentrations in liver, blood, and fish carcass. In addition, two compartments were added, one for the fish gonads and the other corresponding to the rest of the fish organs removed during dissection, the GIT, and the kidney.

Data on BPA excretion were scarce in the literature. Lindholst *et al.* (2001) and (2003) studied how BPA was eliminated by rainbow trout and zebrafish. BPA gluc, and BPA sulf concentrations were measured in trout bile, assuming that the main pathway of excretion was feces. The model structure was adapted to these assumptions. BPA excretion was therefore modeled as branchial (Equation 3), BPA gluc, and BPA sulf excretion by the bile through the feces (Equation 4), assuming that metabolite excretion via the gills was extremely low.

$$\frac{d(Q_{excret\ gills})}{dt} = Kx \times UF \times \frac{C_{ven}}{PC_{bw}} \quad (\text{Equation 3})$$

where $Q_{excret\ gills}$ is the amount of chemical excreted by the gills (μg), Kx the exchange coefficient between plasma and water (mL/d), C_{ven} the chemical concentration in venous plasma and PC_{bw} the partition coefficient between blood and water.

$$\frac{d(Q_{bile})}{dt} = (K_{e_{bile}} \times Q_{liver} \times UF) - K_{BG} \times Q_{bile} \quad (\text{Equation 4})$$

where Q_{bile} is the quantity of chemical in bile (μg), $K_{e_{bile}}$ the excretion rate in bile (d^{-1}) and K_{BG} (d^{-1}) the rate constant from bile to GIT lumen.

2.4. Model parametrization

The main physiological parameters for zebrafish, rainbow trout, and three-spined stickleback were taken from the generic model of Grech *et al.* (2019). Some stickleback physiological parameters were modified using our dataset, *i.e.*, the weight of the organs, the fraction of arterial blood flow to organs, and the plasma fraction (Table S3). For each experiment simulated, the physiological parameters were set to the specific values of the species studied and were not included into the calibration process.

2.4.1. Sensitivity analysis

Before calibration, the set of chemical-specific parameters to be calibrated was identified with a sensitivity analysis (SA) using the variance-based Sobol method (Sobol *et al.* 2007; Saltelli *et al.* 2008). The sensitivity of 29 parameters was estimated with uniform distributions $\pm 10\%$. In this SA analysis, partition coefficients were set to the values calculated using the QSAR model as presented in Pery *et al.* (2014) (Table S4). The influence of the parameters was investigated on nine outputs, including blood, liver, and carcass levels at 1, 4, 7, 8 and 14 day. The SA was carried out on the exposure scenario where stickleback was exposed to BPA at $100 \mu\text{g}/\text{L}$ for seven days, followed by seven days of depuration. Details are available in SI (section 3).

2.4.2. Prior definition

All calibrated parameters are available in Table 2. Most prior distributions were set as truncated normal, and the coefficient of variation on the prior values was set to 30% (including uncertainty and inter-individual variability).

Based on the results of the SA, six BPA-related *PCs* were calibrated using the QSAR values as priors. *UF* was also calibrated, and its prior mean was set to 3.5% based on *in vitro* data in human plasma from Edginton and Ritter (2009). An IVIVE approach was applied to determine prior distributions for Michaelis-Menten equation parameters following the stepwise approach proposed by Nichols *et al.* (2006). *In vitro* hepatic glucuronidation and sulfation measured in zebrafish hepatocytes were used to derive Michaelis constant *Km* and maximum reaction velocity *Vmax*. *Km* means for glucuronidation and sulfation were set equal to the values reported in Wang *et al.* (2014) and Ohkimoto *et al.* (2003), respectively, after conversion from μM to $\mu\text{g}/\text{mL}$. Maximum reaction velocity for glucuronidation and sulfation were also

derived from those publications by accounting for the S9 protein content of the stickleback liver (25 mg S9 protein/g liver) and predicted liver weight. Prior means for *PCs* related to BPA metabolites were also calculated using the QSAR model. Ratios were built to avoid correlation between Michaelis Menten parameters, *Km* and *Vmax*, and *PC_{bw}* and *UF*. Calibration was then only performed on those ratios and one of the two correlated parameters (*Km* and *UF*).

Due to a lack of data, BPA gluc and BPA sulf *Ke_{bile}* and plasmatic clearances were calibrated using uniform prior distributions.

2.5. Model calibration and assessment

2.5.1. Calibration on the stickleback dataset

The exposure scenarios describing experiments on the stickleback were carefully implemented in the model. Thus, simulated BPA levels in water over time were adjusted based on the chemical concentration measurements (described in section 2.2). Initial fish weight was 1.85 g for females and 1.67 g for males. Food consumption was adjusted to correctly predict the fish growth using the Dynamic Energy Budget (DEB) equations implemented in the PBTK (Leloutre *et al.* 2018; Grech *et al.* 2019). Finally, the water temperature was set to 16 °C. Details are available in SI. Simulations were then compared to data collected in stickleback.

Parameters were calibrated using experimental stickleback data and Bayesian methods (Monte Carlo Markov Chain, MCMC). See all details in SI (section 4. MCMC calibration).

2.5.2. External evaluation on literature data

The model calibrated on stickleback data was used to predict BPA kinetics in zebrafish and trout. Predictions were obtained using the exposure scenarios described in the five publications cited previously (Lindholst *et al.* 2000; Lindholst *et al.* 2001; Lindholst *et al.* 2003; Fang *et al.* 2016; Eser *et al.* 2021) and compared to the data from these publications (for model simulation inputs see Table S14). In addition, a comparison was performed between the fold changes obtained by Grech *et al.* (2019) for BPA TK data and the current PBTK (see section 7 in SI).

Further investigations were carried out by performing another calibration on the entire set of TK data, which included data in zebrafish, trout, and stickleback. To this objective, the physiological parameters specific to the stickleback were replaced by zebrafish or trout parameters, and the exposure scenarios of each study were carefully implemented for the calibration. The resulting calibrated parameters were then compared to the parameters specific

to the stickleback model. The quality of prediction of both models was compared with fold deviations and the Bayesian Information Criteria (BIC).

Calculations were performed using R version 3.6.1. (R Core Team 2019) and GNU MCSim v6.2.0 (Bois 2009).

3. Results

3.1. Model calibration

3.1.1. Determination of critical parameters

The sensitivity analysis performed prior to calibration (SI section 3. Sensitivity analysis) showed a varying influence of parameters depending on the exposure period. In most cases, BPA concentration in organs was mainly driven by BPA-related parameters, PC_{bw} , UF , and the plasmatic clearance describing BPA gluc synthesis, but also by *plasma* parameter (percentage inverse of the hematocrit). Metabolite concentrations were driven by BPA-related and metabolite-related parameters such as plasmatic clearances. During the depuration phase, the SA showed a significant influence of BPA-related parameters, PC_{bw} , UF , and PC_{pp} , on most outputs. In the particular case of BPA metabolite concentrations, the sensitivity analysis also highlighted the role of metabolite *Ke bile* and UF , specifically at the end of the seven-day depuration.

3.1.1. Stickleback toxicokinetics data

Fish were exposed to nominal BPA concentration levels of 10 and 100 $\mu\text{g/L}$. Water was sampled at seven timepoints, measured concentrations $5.0 \pm 1.2 \mu\text{g/L}$ and $53.0 \pm 19.3 \mu\text{g/L}$ (mean \pm SD). They can be found in SI (Table S5 and S6). Measured concentrations of BPA were used as inputs in the model. The BPA and metabolite concentrations measured in blood, liver, and carcass are reported in SI (Table S7 to S12). An estimation of the accuracy of the measurement in each organ was carried out and is available in SI (Table S13).

The estimated values of the model parameters after calibration on stickleback data are reported in Table 2. Based on the sensitivity analysis described previously, 19 parameters were calibrated. Most of the posterior distributions were different from the prior distributions. However, *gonads:blood PC*, BPA gluc, and *sulf liver:blood PC* did not gain information from the experimental data through the calibration process.

More precisely, the calibrated posterior distribution mean of the unbound fraction UF of BPA was 7% [5;8], twice the prior mean value (3.5% observed in rats by Edginton and Ritter (2009)). Regarding BPA metabolization into BPA gluc, calibrated plasmatic clearances increased compared to the prior and hepatic metabolization decreased, $3.86 \times 10^4 \text{ mL/d/mL}$

$[2.83 \times 10^4; 6.07 \times 10^4]$ and $3.98 \times 10^2 \mu\text{g/d/g}$ $[24.4; 3.13 \times 10^2]$, respectively. In terms of excretion, BPA gluc and BPA sulf $K_{e_{bile}}$ were of the same order of magnitude after calibration: 94.3 d^{-1} $[79.8; 1.97 \times 10^2]$ and 62.8 d^{-1} $[46.8; 1.56 \times 10^2]$, respectively.

Figures 2 and 3 present predicted kinetics for both males and females, for exposure levels 10 and 100 $\mu\text{g/L}$. Overall, for both doses, the predictions are in agreement with the measured concentrations. Some data points are outside the grey area representing the 95% prediction interval. During the depuration phase that followed exposure to 10 $\mu\text{g/L}$, most concentrations were below the LQ (in Figure 2, data points are set to LQ/2 graphically). For this reason, the predictions at this exposure level are lower than the represented data points since no TK data were available to calibrate excretion.

3.1. Model validation and interspecific variability

The PBTK calibrated on stickleback data was then evaluated on data from other species from the literature. A total of 115 data points was represented in Figure 4 against model predictions. In addition, Table 3 contains the percentages of datapoints for each dataset (zebrafish, trout, and stickleback) included within a three-fold factor, between three to ten-fold factors, and over the ten-fold factor, respectively. Finally, in table S15, a comparison of the fold changes (FC) obtained by the PBTK published by Grech *et al.*, (2019) (most recent model applied on BPA) and our BPA PBTK was performed. Briefly, our model outperformed the generic model by reducing by more than 24% data in $\text{FC} > 10$ and increasing by more than 60% data in $\text{FC} < 3$.

3.1.1. Model predictions in zebrafish

Quality of prediction in zebrafish is heterogenous (Table 3): 45% of the predictions are within three-fold of the observations, and 43% superior to a ten-fold interval (12% are between three and ten-fold factors), which is unsatisfactory.

In zebrafish, TK data was available in whole-body and organs for males and females and included metabolite concentrations. At the exception of BPA concentrations in whole-body homogenates measured by Lindholst *et al.* (2003), model predictions generally overestimate concentrations in both zebrafish organs and whole-body. Predictions in the liver are the most accurate, with most data points within the three-fold range. For gonads and the brain, the predictions that best fit the observed data correspond to the lowest exposure level (2 $\mu\text{g/L}$). For the highest exposure levels (200 and 900 $\mu\text{g/L}$), the PBTK overestimates concentrations ten-fold. BPA depuration, measured by Lindholst *et al.* (2003) as normalized concentrations, is correctly predicted, within three-fold.

BPA gluc and BPA sulf levels were also measured in zebrafish whole-body homogenates and are shown on the right panel of Figure 4. Overall, predictions are within ten-fold of the observations (except one data point for BPA gluc during the depuration phase). The same pattern is observed for the predicted concentrations of BPA gluc and sulf. The model fits well the highest concentrations but generally underestimates the lowest concentrations (i.e., the beginning of the synthesis of metabolites).

3.1.2. Model predictions in trout

Considering predictions in trout, datapoints falling out of the ten-fold interval represent 29% of the trout dataset. A total of 41% of the points are included in the three-fold range, suggesting accurate predictions of BPA TK in trout (30% between three-fold and ten-fold factor).

In rainbow trout, data on kinetics of BPA were available in three organs, muscle, liver, and blood. As shown in Figure 4, the PBTK calibrated on stickleback data, with trout physiological parameters, seems to underestimate concentrations in trout. The kinetics predicted in the liver are reasonably in accordance with observations. However, whereas quality of prediction is satisfactory with Lindholst *et al.*'s (2001) data, it is far more variable with the data from Lindholst *et al.* (2000). As for plasma, predictions range between three and ten-fold factor from observations. Finally, the PBTK fails to predict muscle kinetics, with a ten-fold underprediction.

BPA gluc predicted concentrations in plasma are mostly within three-fold of the observations. In addition, BPA gluc accumulation in bile is particularly well predicted by the model. However, BPA sulf accumulation in bile after a seven-day exposure is overpredicted.

3.1.3. Interspecific calibration

A final calibration was performed on the whole dataset gathered to describe BPA TK in fish, including data in zebrafish, trout, and stickleback. As for the predictions of the model calibrated on stickleback data, the Table 3 contains the percentages of datapoints within the three-fold and the ten-fold factors for each dataset. Predictions resulting from the multiple species calibration were generally improved compared to the calibration on stickleback data. In details, 95% and 96% were within the ten-fold range in trout and zebrafish, respectively.

A comparison of six calibrated parameters from the two calibrations (stickleback only and multi-species dataset) is shown in Figure 5. As it can be seen, this calibration results in a slight increase of BPA UF , PC_{fat} , and PC_{pp} in comparison with parameters calibrated on the stickleback dataset only. Those modifications slightly improve the fit of TK simulations in trout muscle, plasma, and liver (Figure S7 and S8). For zebrafish TK data, it results in an overall

better fit for the data of Fang *et al.* (2016), but no improvement concerning the simulations of Eser *et al* and Lindholm *et al*'s data. In terms of metabolization parameters, BPA gluc K_m is similar in both calibrations. Multi-species calibration leads to a decrease of BPA gluc clearance in parallel with the increase of hepatic V_{max} .

In Figure S9, it can be seen that the calibration on the multi-species dataset resulted in simulations of poorer accuracy in the stickleback carcass and blood, for BPA, compared to the calibration on the stickleback dataset. Surprisingly, overall a slight improvement could be suggested by the fold factors: 84% (82% previously) of the points fell within the three-fold range and 12% (14% previously) were comprised within three and ten-fold. Nevertheless, as expected, the comparison of the BIC calculated for each model and available in Table 3 shows that the model calibrated on stickleback data only was the overall best model with a BIC smaller than the one from the calibration on multi-species data.

4. Discussion

Fish have been used as a model species for endocrine-disrupting effects for many reasons, including their ease of use in laboratory experiments, the ubiquity of endocrine chemicals in water, and also because some species, such as three-spined stickleback, have shown specific biomarkers indicative of the presence of EDCs (Tyler *et al.* 1998; Jolly *et al.* 2009). In particular, BPA effects, and to a lesser extent, BPA kinetics, were the subject of several publications (Flint *et al.* 2012; David *et al.* 2019; Faheem & Bhandari 2021). In this work, we improved a generic PBTK developed for four different species to specifically predict the toxicokinetics of BPA and its metabolites in stickleback. Comparison between predictions and BPA TK data retrieved from the literature showed that the model was also valuable for predicting the fate of BPA in zebrafish and trout.

4.1. Adaptation of a generic PBTK

In this work, the generic model from Grech *et al.* (2019) was used as a basis to build a specific PBTK for BPA. Indeed, previous PBTK developed in fish and applied to predict BPA TK were not particular to this chemical (Pery *et al.* 2014; Grech *et al.* 2019). Accordingly, in those models, metabolization was simplified to stay generic. In Pery *et al.* (2014), metabolization parameters were fitted to predict BPA uptake and excretion accurately on only one whole body dataset. In Grech *et al.* (2019), K_m and V_{max} were calculated using *in vitro* data from Ohkimoto *et al.* (2003), and not calibrated on TK data. Thus, it was assumed that the implementation of BPA sulfation was sufficient to predict BPA kinetics correctly. However, those approximations did not allow the authors to propose accurate predictions for BPA metabolites. The choice to build a specific PBTK was justified by the improvement in model accuracy. Thus, the simulations of our PBTK clearly outperformed the more recent PBTK applied to BPA (Table S15).

In our case and based on previous BPA PBTK, Michaelis Menten equations were chosen to describe hepatic metabolization of BPA into BPA gluc and BPA sulf (Yang *et al.* 2015; Karrer *et al.* 2018; Grech *et al.* 2019). Based on BPA gluc and sulf levels measured in Lindholst *et al.* (2003) and the present study, enzyme maximal rate for BPA gluc synthesis was though to largely exceed the one describing BPA sulf synthesis. An *in vitro*-*in vivo* extrapolation (IVIVE) approach was performed as described in Nichols *et al.* (2006) to calculate Michaelis Menten prior means. Surprisingly, in the particular case of BPA gluc synthesis, V_{max} value measured *in vitro* using zebrafish UDP-glucuronosyltransferase (UGT) proteins was particularly low regarding BPA sulf V_{max} (Ohkimoto *et al.* 2003; Wang *et al.* 2014). In addition, when only hepatic metabolization was assumed, the calibrated model fails to simulate observed data in stickleback (results not shown). Generally, in fish, the liver is considered as the main site of

metabolization and *in vitro* studies only focused on metabolite formation in this organ. Nonetheless, extrahepatic phase II enzyme expressions have been suspected (Nichols *et al.* 2006). In Barron *et al.* (1989), metabolization occurring in gills was responsible for the limited accumulation of phthalates. Adding a second metabolization site in our model allowed us to obtain an excellent fit to the stickleback data, and more interestingly, a satisfying prediction of the BPA gluc accumulation in bile observed in trout (Lindholm *et al.* 2003). Therefore, this substantial accumulation in bile could not be necessarily the result of high hepatic metabolization as it was supposed in the first place. This result tends to demonstrate that the liver may not be the only major site of the metabolization of BPA. In addition, our modeling analysis suggests that metabolization occurs to a larger extent in the plasma. Yet, as our model did not explicitly include a gill compartment, the high plasmatic metabolization could occur in fact in the gills, or in any other part of the fish, and was secondarily released in plasma. This finding would be in agreement with evidence of UGT expression responsible for the glucuronidation of xenobiotics which has been reported in various tissues, including the intestine, gill, kidney, or adipose tissue (Leaver *et al.* 2007). Thus, one possibility could be that BPA is highly metabolized in the gills. To address this question, future *in vitro* metabolism studies in fish, particularly bisphenol metabolization, should include hepatic cells and cells from tissues known to express highly UGT genes.

Another adaptation was proposed in the structure of our BPA model. In the former model of Pery *et al.* (2014) and Grech *et al.* (2019), a QSAR method based on the work of Bertelsen *et al.* (1998) was used to calculate the partition coefficients of each compartment of the model: no calibration of the parameters was performed. Nevertheless, as it can be noticed in Grech *et al.* (2019), the model failed to predict BPA accumulation in organs. In fact, to calculate *PCs* for BPA and BPA metabolites, it was assumed that both parent and metabolites were mainly in their neutral form in the physiological condition. Nonetheless, it must be seen as an approximation because, in the physiological condition, BPA gluc is known to be present in both forms, ionized and non-ionized. A more complex equation could have been used to calculate the *PCs* of the different chemicals (Endo *et al.* 2013; Grech *et al.* 2017). However, in our work, the same QSAR equations were used to calculate the *PC* prior values (i.e. starting point of the calibration), and then, Bayesian inference was used to provide information on those uncertain parameters and get closer to their actual values (Bois & Brochot 2016). Overall, the slight deviations between prior and posterior mean values seem to support this strategy.

4.2. Model performance

The model performance was evaluated on a total of five publications measuring BPA uptake and depuration in fish. More than one hundred concentrations were predicted in various

organs, following multiple doses and diverse exposure and depuration durations. Our experimental data were kept for calibration as the exposure scenarios were properly designed and quantified to identify toxicokinetic parameters (metabolism, excretion process...). One of the advantages of using a model developed for four different fish species is to adapt all species-specific physiological parameters in our simulations. Indeed, in Grech *et al.* (2019), it was shown that when adjusted to fish species physiology, predictions for various chemicals were in agreement with literature data, both in whole body and organ concentrations. Nevertheless, some issues were identified regarding BPA physico-chemical properties and uncertainties on actual exposure.

For example, in Lindholst *et al.* (2001), BPA concentrations in water were measured to determine actual concentrations and showed a narrow SEM of 0.004 μM on 0.43 μM over the whole seven-day exposure period. For this reason, in our work, it was decided to use a constant dose in the modeling of this experiment. Nevertheless, as it can be seen on Figure S8, BPA levels measured in organs by Lindholst *et al.* (2001) showed a clear decrease between the second and fifth day of the exposure. The authors did not suggest any explanation for this unexpected variation of BPA concentration. In addition, this pattern was not observed in any other BPA exposure found in the literature. It could tend to demonstrate that the actual quantity in water in Lindholst *et al.* (2001) was far more variable than the one reported. Therefore, the discrepancy between the external and the internal dose in the organs could explain why the resulting predictions are sometimes distant from the observations.

Another issue was identified with a recent publication of BPA uptake in zebrafish whole-body. Indeed, in Eser *et al.* (2021), zebrafish were exposed to the nominal dose of 90 $\mu\text{g/L}$, and body burden was analytically measured and raised 11.46 ng/mL after a five-day exposure. In Lindholst *et al.* (2003), the same experiment was performed (nominal dose 100 $\mu\text{g/L}$), and body burden reached 569 ng/mL at steady-state (reached within the first 24 hours of exposure). The slight difference between the two nominal doses could hardly explain the considerable discrepancy, a 50-fold difference, between the measured whole-body concentrations. When used to predict BPA concentrations in zebrafish, the PBTK calibrated on stickleback data tends to overestimate BPA uptake, except the data of Lindholst *et al.* (2003). It could highlight an analytical issue. For example, concerns were raised about the stability of the metabolites in the different matrices before analysis (Ye *et al.* 2007; Dekant & Völkel 2008; Ougier *et al.* 2021). Thus, metabolites deconjugation could lead to underestimating BPA metabolite concentration and overestimating BPA concentrations in the different organs.

More generally, errors associated with measured concentrations in Figure 4 were not shown for sake of clarity due to the large number of datapoints. However, it must be taken into

account that uncertainty and variability associated with measurements was particularly high in some cases. For example, BPA sulf concentration measured in trout bile was highly variable, with a mean value of 267 ng/mL and an SD of 277 ng/mL. This point could explain, at least partially, the sometimes-large discrepancies between predictions and observations.

4.3. Limits of calibration on one species

In this work, the model was calibrated using our dataset in stickleback to increase the reliability of the PBTK. Indeed, as previously mentioned, BPA experiments on fish from the literature sometimes lacked information to perfectly describe the exposure scenarios in the model's inputs. However, the limits of using a single species were highlighted when evaluating the predictions in fish organs. Because no measurement was available in compartments other than blood, liver, and carcass, the ability of the model to correctly predict concentrations in different compartments remained uncertain. Evaluation on datasets obtained in other species showed that the PBTK could predict BPA kinetics in zebrafish, for the lowest concentration levels, even in the brain and the gonads. Predictions were less accurate for zebrafish exposed to 20 to 90 times the environmentally relevant dose (outside the doses of our calibration dataset): at some point, the model failed to simulate the behavior of BPA correctly. When including all the species in the calibration process, the resulting fit to the data was notably improved for the trout but not for zebrafish (see Table 3). Since some physiological parameters, such as relative blood flow to organs in zebrafish, were scaled using data from rainbow trout due to the lack of data regarding fish physiology (Grech *et al.* 2019), one possibility could be that those approximations increase model error. Nonetheless, the discrepancy between observations and predictions could also be due to non-physiological parameters specific to the species.

For example, in terms of metabolization, a difference was observed between the calibration on stickleback or multi-species data (Figure 5). Thus, unlike the K_m , which were similar in both calibrations, hepatic V_{max} was different between the two calibrations for both BPA gluc and BPA sulf. The same result was observed *in vitro* in Lavado and Schlenk (2011) for parathion, fenthion, and chlorpyrifos metabolism in rainbow trout and coho salmon (*Oncorhynchus kisutch*). According to the authors, sharing the same binding affinity (K_m) would indicate that the enzymes responsible for the metabolization would be similar in structure. Still, the catalytic efficiencies were different likely due to varying protein content between species. Our results seem to indicate that the stickleback BPA gluc and BPA sulf metabolism may slightly differ from the trout and the zebrafish. Consequently, a calibration containing TK data from the three species would result in a trade-off V_{max} posterior value.

Another critical parameter, highlighted by the sensitivity analysis, could be the unbound fraction in plasma. This parameter which depends on plasma composition is expected to be species-dependent (De Smet *et al.* 1998; Noël *et al.* 2010; Henneberger *et al.* 2020). Initially, UF deviates from its prior mean in the calibration on stickleback data and reaches around 7%. This parameter measures chemical bound to plasmatic proteins, mainly albumin in mammals. The posterior distribution obtained in fish is slightly higher than the values reported in the literature. More precisely, when accounted for, UF used in rat and human PBPK are set to around 5% (Csanády *et al.* 2002; Kawamoto *et al.* 2007; Edginton & Ritter 2009). However, UF could reach 10% in mammals, as stated by Collet (2012). Nevertheless, fish plasma composition could not reflect mammal plasma composition. In Henneberger *et al.* (2020), it was shown that trout albumin could differ from human albumin and that some chemicals known to have a low UF in human plasma could have a high UF in trout. Moreover, transposition to other fish species should be done carefully as zebrafish plasma would not contain any albumin-like proteins resulting in a UF different from trout UF (Noël *et al.* 2010). Nevertheless, the UF resulting from the multi-species calibration did not strongly differ from the calibration on stickleback data indicating a similar UF for those species or a stickleback value being an average between zebrafish and trout UF .

5. Conclusion

An expected output of this work is to propose an integrating approach to link internal concentrations to BPA effects in three-spined stickleback in the future. Thus, this work consisted of the first step of a scaling-up process where environmentally relevant concentrations of BPA are linked to bioaccumulation in fish organs. The structure of the model was built to allow prediction of BPA concentrations and its metabolites in various organs. The model was then calibrated based on TK data resulting from environmentally relevant exposure to BPA. The calibrated model was shown able to accurately simulate internal concentrations in stickleback, and to some extent concentrations in zebrafish and trout. However, for those species, the accuracy was limited by the stickleback data used in the calibration process. Since BPA effects were measured in stickleback, it should not prevent the scaling-up process to be completed.

Funding information

This work was supported by the French National program EC2CO (Ecosphère Continentale et Côtière) as part of the DERBI project and by the French Ministry of ecological transition (P190). The authors wish to thank Cleo Tebby for its contribution in the calibration process and its careful proofreading.

References

- Barron, M.G., Schultz, I.R. & Hayton, W.L. (1989). Presystemic branchial metabolism limits di-2-ethylhexyl phthalate accumulation in fish. *Toxicology and Applied Pharmacology*, 98, 49-57.
- Bertelsen, S.L., Hoffman, A.D., Gallinat, C.A., Elonen, C.M. & Nichols, J.W. (1998). Evaluation of log K_{ow} and tissue lipid content as predictors of chemical partitioning to fish tissues. *Environmental Toxicology and Chemistry*, 17, 1447-1455.
- Bois, F.Y. (2009). GNU MCSim: Bayesian statistical inference for SBML-coded systems biology models. *Bioinformatics*, 25, 1453-1454.
- Bois, F.Y. & Brochot, C. (2016). Modeling Pharmacokinetics. In: *In Silico Methods for Predicting Drug Toxicity* (ed. Benfenati, E). Springer, pp. 37-62.
- Boucher, J.G., Boudreau, A., Ahmed, S. & Atlas, E. (2015). In Vitro Effects of Bisphenol A β -D-Glucuronide (BPA-G) on Adipogenesis in Human and Murine Preadipocytes. *Environmental health perspectives*, 123, 1287-1293.
- Brinkmann, M., Schlechtriem, C., Reininghaus, M., Eichbaum, K., Buchinger, S., Reifferscheid, G. *et al.* (2016). Cross-Species Extrapolation of Uptake and Disposition of Neutral Organic Chemicals in Fish Using a Multispecies Physiologically-Based Toxicokinetic Model Framework. *Environmental Science & Technology*, 50, 1914-1923.
- Collet, S. (2012). Développement d'une approche toxicocinétique/toxicodynamique basée sur des mécanismes physiologiques pour évaluer les effets oestrogéniques du Bisphénol A.
- Csanády, G., Oberste-Frielinghaus, H., Semder, B., Baur, C., Schneider, K. & Filser, J. (2002). Distribution and unspecific protein binding of the xenoestrogens bisphenol A and daidzein. *Archives of toxicology*, 76, 299-305.
- David, V., Joachim, S., Porcher, J.-M. & Beaudouin, R. (2019). Modelling BPA effects on three-spined stickleback population dynamics in mesocosms to improve the understanding of population effects. *Science of The Total Environment*, 692, 854-867.
- De Smet, H., Blust, R. & Moens, L. (1998). Absence of albumin in the plasma of the common carp *Cyprinus carpio*: binding of fatty acids to high density lipoprotein. *Fish Physiology and Biochemistry*, 19, 71-81.
- Dekant, W. & Völkel, W. (2008). Human exposure to bisphenol A by biomonitoring: methods, results and assessment of environmental exposures. *Toxicology and Applied Pharmacology*, 228, 114-134.
- Dodds, E.C., Goldberg, L., Lawson, W. & Robinson, R. (1938). OEstrogenic Activity of Certain Synthetic Compounds. *Nature*, 141, 247-248.
- Edginton, A.N. & Ritter, L. (2009). Predicting Plasma Concentrations of Bisphenol A in Children Younger Than 2 Years of Age after Typical Feeding Schedules, using a Physiologically Based Toxicokinetic Model. *Environmental health perspectives*, 117, 645-652.
- Endo, S., Brown, T.N. & Goss, K.-U. (2013). General Model for Estimating Partition Coefficients to Organisms and Their Tissues Using the Biological Compositions and Polyparameter Linear Free Energy Relationships. *Environmental Science & Technology*, 47, 6630-6639.
- Erickson, R.J. & McKim, J.M. (1990). A model for exchange of organic chemicals at fish gills: flow and diffusion limitations. *Aquatic Toxicology*, 18, 175-197.
- Eser, B., Tural, R., Gunal, A.C. & Sepici Dincel, A. (2021). Does bisphenol A bioaccumulate on zebrafish? Determination of tissue bisphenol A level. *Biomedical Chromatography*, n/a, e5285.
- Faheem, M. & Bhandari, R.K. (2021). Detrimental Effects of Bisphenol Compounds on Physiology and Reproduction in Fish: A Literature Review. *Environmental Toxicology and Pharmacology*, 81, 103497.
- Fang, Q., Shi, Q., Guo, Y., Hua, J., Wang, X. & Zhou, B. (2016). Enhanced Bioconcentration of Bisphenol A in the Presence of Nano-TiO₂ Can Lead to Adverse Reproductive Outcomes in Zebrafish. *Environmental Science & Technology*, 50, 1005-1013.

- Flint, S., Markle, T., Thompson, S. & Wallace, E. (2012). Bisphenol A exposure, effects, and policy: A wildlife perspective. *Journal of Environmental Management*, 104, 19-34.
- Forbes, V.E., Calow, P. & Sibly, R.M. (2008). The extrapolation problem and how population modeling can help. *Environmental Toxicology and Chemistry*, 27, 1987-1994.
- Gerlowski, L.E. & Jain, R.K. (1983). Physiologically Based Pharmacokinetic Modeling: Principles and Applications. *Journal of Pharmaceutical Sciences*, 72, 1103-1127.
- Gramec Skledar, D. & Peterlin Mašič, L. (2016). Bisphenol A and its analogs: Do their metabolites have endocrine activity? *Environmental Toxicology and Pharmacology*, 47, 182-199.
- Grech, A., Brochot, C., Dorne, J.-L., Quignot, N., Bois, F.Y. & Beaudouin, R. (2017). Toxicokinetic models and related tools in environmental risk assessment of chemicals. *Science of The Total Environment*, 578, 1-15.
- Grech, A., Tebby, C., Brochot, C., Bois, F.Y., Bado-Nilles, A., Dorne, J.L. *et al.* (2019). Generic physiologically-based toxicokinetic modelling for fish: Integration of environmental factors and species variability. *Science of The Total Environment*, 651, 516-531.
- Gu, Z.Y., Jia, R., He, Q., Cao, L.P., Du, J.L., Jeney, G. *et al.* (2020). Oxidative stress, ion concentration change and immune response in gills of common carp (*Cyprinus carpio*) under long-term exposure to bisphenol A. *Comparative Biochemistry and Physiology C-Toxicology & Pharmacology*, 230, 10.
- Henneberger, L., Klüver, N., Mühlenbrink, M. & Escher, B. (2020). Trout and Human Plasma Protein Binding of Selected Pharmaceuticals Informs the Fish Plasma Model. *Environmental Toxicology and Chemistry*, n/a.
- Inoue, H., Tsuruta, A., Kudo, S., Ishii, T., Fukushima, Y., Iwano, H. *et al.* (2005). Bisphenol a glucuronidation and excretion in liver of pregnant and nonpregnant female rats. *Drug Metabolism and Disposition*, 33, 55-59.
- Inoue, H., Yuki, G., Yokota, H. & Kato, S. (2003). Bisphenol A glucuronidation and absorption in rat intestine. *Drug Metabolism and Disposition*, 31, 140-144.
- Jolly, C., Katsiadaki, I., Morris, S., Le Belle, N., Dufour, S., Mayer, I. *et al.* (2009). Detection of the anti-androgenic effect of endocrine disrupting environmental contaminants using in vivo and in vitro assays in the three-spined stickleback. *Aquatic Toxicology*, 92, 228-239.
- Karrer, C., Roiss, T., Goetz, N.v., Skledar, D.G., Mašič, L.P. & Hungerbühler, K. (2018). Physiologically Based Pharmacokinetic (PBPK) Modeling of the Bisphenols BPA, BPS, BPF, and BPAF with New Experimental Metabolic Parameters: Comparing the Pharmacokinetic Behavior of BPA with Its Substitutes. *Environmental health perspectives*, 126, 077002.
- Kawamoto, Y., Matsuyama, W., Wada, M., Hishikawa, J., Chan, M.P.L., Nakayama, A. *et al.* (2007). Development of a physiologically based pharmacokinetic model for bisphenol A in pregnant mice. *Toxicology and Applied Pharmacology*, 224, 182-191.
- Kurebayashi, H., Betsui, H. & Ohno, Y. (2003). Disposition of a low dose of ¹⁴C-bisphenol A in male rats and its main biliary excretion as BPA glucuronide. *Toxicological Sciences*, 73, 17-25.
- Lavado, R. & Schlenk, D. (2011). Microsomal biotransformation of chlorpyrifos, parathion and fenthion in rainbow trout (*Oncorhynchus mykiss*) and coho salmon (*Oncorhynchus kisutch*): Mechanistic insights into interspecific differences in toxicity. *Aquatic Toxicology*, 101, 57-63.
- Leaver, M.J., Wright, J., Hodgson, P., Boukouvala, E. & George, S.G. (2007). Piscine UDP-glucuronosyltransferase 1B. *Aquatic Toxicology*, 84, 356-365.
- Leloutre, C., Péry, A.R.R., Porcher, J.-M. & Beaudouin, R. (2018). A bioenergetics model of the entire life cycle of the three-spined stickleback, *Gasterosteus aculeatus*. *Ecology of Freshwater Fish*, 27, 116-127.
- Lindholst, C., Pedersen, K.L. & Pedersen, S.N. (2000). Estrogenic response of bisphenol A in rainbow trout (*Oncorhynchus mykiss*). *Aquatic Toxicology*, 48, 87-94.
- Lindholst, C., Pedersen, S.N. & Bjerregaard, P. (2001). Uptake, metabolism and excretion of bisphenol A in the rainbow trout (*Oncorhynchus mykiss*). *Aquatic Toxicology*, 55, 75-84.
- Lindholst, C., Wynne, P.M., Marriott, P., Pedersen, S.N. & Bjerregaard, P. (2003). Metabolism of bisphenol A in zebrafish (*Danio rerio*) and rainbow trout (*Oncorhynchus mykiss*) in relation to

- estrogenic response. *Comparative Biochemistry and Physiology Part C: Toxicology & Pharmacology*, 135, 169-177.
- Little, A.G. & Seebacher, F. (2015). Temperature determines toxicity: bisphenol A reduces thermal tolerance in fish. *Environmental Pollution*, 197, 84-89.
- Matthews, J.B., Twomey, K. & Zacharewski, T.R. (2001). In vitro and in vivo interactions of bisphenol A and its metabolite, bisphenol A glucuronide, with estrogen receptors alpha and beta. *Chemical Research in Toxicology*, 14, 149-157.
- Mazur, C.S., Kenneke, J.F., Hess-Wilson, J.K. & Lipscomb, J.C. (2010). Differences between Human and Rat Intestinal and Hepatic Bisphenol A Glucuronidation and the Influence of Alamethicin on In Vitro Kinetic Measurements. *Drug Metabolism and Disposition*, 38, 2232-2238.
- Mit, C., Tebby, C., Gueganno, T., Bado-Nilles, A. & Beaudouin, R. (2021). Modeling acetylcholine esterase inhibition resulting from exposure to a mixture of atrazine and chlorpyrifos using a physiologically-based kinetic model in fish. *Science of The Total Environment*, 773, 144734.
- Nichols, J.W., McKim, J.M., Andersen, M.E., Gargas, M.L., Clewell, H.J. & Erickson, R.J. (1990). A physiologically based toxicokinetic model for the uptake and disposition of waterborne organic chemicals in fish. *Toxicology and Applied Pharmacology*, 106, 433-447.
- Nichols, J.W., Schultz, I.R. & Fitzsimmons, P.N. (2006). In vitro-in vivo extrapolation of quantitative hepatic biotransformation data for fish. I. A review of methods, and strategies for incorporating intrinsic clearance estimates into chemical kinetic models. *Aquatic Toxicology*, 78, 74-90.
- Noël, E.S., Reis, M.D., Arain, Z. & Ober, E.A. (2010). Analysis of the Albumin/alpha-Fetoprotein/Afamin/Group specific component gene family in the context of zebrafish liver differentiation. *Gene Expression Patterns*, 10, 237-243.
- Ohkimoto, K., Sugahara, T., Sakakibara, Y., Suiko, M., Liu, M.-Y., Carter, G. *et al.* (2003). Sulfonation of environmental estrogens by zebrafish cytosolic sulfotransferases. *Biochemical and Biophysical Research Communications*, 309, 7-11.
- Ougier, E., Zeman, F., Antignac, J.-P., Rousselle, C., Lange, R., Kolossa-Gehring, M. *et al.* (2021). Human biomonitoring initiative (HBM4EU): Human biomonitoring guidance values (HBM-GVs) derived for bisphenol A. *Environment International*, 154, 106563.
- Pandey, M., Ghorai, S.M. & Rai, U. (2018). Bisphenol A mediated effects on innate immunity in freshwater teleost spotted snakehead *Channa punctatus* murrel. *Fisheries Science*, 84, 25-31.
- Pery, A.R.R., Devillers, J., Brochot, C., Mombelli, E., Palluel, O., Piccini, B. *et al.* (2014). A Physiologically Based Toxicokinetic Model for the Zebrafish *Danio rerio*. *Environmental Science & Technology*, 48, 781-790.
- Qiu, W.H., Shen, Y., Pan, C.Y., Liu, S., Wu, M.H., Yang, M. *et al.* (2016). The potential immune modulatory effect of chronic bisphenol A exposure on gene regulation in male medaka (*Oryzias latipes*) liver. *Ecotoxicology and Environmental Safety*, 130, 146-154.
- R Core Team (2019). R: A Language and Environment for Statistical Computing. R Foundation for Statistical Computing Vienna, Austria.
- Saltelli, A., Chan, K. & Scott, E.M. (2008). *Sensitivity Analysis*. John Wiley & Sons, Ltd edn, New York.
- Shin, B.S., Kim, C.H., Jun, Y.S., Kim, D.H., Lee, B.M., Yoon, C.H. *et al.* (2004). Physiologically based pharmacokinetics of bisphenol a. *Journal of Toxicology and Environmental Health, Part A*, 67, 1971-1985.
- Sobol, I.M., Tarantola, S., Gatelli, D., Kucherenko, S.S. & Mauntz, W. (2007). Estimating the approximation errors when fixing unessential factors in global sensitivity analysis. *Reliability Engineering & System Safety*, 92, 957-960.
- Tebby, C., Brochot, C., Dorne, J.-L. & Beaudouin, R. (2019). Investigating the interaction between melamine and cyanuric acid using a Physiologically-Based Toxicokinetic model in rainbow trout. *Toxicology and Applied Pharmacology*, 370, 184-195.
- Teeguarden, J.G., Waechter, J.M., Jr., Clewell, H.J., III, Covington, T.R. & Barton, H.A. (2005). Evaluation of Oral and Intravenous Route Pharmacokinetics, Plasma Protein Binding, and Uterine Tissue

- Dose Metrics of Bisphenol A: A Physiologically Based Pharmacokinetic Approach. *Toxicological Sciences*, 85, 823-838.
- Tyler, C.R., Jobling, S. & Sumpter, J.P. (1998). Endocrine Disruption in Wildlife: A Critical Review of the Evidence. *Critical Reviews in Toxicology*, 28, 319-361.
- Vandenberg, L.N., Hauser, R., Marcus, M., Olea, N. & Welshons, W.V. (2007). Human exposure to bisphenol A (BPA). *Reproductive Toxicology*, 24, 139-177.
- Vidal, A., Babut, M., Garric, J. & Beaudouin, R. (2019). Elucidating the fate of perfluorooctanoate sulfonate using a rainbow trout (*Oncorhynchus mykiss*) physiologically-based toxicokinetic model. *Science of The Total Environment*, 691, 1297-1309.
- Wang, Y., Huang, H. & Wu, Q. (2014). Characterization of the zebrafish Ugt repertoire reveals a new class of drug-metabolizing UDP glucuronosyltransferases. *Molecular Pharmacology*, 86, 62-75.
- Wu, M., Xu, H., Shen, Y., Qiu, W. & Yang, M. (2011). Oxidative stress in zebrafish embryos induced by short-term exposure to bisphenol A, nonylphenol, and their mixture. *Environmental Toxicology and Chemistry*, 30, 2335-2341.
- Yang, X., Doerge, D.R., Teeguarden, J.G. & Fisher, J.W. (2015). Development of a physiologically based pharmacokinetic model for assessment of human exposure to bisphenol A. *Toxicology and Applied Pharmacology*, 289, 442-456.
- Ye, X., Bishop, A.M., Reidy, J.A., Needham, L.L. & Calafat, A.M. (2007). Temporal stability of the conjugated species of bisphenol A, parabens, and other environmental phenols in human urine. *Journal of Exposure Science & Environmental Epidemiology*, 17, 567-572.

Table lists

Table 1. Summary of experimental data on BPA toxicokinetics.....	2
Table 2. Parameter prior distribution and posterior values obtained after calibration on stickleback TK data	3
Table 3. Comparison of the Bayesian information criteria (BIC) and folds obtained by simulating data in zebrafish, trout, and stickleback, with the models calibrated on stickleback and multi-species data	4

Table 1. Summary of experimental data on BPA toxicokinetics

Species	Exposure scenario	Nominal dose of BPA (µg/L)	Matrix	Metabolite(s)	Study reference
<i>Danio rerio</i>	7d uptake and 7d depuration	100	Whole-body	BPA gluc and BPA sulf	Lindholst <i>et al.</i> , 2003
	21d uptake (continuous)	2, 20, 200	Liver, gonads, brain (male and female)		Fang <i>et al.</i> , 2016
	21d uptake (continuous)	90, 900	Whole-body		Eser <i>et al.</i> , 2021
<i>Oncorhynchus mykiss</i>	12d uptake (continuous)	10, 40, 70, 100, 500	Muscle and liver		Lindholst <i>et al.</i> , 2000
	7d uptake (continuous) Intraperitoneal (one dose)	100 154 µmol/kg	Plasma, liver, and muscle	BPA gluc	Lindholst <i>et al.</i> , 2001
	8d uptake (continuous)	100	Bile	BPA gluc and BPA sulf	Lindholst <i>et al.</i> , 2003

Table 2. Parameter prior distribution and posterior values obtained after calibration on stickleback TK data

Chemical	Parameter name	Abbreviation	Unit	Prior distribution*	Posterior distribution	
					MPV**	95% IC
BPA	Unbound fraction	<i>Unbound_fraction</i>	No unit	TN(0.035,0.3,0.001,1)	0.07	0.05;0.08
	Blood:water partition coefficient	<i>PC_blood_water</i>	No unit	Calculated using an intermediate ratio	0.35	0.25;0.45
	Liver:blood partition coefficient	<i>PC_liver</i>	No unit	TN(2.69,0.3,1×10 ⁻⁶ , 1×10 ⁶)	4.81	2.90;5.30
	Gonads:blood partition coefficient	<i>PC_gonads</i>	No unit	TN(5.63,0.3,1×10 ⁻⁶ , 1×10 ⁶)	5.56	1.73;8.79
	Fat:blood partition coefficient	<i>PC_fat</i>	No unit	TN(24.26,0.3, 1×10 ⁻⁶ , 1×10 ⁶)	0.63	0.10;11.6
	Richly perfused:blood partition coefficient	<i>PC_brain</i>	No unit	TN(1.74,0.3, 1×10 ⁻⁶ , 1×10 ⁶)	0.18	3.72×10 ⁻² ;2.06
	Poorly perfused:blood partition coefficient	<i>PC_pp</i>	No unit	TN(1.68,0.3, 1×10 ⁻⁶ , 1×10 ⁶)	0.52	0.23;0.67
	Km gluco	<i>Km_gluco</i>	µg/mL	TN(24.3, 0.3, 1×10 ⁻⁶ , 1×10 ⁶)	40.0	10.3;40.0
	Km sulfo	<i>Km_sulfo</i>	µg/mL	TN(7.1,0.3, 1×10 ⁻⁶ , 1×10 ⁶)	7.57	3.24;10.9
	Vmax gluco	<i>Vmax_gluco</i>	µg/d/g	Calculated using an intermediate ratio	3.98×10 ²	24.4;3.13×10 ²
	Vmax sulfo	<i>Vmax_sulfo</i>	µg/d/g	Calculated using an intermediate ratio	11.4	2.03;87.8
	Plasmatic clearance gluco	<i>Cl_plasma_gluco</i>	mL/d/mL	U(1×10 ⁻⁶ , 1×10 ⁶)	3.86×10 ⁴	2.83×10 ⁴ ; 6.07×10 ⁴
	Plasmatic clearance sulfo	<i>Cl_plasma_sulfo</i>	mL/d/mL	U(1×10 ⁻⁶ , 1×10 ⁶)	3.76×10 ²	1.99×10 ² ; 4.86×10 ²
BPA gluc	Liver:blood partition coefficient	<i>PC_liver_gluco</i>	No unit	TN(3.50,0.3,1×10 ⁻¹⁰ , 1×10 ⁶)	3.30	2.12;5.75
	Rob:blood partition coefficient	<i>PC_rob_gluco</i>	No unit	TN(6.30,0.3,1×10 ⁻¹⁰ , 1×10 ⁶)	0.14	0.12;0.22
	Ke bile	<i>Ke_bile_gluco</i>	1/d	U(1×10 ⁻⁶ ,1×10 ⁶)	94.3	79.8; 1.97×10 ²
BPA sulf	Liver:blood Partition coefficient	<i>PC_liver_sulfo</i>	No unit	TN(3.80,0.3,1×10 ⁻¹⁰ , 1×10 ⁶)	3.68	2.62;6.81
	Rob:blood Partition coefficient	<i>PC_rob_sulfo</i>	No unit	TN(7.0,0.3,1×10 ⁻¹⁰ , 1×10 ⁶)	0.31	0.25;0.51
	Ke bile	<i>Ke_bile_sulfo</i>	1/d	U(1×10 ⁻⁶ , 1×10 ⁶)	62.8	46.8;1.56×10 ²

*TN stands for the truncated normal law (prior, coefficient variation, lowest bound, highest bound); U stands for the uniform law (lowest bound, highest bound)

**MPV stands for the Most Probable Value (mode)

Table 3. Comparison of the Bayesian information criteria (BIC) and folds obtained by simulating data in zebrafish, trout, and stickleback, with the models calibrated on stickleback and multi-species data

		Simulated dataset									
		Stickleback			Zebrafish			Trout			
		BIC	Fold			Fold			Fold		
<3	3-10		>10	<3	3-10	>10	<3	3-10	>10		
Calibration dataset	Stickleback	93.7	82%	14%	4%	45%	12%	43%	41%	30%	29%
	Multi-species	108.3	84%	12%	4%	45%	12%	43%	45%	50%	5%

Figure lists

Figure 1. Schematic representation of the BPA PBTK. 2

Figure 2. Model simulations in blood, liver and carcass of three-spined stickleback exposed at 10 µg/L after specific data calibration compared to experimental datapoints..... 3

Figure 3. Model simulations in blood, liver and carcass of three-spined stickleback exposed at 100 µg/L after specific data calibration compared to the experimental datapoints..... 4

Figure 4. Comparison between BPA, BPA gluc and BPA sulf concentrations measured in zebrafish and rainbow trout and model prediction..... 5

Figure 5. Comparison of a set of six parameters calibrated using stickleback TK data and multi-species TK data. 6

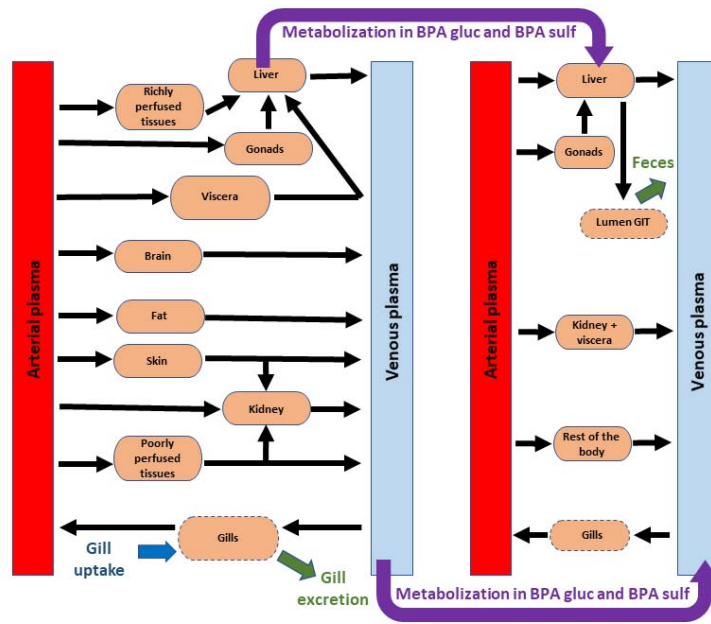


Figure 1. Schematic representation of the BPA PBTK.

Uptake by the gills is symbolized in blue. Metabolization occurs in the liver and venous plasma (purple). Excretion by the gill and the feces via the bile is symbolized in green.

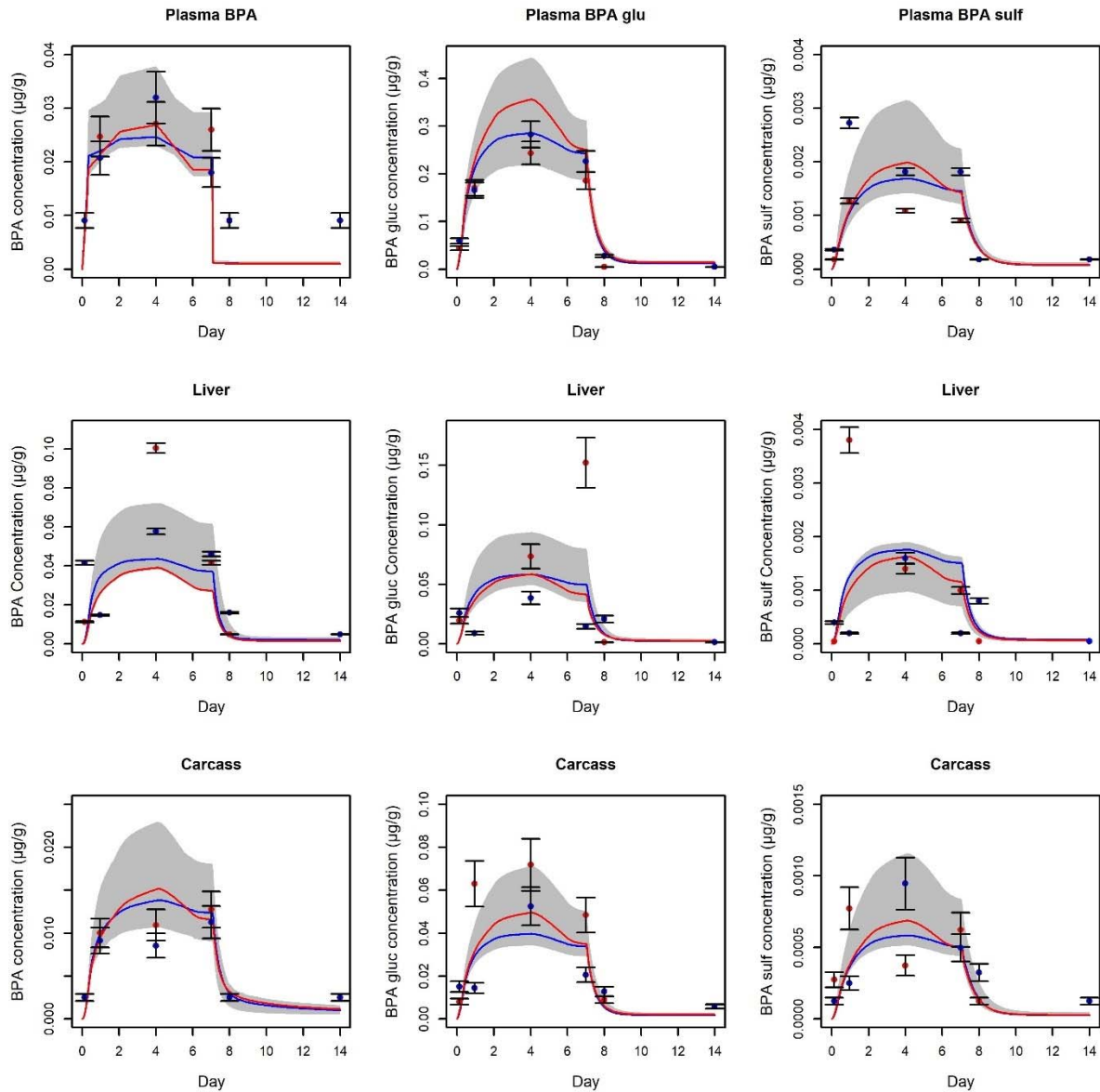


Figure 2. Model simulations in blood, liver and carcass of three-spined stickleback exposed at 10 µg/L after specific data calibration compared to experimental datapoints.

Concentrations are represented in blue for males and in red for females. The solid line represents the model predictions and the dots the measured concentration (pool of two fish). The grey area is the 95% prediction interval, computed from the posterior distributions. The simulations were made using the last 333 iterations of the three MCMC chains. Intervals of credibility are build using the estimated precision of measurement for each organ and each compound.

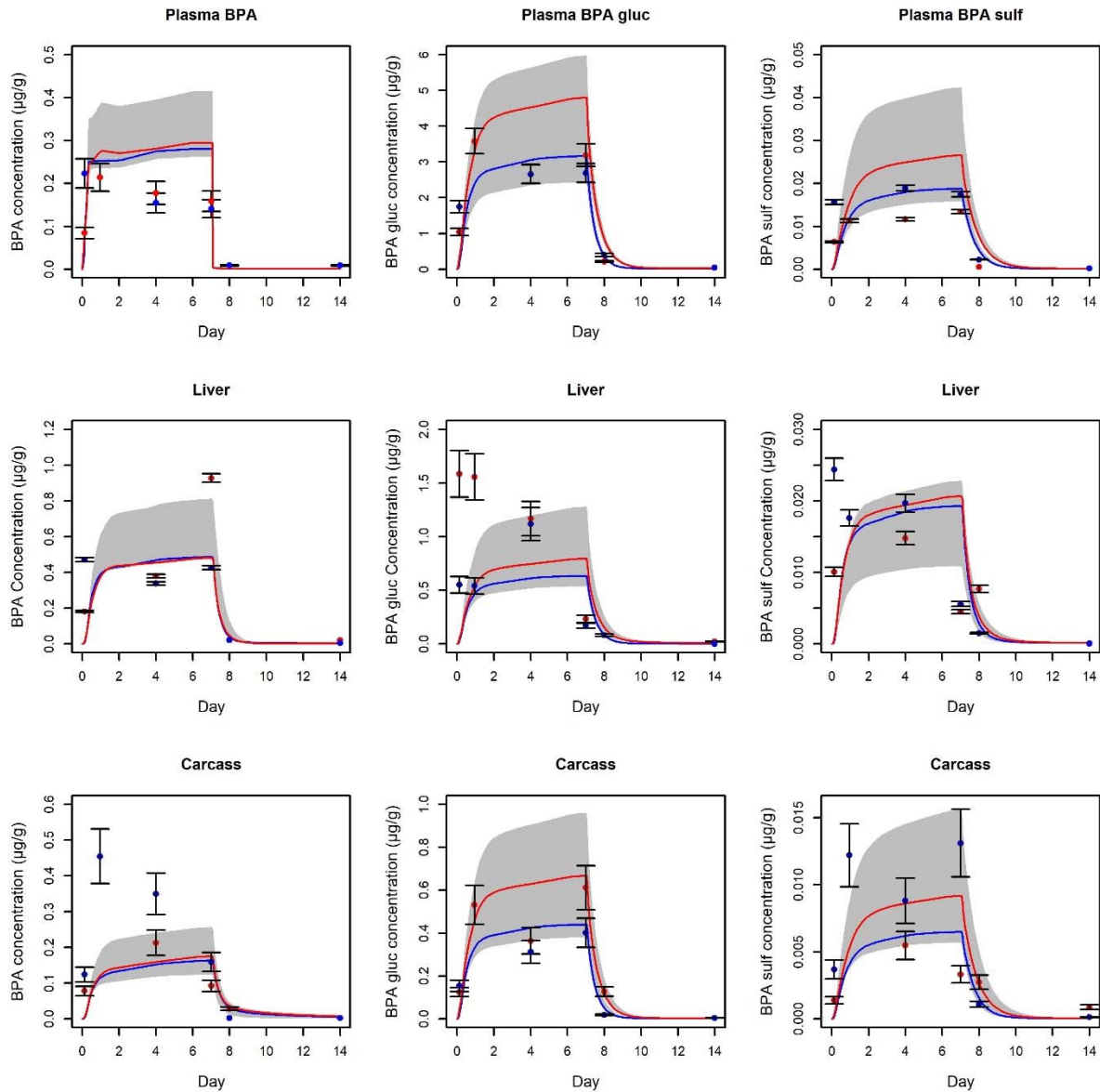


Figure 3. Model simulations in blood, liver and carcass of three-spined stickleback exposed at 100 µg/L after specific data calibration compared to the experimental datapoints.

Concentrations are represented in blue for males, and in red for females. The solid line represents the model predictions and the dots the measured concentration (pool of two fish). The grey area is the 95% prediction interval, computed from the posterior distributions. The simulations were made using the last 333 iterations of the three MCMC chains. Intervals of credibility are build using the estimated precision of measurement for each organ and each compound.

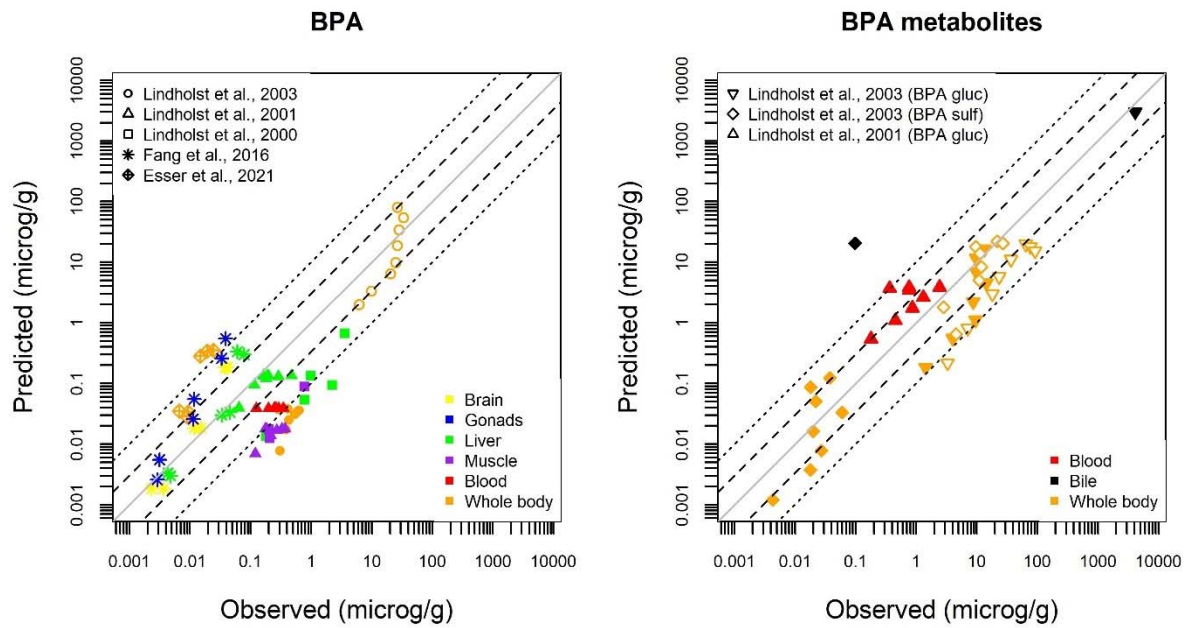


Figure 4. Comparison between BPA, BPA gluc and BPA sulf concentrations measured in zebrafish and rainbow trout and model prediction.

Experimental datasets used are indicated in the legend as for the different matrices where concentrations were measured. Uptake is symbolized by the full points. Depuration was measured as normalized whole-body concentrations in Lindholst et al. (2003) and are represented by the empty points. The grey line corresponds to the identity line, then the 3-fold range and the 10-fold range.

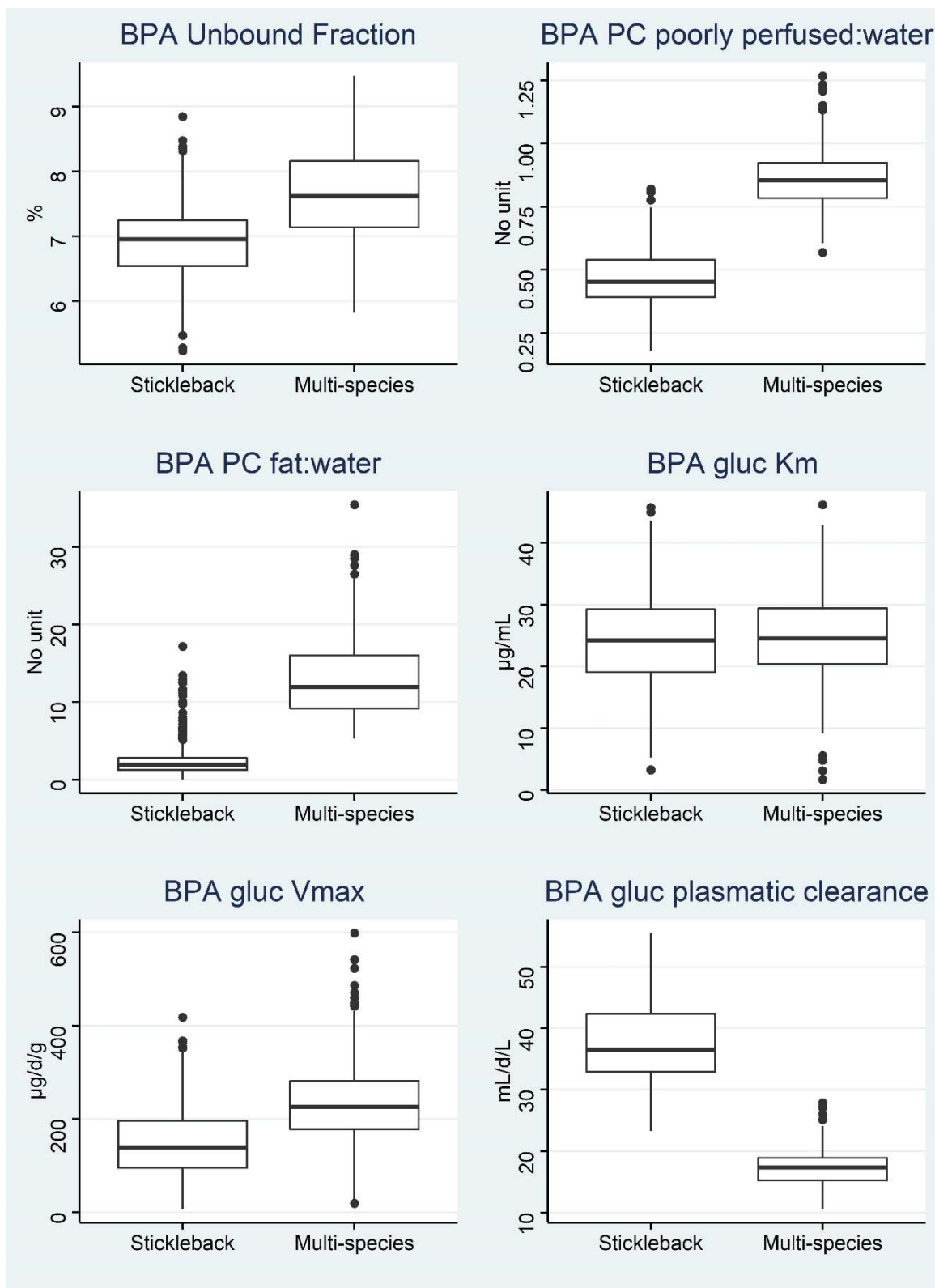


Figure 5. Comparison of a set of six parameters calibrated using stickleback TK data and multi-species TK data.

Boxplots were made using the last 333 iterations of the three MCMC chains calibrated on monospecific TK data (stickleback) and a mix of TK data from stickleback, zebrafish and trout (Multi-species).

Supporting information to “Adaptation of a generic PBTK to model BPA TK in three-spined stickleback”

1. Chemical analysis	2
1.1. Standards and reagents.....	2
1.2. Sample processing.....	2
1.3. LC-MS/MS.....	3
1.4. BPA and metabolites quantification.....	4
2. Generic model structure	5
2.1. Model compartment	5
2.2. Physiological parameters	5
3. Sensitivity analysis.....	6
4. MCMC calibration.....	11
4.1. Parametrization.....	11
4.2. Calibration results	11
5. Literature dataset.....	11
5.1. Literature scenario: model simulation inputs	11
6. Stickleback dataset.....	11
6.1. Analysis results in water.....	12
6.2. Analysis results in the three matrices	12
7. Model evaluation	14
7.1. Model simulation inputs	14
7.2. Comparison of the Grech <i>et al</i> 's model and the BPA PBTK.....	15
8. Multi-species calibration	16
8.1. Internal evaluation of the model	16
9. MCSim code.....	20
9.1. Model code for MCSim.....	20
9.2. MCMC code for MCSim	27
10. References.....	34

1. Chemical analysis

1.1. Standards and reagents

Analytical standard of Bisphenol A (BPA) was obtained from Sigma-Aldrich (Saint Quentin Fallavier, France). Bisphenol A sodium monosulfate (BPA-S) and Bisphenol A glucuronide (BPA-Glu) were acquired from US Biological Clinisciences (Nanterre, France). Isotopically labeled internal standards of Bisphenol A-D4 (BPA-D4) and bisphenol A Glucuronid \times 10-13C12 were purchased from CDN ISOTOPES (Quebec, Canada). All standards were greater than 98% purity. Water (Optima LC/MS grade), acetonitrile (ACN), and MeOH (ULC/MS grade) were furnished by Fisher Chemical (Illkirch, France) and Biosolve Chimie SARL (Dieuze, France), respectively. Ammonium Fluoride (NH₄F) (purity > 99,99%) was obtained from Sigma-Aldrich.

Individual stock solutions were prepared at concentrations of 1000 μ g/ml in methanol (MeOH) and stored at -23°C. Working solutions were prepared daily by appropriate dilution of an intermediate stock solution (10 μ g/ml of each compound in MeOH) held at -23°C.

1.2. Sample processing

Water

BPA water concentration was monitored at each sampling time to measure the actual exposure concentrations in the aquarium. After 10 min in an ultrasonic bath, an aliquot (900 μ l) of the water sample was added to 100 μ l of MeOH containing the internal standards BPA-D4 and BPA-Glu-13C12 200 ng/ml. After homogenization, 10 μ l of this mixture were injected and analyzed in LC-MS/MS.

Stickleback blood and liver

A liquid-liquid microextraction was performed onto 20 mg of fresh liver or 20 μ l of blood in 2 ml-screw tubes. Then, 1ml ACN/MeOH (50:50, v/v) was added, and the tube was vortexed 5s, then shook 120s with a Beadbug homogenizer (320 rpm). Next, the tube was placed 5 minutes in an ultrasonic bath before centrifugation at 4°C for 10 minutes at 10 000 rpm. Then, 800 μ l of supernatant were transferred in a new 2 ml-tube before evaporating to dryness in a miVac Centrif1000 μ g/ml concentrations) for 45 min at 35°C. The dry residue was dissolved in 800 μ l H₂O/MeOH (90:10, v/v), and 5 μ l of this mixture was injected in LC-MS/MS for analysis.

Stickleback carcass

Bheldanalysis, the carcasses were freeze-dried for 48h, subsequently ground with a mortar. Then, as described above, the microextraction was performed onto 25 mg of the freeze-dried carcass. However, an additional step was necessary: the extract was first frozen for 3 hours at -23°C, then an aliquot (250 µl) was removed and evaporated to dryness to quantify BPA-Glu metabolite. A second aliquot of the extract (600 µl) was purified before evaporation with the dSPE PSA/C18 (Macherey Nagel) clean-up to increase BPA and BPA-S sensitivity. The dry residues were dissolved in the same volumes of H₂O/MeOH (90:10, v/v) before LC-MS/MS injection.

1.3. LC-MS/MS

A Waters H-Class liquid chromatography system (Waters, Saint Quentin en Yvelines, France) was used for chromatographic separation. This one was performed with a Waters BEH C18 column (100 × 2,1 mm; 1,7 µm) with a mobile phase composed of (A) 1mM NH₄F in water and (B) MeOH with the following gradient: 20–100% (B) for 5 min followed by 100% (B) for 2 min. The column was then equilibrated at the initial conditions for 2 min. The flow rate was fixed at 0,3 mL/min, the oven temperature was set at 40 °C, and the injection volume was 5 µL for fish and 10 µl for aquarium water. The chromatographic system was coupled with Waters's Xevo TQ-S triple quadrupole mass spectrometer. Electrospray ionization was performed in the negative mode with the following optimized parameters: capillary voltage -2400V, desolvation temperature 550 °C, source temperature 150 °C, and nitrogen desolvation and nebulizer gas flow 900 L/h and 150 L/h, respectively. For each compound, the IntelliStart™ Software was used to automatically select the m/z value for the precursor ion [M-H] and product ions, cone voltage, and collision energy. Thus, two multiple reaction monitoring (MRM) transitions were optimized. The target ion transition with the highest intensity (MRM1) was used for quantitation, whereas the second target ion transition (MRM2) was used for confirmation. The ion transitions, cone voltages, collision energies, and dwell times for the analytes are displayed in Table S1.

Table S1. Retention time (Tr), transitions used for the quantification (MRM1) and confirmation (MRM2), dwell time, and optimized source parameters.

Compound	Tr (min)	Transitions	Dwell time (ms)	Cone voltage (V)	Collision energy (eV)
BPA	4.9	MRM 1 : 227.1 -> 212.1	24	21	21
		MRM 2 : 227.1 -> 133.1	24	21	27
BPA-S	2.8	MRM 1 : 307.1 -> 212.1	24	49	35
		MRM 2 : 307.1 -> 227.1	24	49	27
BPA-Glu	2.3	MRM 1 : 403.1 -> 133.0	24	9	19
		MRM 2 : 403.1 -> 117.0	24	9	33

1.4. BPA and metabolites quantification

BPA and metabolites were quantified with a matrix-matched calibration with eight levels, using the isotopically labeled internal standards. The obtained limits of quantification are displayed in Table S2 for each matrix.

Table S2. Quantification limits for each matrix (ng/g or ng/ml)

	BPA	BPA-S	BPA-Glu
Liver (ng/g)	10	0.1	3
Blood (ng/g)	10	0.2	5
Carcass (ng/g)	20	1	5
Water (ng/ml)	0.5	0.2	0.4

2. Generic model structure

2.1. Model compartment

The PBTK model used is based on the generic model developed by Grech *et al.* (2019). This model has been successfully applied to four different species, including rainbow trout, zebrafish, fathead minnow, and three-spined stickleback. It comprises twelve well-mixed blood flow limited compartments: arterial and venous blood, gills, gastrointestinal tract (GIT), skin, kidney, fat, liver, gonads, brain, poorly perfused tissues (PPT), and richly perfused tissues (RPT). Cardiac output, oxygen consumption rate, and afferent oxygen concentration are modulated by temperature by using Arrhenius' function. It also includes a growth sub-model based on DEB theory, depending on temperature and food level. Absorption can be driven by GIT or gills. In terms of excretion, branchial, urinary, fecal, and biliary excretion routes have been modeled. Physiological parameter values were subject to an extensive literature search. The structure of the model is available in 7. Model structure.

2.2. Physiological parameters

Physiological parameters were retrieved from the generic model by Grech *et al.* (2019). Rainbow trout and zebrafish physiological parameters can be found in the supporting information available online with the previously cited paper. For the particular case of the three-spined stickleback, few physiological parameters were adapted to our dataset, especially relative weights measured during dissection and plasma fraction calculated with the hematocrit fraction (plasma = 1-hematocrit) retrieved in Dalziel *et al.* (2012). In addition, because blood flow to organs was directly based on the relative volume of each organ, relative blood flows were also modified and are available in table S3.

Table S3. Stickleback specific physiological data retrieved from Grech et al., 2018 and updated (in bold)

Parameters (fraction)	Mean value	
	Male	Female
Relative weight		
Adipose tissues	0.0168	0.0168
Blood	0.009	0.011
Brain	0.012	0.010
GIT	0.055	0.066
Gonads	0.008	0.028
Kidney	0.013	0.008
Liver	0.055	0.065
PPT	0.7662	0.7162
RPT	0.032	0.025
Skin	0.036	0.061
Relative blood flow		
Adipose tissues	0.0095	0.0095
Brain	0.039	0.0251
GIT	0.088	0.0816
Gonads	0.0054	0.002
Kidney	0.12	0.07
Liver	0.054	0.054
PPT	0.55	0.62
RPT	0.12	0.1033
Skin	0.019	0.0242
Plasma	0.55	0.55

3. Sensitivity analysis

The sensitivity analysis was carried out on the exposure scenario on three-spined stickleback to 100µg/L of BPA for seven days followed by seven days of depuration and using the variance-based Sobol method (Sobol *et al.* 2007; Saltelli *et al.* 2008). The influence of 29 parameters (presented in Table S4) was investigated on nine outputs including blood, liver, and carcass concentrations. Partition coefficients were calculated using the QSAR method described in Grech *et al.* (2019) and originally from Bertelsen *et al.* (1998). LogKow was set to 3.32 for BPA, 1.46 for BPA gluc, and 1.19 for BPA sulf, thus considering only the neutral molecular form at pH=7 for all compounds.

In the following, a selection of six SA showing the top ten most influential parameters on BPA, BPA gluc, and BPA sulf concentrations in the whole body, liver, and plasma are presented (figure S2 to S7).

Table S4. Mean parameter values used in the sensitivity analysis

<i>Parameter</i>	<i>Value</i>
<i>Plasma</i>	0.55
<i>Unbound_fraction</i>	0.035
<i>Unbound_fraction_gluco</i>	0.95
<i>Unbound_fraction_sulfo</i>	0.95
<i>Ratio_PC_UF</i>	1681
<i>PC_liver</i>	2.69
<i>PC_gonads</i>	5.63
<i>PC_brain</i>	1.88
<i>PC_fat</i>	24.3
<i>PC_skin</i>	1.19
<i>PC viscera</i>	1.13
<i>PC_kidney</i>	4.25
<i>PC_rp</i>	1.74
<i>PC_pp</i>	1.70
<i>Km_gluco</i>	24.3
<i>Ratio_Vmax_Km_gluco</i>	8.6
<i>Km_sulfo</i>	7.1
<i>Ratio_Vmax_Km_sulfo</i>	17070
<i>Cl_plasma_gluco</i>	10000
<i>Cl_plasma_sulfo</i>	1000
<i>PC_liver_gluco</i>	3.5
<i>PC_gonads_gluco</i>	6.92
<i>PC_rob_gluco</i>	6.3
<i>PC_liver_sulfo</i>	3.8
<i>PC_gonads_sulfo</i>	7.28
<i>PC_rob_sulfo</i>	7
<i>PC_abdo_cavity_sulfo</i>	7.46
<i>Ke_bile_gluco</i>	100
<i>Ke_bile_sulfo</i>	100
<i>Ke_feces</i>	100

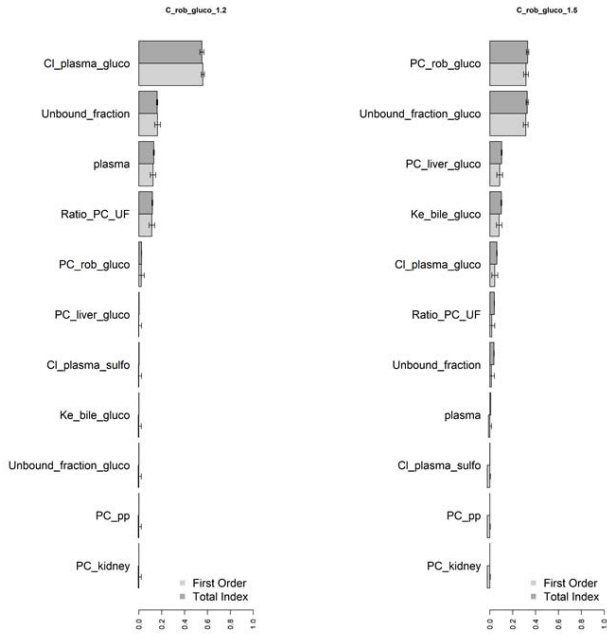


Figure S2. Sensitivity analysis on BPA gluc concentrations in stickleback carcass after 1 and 14 days of exposure. The top ten most influential parameters are represented.

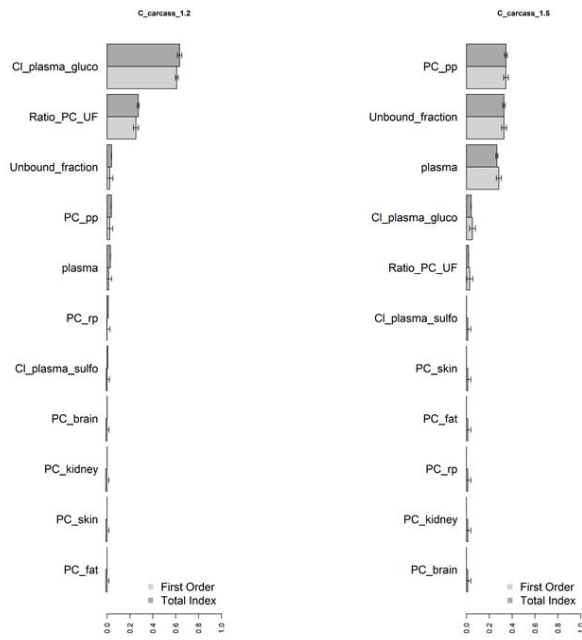


Figure S1. Sensitivity analysis on BPA concentrations in stickleback carcass after 1 and 14 days of exposure. The top ten most influential parameters are represented.

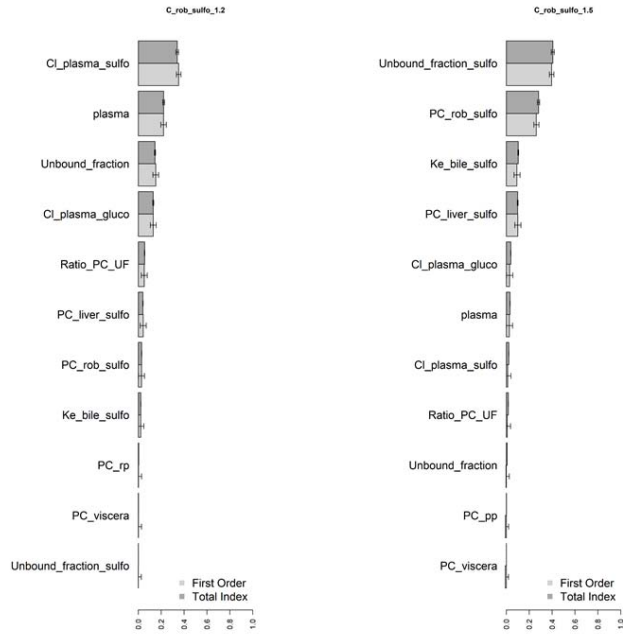


Figure S4. Sensitivity analysis on BPA sulf concentrations in stickleback carcass after 1 and 14 days of exposure. The top ten most influential parameters are represented.

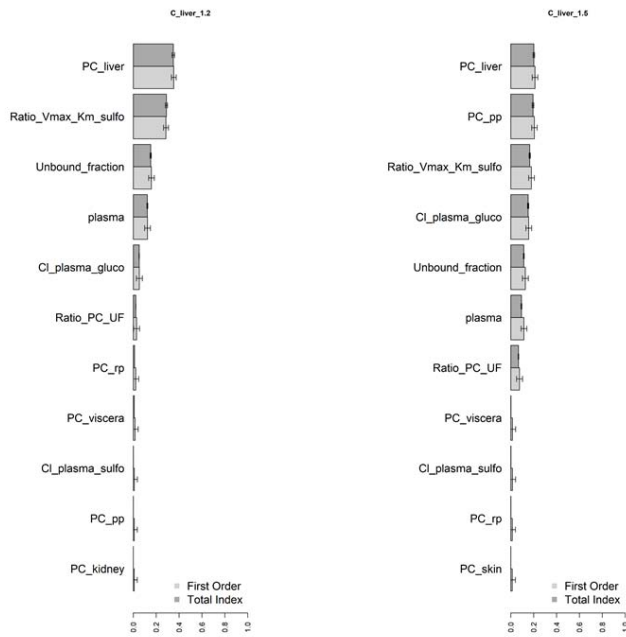


Figure S3. Sensitivity analysis on BPA concentrations in stickleback liver after 1 and 14 days of exposure. The top ten most influential parameters are represented.

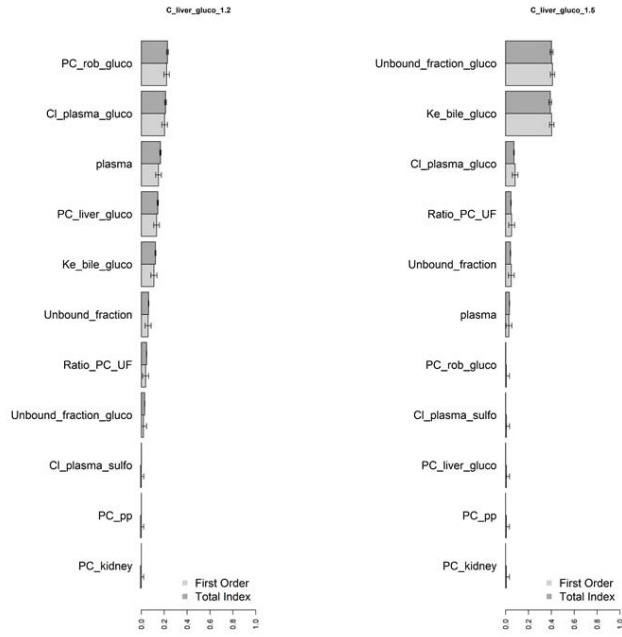


Figure S6. Sensitivity analysis on BPA gluc concentrations in stickleback liver after 1 and 14 days of exposure. The top ten most influential parameters are represented.

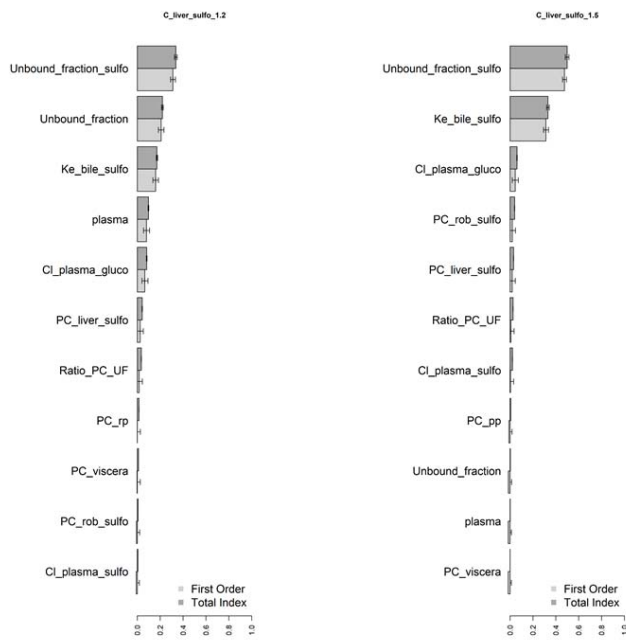


Figure S5. Sensitivity analysis on BPA gluc concentrations in zebrafish plasma after 1 and 14 days of exposure following Lindholm et al. 2003. The top ten most influential parameters are represented.

4. MCMC calibration

4.1. Parametrization

Calibration was carried out using GNU MCSim v6.2.0 (Bois 2009). Prior distributions are described in Table 2. Data likelihoods are available in section 7. Model code. MCSim gives the possibility to specify a distribution for the data. The probability of realization of modeled outputs was then described with LogNormal distribution with a variation coefficient of 100% to consider inter-individual variability.

4.2. Calibration results

Parameters were calibrated using Monte Carlo Markov Chains, with three chains of 20 000 iterations each. Convergence was assessed in R 3.6.1 (R Core Team 2019) with the package coda by checking that autocorrelations were low (i.e., that the chains were well mixed), that estimates lay well within the prior boundaries, and that the Gelman-Rubin index was close to 1.

5. Literature dataset

5.1. Literature scenario: model simulation inputs

Material and methods from the five publications were analyzed to provide the most complete inputs for the simulations of the different exposure (Table S5).

Reference	Fish characteristics	Environmental condition	Study design
<i>Lindholst et al., 2000</i>	Species: rainbow trout Age: juvenile Sex: _ Weight: 90-130g N: 50	Temperature: 15°C Tank: 50L Flow rate: 80L/d Food: not fed	Dose: 10,40,70,100,500 µg/L Duration: 12d Sample times:1
<i>Lindholst et al., 2001</i>	Species: rainbow trout Age: juvenile Sex: _ Weight: 90-130g N: 90	Temperature: 15°C Tank: 400L Flow rate: 960L/d Food: not fed	Dose: 100µg/L Duration: 7d Sample times: 9
<i>Lindholst et al., 2003</i>	Species: zebrafish Age: adult Sex: _ Weight: _ N:150	Temperature: 27°C Tank: 100L Flow rate: 800L/d Food: not fed	Dose: 100 µg/L Duration: 14d Sample times: 17
<i>Fang et al., 2016</i>	Species: zebrafish Age: four-month old Sex: male-female Weight: _ N: 48	Temperature: 28°C Tank: 20L Flow rate: _ Food: _	Dose: 2, 20, 200µg/L Duration: 21d Sample times: 1
<i>Eser et al. 2021</i>	Species: zebrafish Age: adult Sex: _ Weight: _ N: 84	Temperature: 28°C Tank: 10L Flow rate: no flow (static) Food: not fed	Dose: 90µg/L, 900µg/L Duration: 21d Sample times: 3

6. Stickleback dataset

6.1. Analysis results in water

Water from aquariums where fish were exposed to BPA was sampled at various times and analyzed. Data are presented in table S5 for 10 µg/L nominal concentration and table S6 for 100 µg/L nominal concentration. The limit of quantification (LQ) was estimated to be 0.5, 0.35, and 0.20 ng/mL for BPA, BPA gluc, and BPA sulf. The limit of detection (LD) was estimated to be 0.3, 0.1, and 0.15 ng/mL for BPA, BPA gluc, and BPA sulf.

Table S5. Measured concentrations in water (nominal concentration 10 µg/L)

	BPA (ng/ml)	BPA glu (ng/ml)	BPA sulf (ng/ml)
	Female- Male	Female- Male	Female- Male
2h	< LQ - < LQ	nd – nd	nd – nd
4h	< LQ - < LQ	nd – nd	nd – nd
8h	4.5 - 5	nd – nd	nd – nd
24h	2.2 - 5.2	nd – nd	nd – nd
48h	6.1 - 5.7	nd – nd	nd – nd
72h	6.4 - 5.8	nd – nd	nd – nd
168h	4.4 - 4.8	nd – nd	nd – nd

Table S6. Measured concentrations in water (nominal concentration 100 µg/L)

	BPA (ng/ml)	BPA glu (ng/ml)	BPA sulf (ng/ml)
	Female- Male	Female- Male	Female- Male
2h	17.3 - X	nd – nd	nd – nd
4h	23.1 – 25.4	nd – nd	nd – nd
8h	57.9 – X	nd – nd	nd – nd
24h	65.7 – 59.2	1.3 – 1.1	nd – nd
48h	64.2 – 59.6	1.5 – 1.5	nd – nd
72h	66.8 – 64.7	0.8 – 0.8	nd – nd
168h	70.1 – 65.9	2.3 – 1.4	nd – nd

6.2. Analysis results in the three matrices

The liver, blood, and carcass of the fish were also sampled and analyzed to quantify BPA, BPA gluc, and BPA sulf concentrations. Table S7 and S8 show concentrations in the liver, table S9 and S10 concentrations in blood, and table S11 and S12 concentrations in the dried carcass. A ratio was applied to the concentrations measured in the dried carcass to extrapolate the concentrations in the wet carcass. This ratio is available in Brey *et al.* (2010). The limit of quantification (LQ) for the liver is estimated to be 10 ng/g for BPA, 3 ng/g for BPA gluc, and 0.1 ng/g for BPA sulf. LQ for blood is estimated to be 10 ng/g for BPA, 5 ng/g for BPA gluc and 0.2 ng/g for BPA sulf. Finally, LQ for carcass is estimated to be 20 ng/g for BPA, 10 ng/g for BPA gluc, and 1 ng/g for BPA sulf.

Table S7 Measured concentrations in female stickleback liver

Sample	[BPA] (ng/g)		[BPA-Sulf] (ng/g)		[BPA-Gluc] (ng/g)	
	10 µg/L	100 µg/L	10 µg/L	100 µg/L	10 µg/L	100 µg/L
Nominal concentration						

Table S11. Measured concentrations in female stickleback dried carcass

Sample	[BPA] (ng/g)		[BPA-Sulf] (ng/g)		[BPA-Gluc] (ng/g)	
	10 µg/L	100 µg/L	10 µg/L	100 µg/L	10 µg/L	100 µg/L
Nominal concentration	10 µg/L	100 µg/L	10 µg/L	100 µg/L	10 µg/L	100 µg/L
DAY 0.25	< LQ	313,0	1,1	5,5	32,5	499,8
DAY 1	40,2	2634,1	3,1	63,0	252,9	2134,9
DAY 4	43,9	853,1	1,5	22,0	288,5	1460,8
DAY 7	51,1	369,7	2,5	13,3	194,5	2454,7
DAY 8	< LQ	113,9	< LQ	11,0	35,7	507,9
DAY 14	< LQ	< LQ	< LQ	3,5	23,0	15,7

Table S12. Measured concentrations in male stickleback dried carcass

Sample	[BPA] (ng/g)		[BPA-Sulf] (ng/g)		[BPA-Gluc] (ng/g)	
	10 µg/L	100 µg/L	10 µg/L	100 µg/L	10 µg/L	100 µg/L
Nominal concentration	10 µg/L	100 µg/L	10 µg/L	100 µg/L	10 µg/L	100 µg/L
DAY 025	< LQ	498,5	< LQ	14,8	60,1	617,6
DAY 1	36,6	1825,8	1	49,0	57,8	3993,4
DAY 4	34,3	1403,5	3,8	35,4	210,6	1253,3
DAY 7	45,2	639,3	2	52,6	82,6	1609,7
DAY 8	< LQ	< LQ	1,3	4,4	51,3	74,3
DAY 14	< LQ	< LQ	< LQ	< LQ	23,2	19,8

Table S13. Estimated accuracy of chemical measurement in liver, carcass and blood

	liver	carcass	blood
BPA	2,6	16,7	15,1
BPA sulf	6,4	19,2	3,6
BPA gluc	13,8	16,9	9,8

7. Model evaluation

7.1. Model simulation inputs

Inputs for the different exposure scenarios from the literature were chosen according to the content of Table S14.

Table S14. Model simulation inputs

Reference	Fish characteristics	Environmental condition	Study design
<i>Lindholst et al., 2000</i>	Species: rainbow trout Age: juvenile Sex: _ Weight: 90-130g N: 50	Temperature: 15°C Tank: 50L Flow rate: 80L/d Food: not fed	Dose: 10,40,70,100,500 µg/L Duration: 12d Route: water Sample times:1
<i>Lindholst et al., 2001</i>	Species: rainbow trout Age: juvenile Sex: _ Weight: 90-130g N: 90	Temperature: 15°C Tank: 400L Flow rate: 960L/d Food: not fed	Dose: 100µg/L Duration: 7d Route: water Sample times: 9
<i>Lindholst et al., 2003</i>	Species: zebrafish Age: adult Sex: _ Weight: _ N:150	Temperature: 27°C Tank: 100L Flow rate: 800L/d Food: not fed	Dose: 100 µg/L Duration: 14d Route: water Sample times: 17
<i>Fang et al., 2016</i>	Species: zebrafish Age: four-month old Sex: male-female Weight: _ N: 48	Temperature: 28°C Tank: 20L Flow rate: _ Food: _	Dose: 2, 20, 200µg/L Duration: 21d Route: water Sample times: 1
<i>Eser et al. 2021</i>	Species: zebrafish Age: adult Sex: _ Weight: _ N: 84	Temperature: 28°C Tank: 10L Flow rate: no flow (static) Food: not fed	Dose: 90µg/L, 900µg/L Duration: 21d Route: water Sample times: 3

7.2. Comparison of the Grech *et al.*'s model and the BPA PBTK

In the following, fold changes are defined as

$$FC = e^{|\log(Pred) - \log(Obs)|}$$

with Pred the predicted values and Obs the observed values as proposed in Grech *et al.* (2018) to allow comparison between models.

In details, BPA exposure from the literature which were both presented in the cited paper and our work were used. It excludes the intra-peritoneal exposure in Lindholst *et al.* (2001) simulated in Grech *et al.* (2018). It also excludes depuration phase for zebrafish in Lindholst *et al.* (2003) and BPA metabolite TK data as well. As it can be seen the PBTK specific to BPA outperformed the generic PBTK presented in Grech *et al.* (2018). It increased $FC < 3$ by 63% and decreased $FC > 10$ by 25%.

Table S15. Comparison of the generic PBTK presented in Grech *et al.* (2018) and the BPA PBTK

Model	FC < 3	3 < FC < 10	FC > 10
BPA PBTK	31%	35%	34%
PBTK in Grech <i>et al.</i> , 2018	19%	36%	45%

8. Multi-species calibration

Calibration was carried out using a mix of TK data in zebrafish, rainbow trout and three-spined stickleback (original TK dataset). This work was completed to assess the effect of adding the other species on parameters, notably BPA unbound fraction and Michaelis Menten parameters. In addition, a particular attention was given to simulations in trout muscle. Exhaustive results from the calibration are shown in the table S14.

Table S16. Parameter posterior values obtained after monospecific calibration

Chemical	Parameter name	Abbreviation	Unit	Prior distribution*	Posterior distribution	
					MPV**	95% IC
BPA	Unbound fraction	<i>Unbound_fraction</i>	No unit	TN(0.035,0.3,0.001,1)	0.08	0.07;0.09
	Blood:water partition coefficient	<i>PC_blood_water</i>	No unit	Calculated using an intermediate ratio	0.5	0.4;0.6
	Liver:blood partition coefficient	<i>PC_liver</i>	No unit	TN(2.69,0.3,1×10 ⁻⁶ , 1×10 ⁶)	4.1	3.3;5.2
	Gonads:blood partition coefficient	<i>PC_gonads</i>	No unit	TN(5.63,0.3,1×10 ⁻⁶ , 1×10 ⁶)	0.9	0.6;2.0
	Fat:blood partition coefficient	<i>PC_fat</i>	No unit	TN(24.26,0.3, 1×10 ⁻⁶ , 1×10 ⁶)	12.7	6.7;25.6
	Brain:blood partition coefficient	<i>PC_brain</i>	No unit	TN(1.88,0.3, 1×10 ⁻⁶ , 1×10 ⁶)	1.1	0.7;1.8
	Richly perfused:blood partition coefficient	<i>PC_brain</i>	No unit	TN(1.74,0.3, 1×10 ⁻⁶ , 1×10 ⁶)	0.7	0.04 ;2.0
	Poorly perfused:blood partition coefficient	<i>PC_pp</i>	No unit	TN(1.68,0.3, 1×10 ⁻⁶ , 1×10 ⁶)	0.9	0.7;1.1
	Km gluco	<i>Km_gluco</i>	µg/mL	TN(24.3, 0.3, 1×10 ⁻⁶ , 1×10 ⁶)	18.3	10.8;38.7
	Km sulfo	<i>Km_sulfo</i>	µg/mL	TN(7.1,0.3, 1×10 ⁻⁶ , 1×10 ⁶)	6.3	2.7;11.7
	Vmax gluco	<i>Vmax_gluco</i>	µg/d/g	Calculated using an intermediate ratio	1.7×10 ²	64.1; 4.0×10 ²
	Vmax sulfo	<i>Vmax_sulfo</i>	µg/d/g	Calculated using an intermediate ratio	3.1	0.8;34.4
	Plasmatic clearance gluco	<i>Cl_plasma_gluco</i>	mL/d/m L	U(1×10 ⁻⁶ , 1×10 ⁶)	1.6×10 ⁴	1.3×10 ⁴ ;2.1 ×10 ⁴
	Plasmatic clearance sulfo	<i>Cl_plasma_sulfo</i>	mL/d/m L	U(1×10 ⁻⁶ , 1×10 ⁶)	1.4×10 ²	1.1×10 ² ;2.3 ×10 ²
BPA gluc	Liver:blood partition coefficient	<i>PC_liver_gluco</i>	No unit	TN(3.50,0.3,1×10 ⁻¹⁰ , 1×10 ⁶)	1.1	0.7;3.8
	Rob:blood partition coefficient	<i>PC_rob_gluco</i>	No unit	TN(6.30,0.3,1×10 ⁻¹⁰ , 1×10 ⁶)	0.2	0.2;0.4
	Ke bile	<i>Ke_bile_gluco</i>	1/d	U(1×10 ⁻⁶ ,1×10 ⁶)	83.6	54.9;1.1×10 ²
BPA sulf	Liver:blood Partition coefficient	<i>PC_liver_sulfo</i>	No unit	TN(3.80,0.3,1×10 ⁻¹⁰ , 1×10 ⁶)	4.6	2.4;5.7
	Rob:blood Partition coefficient	<i>PC_rob_sulfo</i>	No unit	TN(7.0,0.3,1×10 ⁻¹⁰ , 1×10 ⁶)	0.4	0.3;0.6
	Ke bile	<i>Ke_bile_sulfo</i>	1/d	U(1×10 ⁻⁶ , 1×10 ⁶)	31.7	27.9;1.2×10 ²

8.1. Internal evaluation of the model

On the example of the model calibrated on stickleback data, the model calibrated on mix data was evaluated by comparing simulations of the calibrated data to observations. Overall,

adding the data from the other species improved the fit for zebrafish and rainbow trout. In details, kinetics from Lindholst *et al.* (2001) is presented on Figure S8. However, this calibration resulted also in a poorer fit to stickleback data for BPA concentration in the carcass and blood. This model overpredicted BPA concentrations in the carcass by a three-factor at 10 µg/L (see Figure S8).

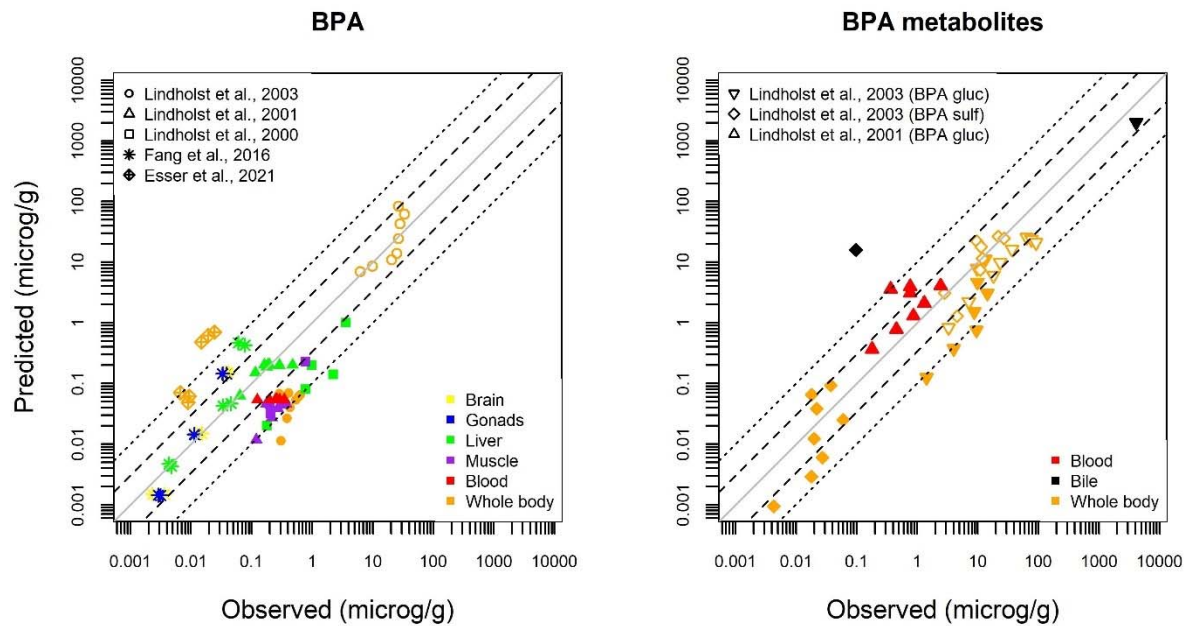


Figure S7. Comparison between BPA, BPA gluc and BPA sulf concentrations measured in zebrafish and rainbow trout and model prediction.

The model was calibrated on data mixing species. Experimental datasets used are indicated in the legend as for the different matrices where concentrations were measured. Uptake is symbolized by the full points. Depuration was measured as normalized whole-body concentrations in Lindholst *et al.* (2003) and are represented by the empty points. The grey line corresponds to the identity line, then the 3-fold range and the 10-fold range.

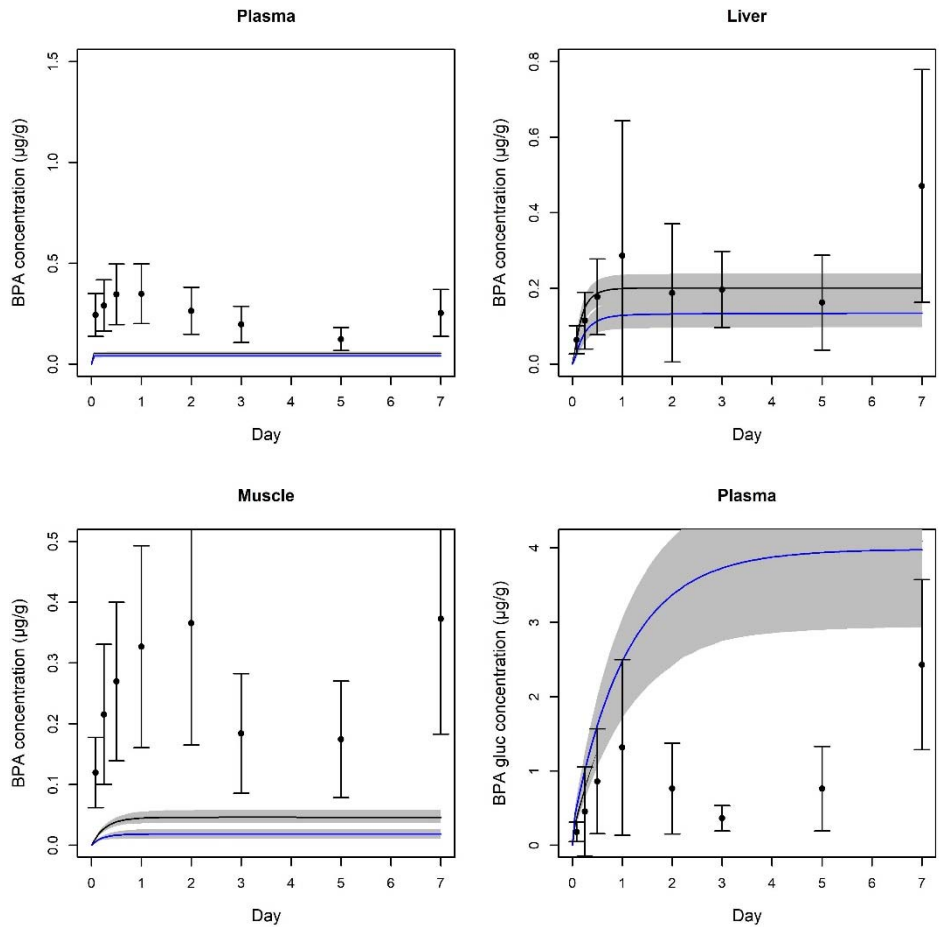


Figure S8. Predicted kinetics in plasma, liver and muscle of rainbow trout by the model calibrated on stickleback data (blue) and calibrated on multi-species data (black) compared to the observation in Lindholm *et al.* (2001).

Predictions are represented by the black solid line (mix) and the blue solid line (SB), respectively. The grey area is the 95% prediction interval computed from the posterior distributions. These 999 simulations were made using every last 333 iterations of each of the three MCMC chains. The dots represent the mean concentration in six fish and the error bar the interval credibility associated to the measurements.

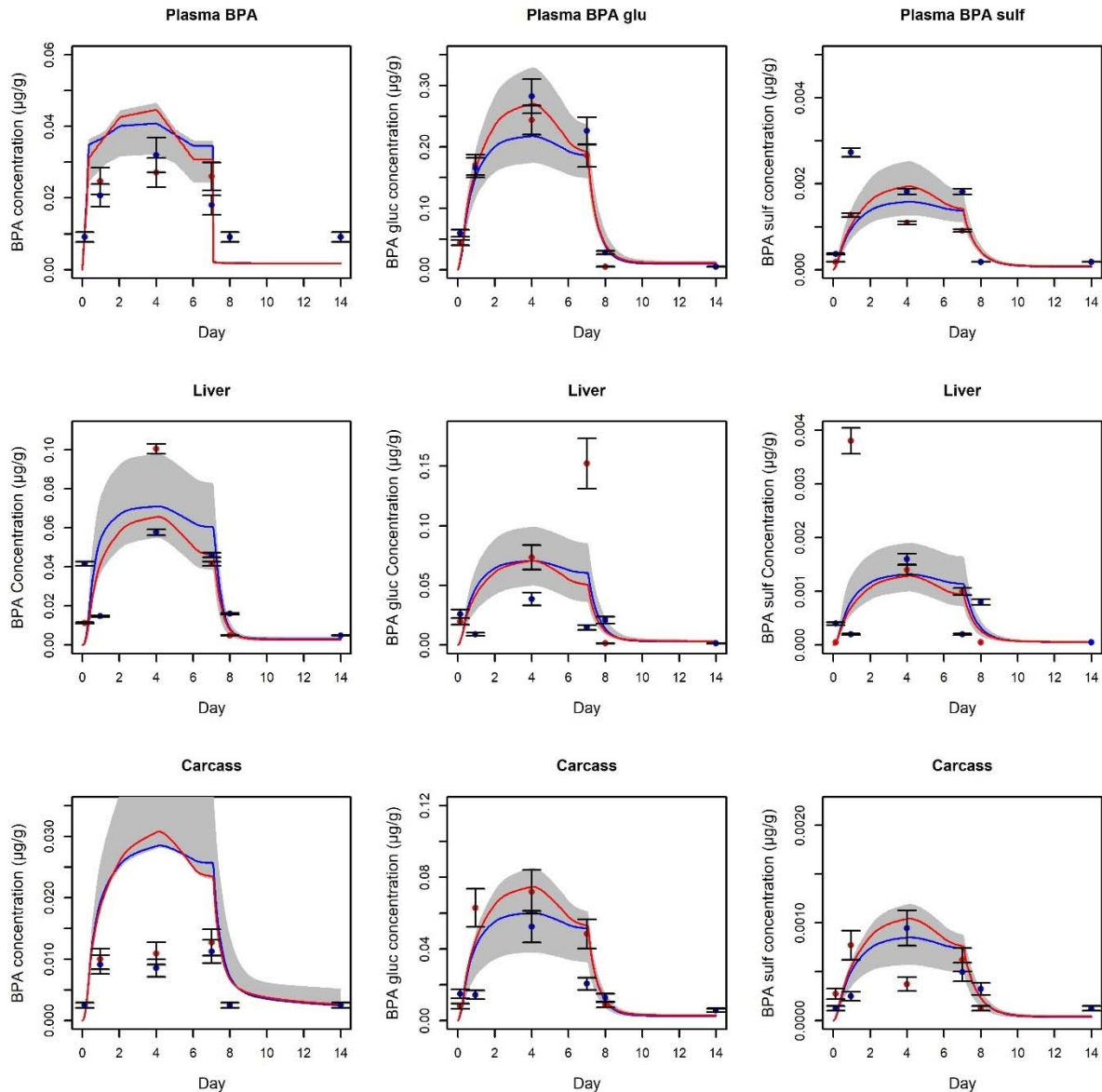


Figure S9. Model simulations in blood, liver and carcass of three-spined stickleback exposed at 10 µg/L after specific data calibration compared to the experimental datapoints.

The model was calibrated on mix data from zebrafish, trout, and stickleback. Concentrations are represented in blue for males, and in red for females. The solid line represents the model predictions and the dots the measured concentration (pool of two fish). The grey area is the 95% prediction interval, computed from the posterior distributions. The simulations were made using the last 333 iterations of the three MCMC chains. Intervals of credibility are build using the estimated precision of measurement for each organ and each compound.

9. MCSim code

9.1. Model code for MCSim

```
####Author : Coarentin Mit
#-----
# (I.) Informations
#-----
#####
# Model BPA
# Base : Vidal - Grech
# Version: XXX
# Update : Hepatic & Plasmatic clearance (BPA gluc and sulf) - ratio_Vmax_Km - ratio_PC_UF
# Date : 02/02/2022
#####
### Units:
##
# Quantity          microg
# Volumes:          mL
# Time:              day
# Flows:             mL/d
# Concentrations:   microg/mL or microg/g
# Vmax:              microg/d/ mL Liver OR microg/d/ g Liver
# Km:               microg/mL
# Masses:            g
# Lenght:           mm
# Temperature:      Celsius
# Ventilation rate: mL/d
# Density of each tissue is considered equal to 1
#####

#-----
# (II.) Model variables
#-----

#-----
# States
#-----

States = {

    L, # Structural length

    #Q_water, # Quantity of BPA in water (microg)
    Q_art, # Quantity of BPA in arterial blood (microg)
    Q_ven, # Quantity BPA in venous blood (microg)
    Q viscera, # ... BPA in viscera (microg)
    Q_lumen_GIT, # ... BPA in lumen (microg)
    Q_gonads, # ... BPA in gonads(microg)
    Q_kidney, # ... BPA in kidney (microg)
    Q_liver, # ... BPA in liver (microg)
    Q_skin, # ... BPA in skin (microg)
    Q_brain, # ... BPA in brain (microg)
    Q_fat, # ... BPA in fat (microg)
    Q_pp, # ... BPA in poorly perfused (microg)
    Q_rp, # ... BPA in richly perfused (microg)

    Q_admin_gills, # ... BPA entering through gills (microg)
    Q_met, # ... BPA metabolized in total (microg)
    Q_excret_feces, # ... BPA fecally excreted (microg)
    Q_excret_gills, # ... BPA excreted by gills (microg)
    Q_bile, # ... BPA in billiary vesicule (microg)
    Q_met_liver_gluc, # ... BPA metabolized in BPAg in liver (microg)
    Q_met_liver_sulfo, # ... BPA metabolized in BPAs in liver (microg)
    Q_met_plasma_gluc, # ... BPA metabolized in BPAg in plasma (microg)
    Q_met_plasma_sulfo, # ... BPA metabolized in BPAg in plasma (microg)
    Q_excret, # Total of BPA quantity excreted (microg)

    # Q_water_gluc, # Quantity of BPA-glucuronide conjugates in water (microg)
    Q_art_gluc, # ... BPA-glucuronide conjugates in arterial blood (microg)
    Q_ven_gluc, # ... BPA-glucuronide conjugates in venous blood (microg)
    Q_lumen_GIT_gluc, # ... BPA-glucuronide conjugates in lumen (microg))
    Q_liver_gluc, # ... BPA-glucuronide conjugates in liver (microg))
    Q_gonads_gluc, # ... BPA-glucuronide conjugates in gonads (microg))
    Q_rob_gluc, # ... BPA-glucuronide conjugates in rest of body (microg))
    Q_abdo_cavity_gluc, # ... BPA-glucuronide conjugates in kidney and viscera (microg))

    Q_excret_gills_gluc, # ... BPA-glucuronide conjugates excreted by gills (microg)
    Q_excret_feces_gluc, # ... BPA-glucuronide conjugates fecally excreted (microg)
    Q_bile_gluc, # ... BPA-glucuronide conjugates in billiary vesicule (microg)
    Q_excret_gluc, # Total of BPA-glucuronide conjugates quantity excreted (microg)

    #Q_water_sulfo, # Quantity of BPA-sulfate conjugates in water (microg)
    Q_art_sulfo, # ... BPA-sulfate conjugates in arterial blood (microg)
    Q_ven_sulfo, # ... BPA-sulfate conjugates in venous blood (microg)
    Q_lumen_GIT_sulfo, # ... BPA-sulfate conjugates in lumen (microg))
    Q_liver_sulfo, # ... BPA-sulfate conjugates in liver (microg))
    Q_gonads_sulfo, # ... BPA-sulfate conjugates in gonads (microg))
    Q_rob_sulfo, # ... BPA-sulfate conjugates in rest of body (microg))
    Q_abdo_cavity_sulfo, # ... BPA-sulfate conjugates in kidney and viscera (microg))

    Q_excret_gills_sulfo, # ... BPA-sulfate conjugates excreted by gills (microg)
    Q_excret_feces_sulfo, # ... BPA-sulfate conjugates fecally excreted (microg)
    Q_bile_sulfo, # ... BPA-sulfate conjugates in billiary vesicule (microg)
    Q_excret_sulfo, # Total of BPA-sulfate conjugates quantity excreted (microg)
```

```

};

#####
#           Outputs
#####

Outputs = {

    C_art,          # ... BPA      in arterial blood (microg.mL-1)
    C_brain, # ... BPA      in brain (microg.mL-1)
    C_ven,         # ... BPA      in venous blood (microg.mL-1)
    C viscera,    # ... BPA      in viscera (microg.mL-1)
    C_gonads, # ... BPA      in gonads(microg.mL-1)
    C_liver, # ... BPA      in liver (microg.mL-1)
    C_skin,       # ... BPA      in skin (microg.mL-1)
    C_fat,        # ... BPA      in fat (microg.mL-1)
    C_pp,         # ... BPA      in pp (microg.mL-1)
    C_rp,         # ... BPA      in rp (microg.mL-1)
    C_carcass,   # ... BPA      in carcass (microg.mL-1)
    C_tot,        # ... BPA      in total (microg.mL-1)
    C_tot_bile, # Total concentration in fish of BPA including the quantity in biliary vesicule (microg.mL-1)

    Q_admin_tot, # ... BPA      absorbed in total (microg)
    Q_elim_tot,  # ... BPA      eliminated in total (microg)
    Q_Body,      # Total of BPA quantity in fish body (microg)

    # C_water_gluc, # Concentration of BPA-glucuronide conjugates in water (microg.mL-1)
    C_art_gluc,    # ... BPA-glucuronide conjugates in arterial blood (microg.mL-1)
1)
    C_ven_gluc,   # ... BPA-glucuronide conjugates in venous blood (microg.mL-1)
    C_gonads_gluc, # ... BPA-glucuronide conjugates in gonads (microg.mL-1)
    C_liver_gluc, # ... BPA-glucuronide conjugates in liver(microg.mL-1)
    C_rob_gluc,   # ... BPA-glucuronide conjugates in rest of fish body
(microg.mL-1)
    C_abdo_cavity_gluc, # ... BPA-glucuronide conjugates in kidney and viscera (microg)
    C_tot_gluc,    # Total concentration of BPA-glucuronide conjugates in fish body (microg.mL-1)
1)
    C_tot_bile_gluc, # Total concentration of BPA-glucuronide conjugates including the quantity in biliary
vesicule.

    # C_water_sulfo, # Concentration of BPA-sulfate conjugates in water (microg.mL-1)
    C_art_sulfo,    # ... BPA-sulfate conjugates in arterial blood (microg.mL-1)
    C_ven_sulfo,   # ... BPA-sulfate conjugates in venous blood (microg.mL-1)
    C_gonads_sulfo, # ... BPA-sulfate conjugates in gonads (microg.mL-1)
    C_liver_sulfo, # ... BPA-sulfate conjugates in liver (microg.mL-1)
    C_rob_sulfo,   # Concentration of BPA-sulfate conjugates in rest of fish body (microg.mL-1)
    C_abdo_cavity_sulfo, # ... BPA-sulfate conjugates in kidney and viscera (microg)
    C_tot_sulfo,   # Total concentration of BPA-sulfate conjugates in fish body (microg.mL-1)
    C_tot_bile_sulfo, # Total concentration in fish of BPA-sulfate conjugates including the quantity in
biliary vesicule.

    #Needed to calibrate excretion in Lindholst 2003
    C_tot_PC,      # Ratio of BPA concentration at time t and at 7d
    C_tot_gluc_PC, # Ratio of BPAG concentration at time t and at 7d
    C_tot_sulfo_PC, # Ratio of BPAs concentration at time t and at 7d

    C_tot_lind,    # Save concentrations of BPA at t = 7d
    C_tot_gluc_lind, # Save concentrations of BPAG at t = 7d
    C_tot_sulfo_lind, # Save concentrations of BPAs at t = 7d

    # Variables computed to evaluate the model
    Mass_Bal,      # Mass balance (microg.mL-1)
    # Mass_Bal_Sys, # Mass balance including quantity in aquarium (microg.mL-1)
    Mass_Bal_gluc, # Mass balance of BPA-glucuronide conjugates(microg.mL-1)
    Mass_Bal_sulfo, # Mass balance of BPA-sulfate conjugate(microg.mL-1)
    BW,            # fish body mass (g)
    Length,       # Physical total length (mm)

    #Other variables
    C_Bisphenol,  # Concentration of bisphenol all forms take into account.

};

#####
#           Inputs
#####

Inputs = {
    Temperature, # Water temperature expressed in degree Celsius
    C_water,     # Concentration of BPA chemical in water (microg.mL-1)
    V_water,     # Volume of aquarium (mL)
    Bw_i,        # Initial mass of fish (g)
    ivQuantity,  # Intravenous quantity (µg)
    f_cst,       # food level 1 = ad-libitum, 0= starvation
    event_bile}; #<input variable> = NDoses(<n>, <list-of-magnitudes>, <list-of-initial-times>);

#####
# (III) Model parameters
#####

#-----
# Physiological parameters
#-----
Bw_Pcard_ref      ;# Body weight of reference for F_card
Bw_VO2_ref        ;# Body weight of reference for VO2 from Macleod, 1996
DEB_V             ;# Energy conductance (mm/d) (DEB model parameter)
DEB_g             ;# Energy investment ratio (SU) (DEB model parameter)
DEB_KM            ;# Somatic maintenance rate coefficient (1/d) (DEB model parameter)
DEB_EHm           ;# Energy at State of maturity at metamorphosis (J)
DEB_EHb           ;# Energy at State of maturity at birth (J)

```

```

DEB_shape ;
a_BW_L ;# a relation BW(g)=F(L(cm))
b_BW_L ;# b relation BW(g)=F(L(cm))

#-----
# Environmental condition
#-----
TA ;# Arrhenius temperature in Kelvin
TR_excretion ;# Arrhenius reference temperature for the excretion processes (Kelvin)
TR_DEB ;# Arrhenius reference temperature for the DEB model(Kelvin)
TR_Fcard ;# Arrhenius reference temperature for cardiac output(Kelvin) -> temperature optimal : 25 C
TR_VO2 ;# Arrhenius reference temperature for respiration(Kelvin)

#-----
# Effective respiratory volume & cardiac output
#-----
F_card_ref ;# Qb_ref_RT * (Bw_ref^(0.75)) / Bw_ref # (mL/d/g) = 28.5 * (7.66^(0.75)) / 7.66 --> allometric
scaling function
V_O2_ref ;# reference oxygen consumption rate (mg/kg/min) --> 2.236044 * 60 * 24 / 1000 mg/g/d from MacLoed, 1966
O2_EE ;# Oxygen extraction efficiency of 71% proposed by Erickson, 1990
Sat ;# dissolved oxygen saturation of 90% proposed by Erickson, 1990
frac_art_ven = (1.0/3.0); # fraction of arterial blood

#-----
# volume scaling factor : fraction of BW (%)
#-----
sc_blood ;# volume scaling factor, expressed in % BW (g)
sc_gonads ;
sc_brain ;
sc_liver ;
sc_fat ;
sc_skin ;
sc viscera ;
sc_kidney ;
sc_rp ;
sc_pp ;

#-----
# Fraction of arterial blood flow
#-----
frac_gonads ;# Fraction of arterial blood flow
frac_brain ;
frac_liver ;
frac_fat ;
frac_skin ;
frac viscera ;
frac_kidney ;
frac_rp ;
frac_pp ;

a_Fpp = 0.4 ;# Fraction of PPT blood going to venous
a_Fs = 0.1 ;# Fraction of skin blood going to venous

plasma ;# Plasma fraction 1 - Haematocrit

#-----
# Exposure quantity (microg)
#-----
WaterQuantity ;
ivQuantity ;

#-----
# Chemical parameters
#-----
Unbound_fraction ; # between 0 and 1
Unbound_fraction_gluco ; # between 0 and 1
Unbound_fraction_sulfo ; # between 0 and 1

#-----
# Partition coefficient (PC QSAR in .R, need adaptation to organ compositions )
#-----
PC_blood_water ; # Partition coef blood water for BPA
PC_liver ; # Partition coef liver ""
PC_gonads ; # Partition coef gonade ""
PC viscera ; # Partition coef viscera ""
PC_fat ; # Partition coef fat for ""
PC_kidney ; # Partition coef kidney ""
PC_skin ; # Partition coef skin ""
PC_brain ; # Partition coef brain ""
PC_rp ; # partition coef rp ""
PC_pp ; # partition coef pp ""

#PC_blood_water_gluco ; # Partition coef blood water for BPA-G
PC_liver_gluco ;
PC_gonads_gluco ;
PC_abdo_cavity_gluco ;
PC_rob_gluco ;

#PC_blood_water_sulfo ; # Partition coef blood water for BPA-S
PC_liver_sulfo ;
PC_gonads_sulfo ;
PC_abdo_cavity_sulfo ;
PC_rob_sulfo ;

#-----
# Metabolism (based on prot.tot in stickleback)
#-----
Km_gluco ;# microg/ml #ohkimoto 2003
Vmax_gluco ;# microg/d/mL liver #ohkimoto 2003

Km_sulfo ;# microg/ml #ohkimoto 2003
Vmax_sulfo ;# microg/d/mL liver #ohkimoto 2003

```

```

#Cl_liver_gluco ; # mL/d/g liver
#Cl_liver_sulfo ; # mL/d/g liver

Cl_plasma_gluco ; # mL/d/mL blood
Cl_plasma_sulfo ; # mL/d/mL blood

#-----
# Excretion
#-----

K_BG ; # Excreted flow from biliary vesicle to faeces (1/d)
Ke_bile ; # Excreted flow of BPA from liver to biliary vesicle (1/d)
Ke_bile_gluco ; # Excreted flow of BPA-G from liver to biliary vesicle (1/d)
Ke_bile_sulfo ; # Excreted flow of BPA-S from liver to biliary vesicle (1/d)

#-----
# Feces and urination
#-----
Ke_feces = 0.83 ; # 1/d estimated from Nichols et al. 2004
urine_rate = 0.05794769 ; # V_burst = 1.2 mL.kg-1 every 29.82 minutes proposed by Curtis 1991 -->
1.2e-03 mL.g BW-1?

#-----
# Other parameters that will be computed in Initialize
#-----
Conv_gluco = (404/228.29); # ratio molar mass BPA-G/BPA
Conv_sulfo = (308/228.29); # ratio molar mass BPA-S/BPA
water_content_blood ; # Bertelsen 1998 in trout
C_tot_lind ; #ug/g
C_tot_gluco_lind ; #ug/g
C_tot_sulfo_lind ; #ug/g
Abs_eff ; #Gills absorption efficiency (0-1)
Ratio_PC_UF;
#Ratio_PC_UF_gluco;
#Ratio_PC_UF_sulfo;
Ratio_Vmax_Km_gluco;
Ratio_Vmax_Km_sulfo;

#####
# (IV) Model initialization
#####
Initialize {

    sc_pp = (1 - sc_blood - sc_gonads - sc_brain - sc_liver - sc_fat
             - sc_skin - sc viscera - sc_kidney -sc_rp);

    frac_pp = (1 - frac_gonads - frac_brain - frac_liver - frac_fat
              - frac_skin - frac viscera - frac_kidney - frac_rp);

    Q_ven = ivQuantity;

    L = pow((Bw_i/ a_BW_L), (1/b_BW_L)) * DEB_shape * 10;

    PC_blood_water = Unbound_fraction * Ratio_PC_UF ;
    #PC_blood_water_gluco = Unbound_fraction_gluco * Ratio_PC_UF_gluco ;
    #PC_blood_water_sulfo = Unbound_fraction_sulfo * Ratio_PC_UF_sulfo ;

    Vmax_gluco = Km_gluco * Ratio_Vmax_Km_gluco ;
    Vmax_sulfo = Km_sulfo * Ratio_Vmax_Km_sulfo ;

} # End of initialize

#####
# (V) ODE equations
#####
Dynamics {

    #Set temperature
    TC_k = Temperature + 273.15; # (degree K)
    TC_c = Temperature; # (degree C)

    # body weight : DEB growth model anisomorphic
    KT_Arrhenius = exp((TA / TR_DEB) - (TA / TC_k));
    DEB_V_t = DEB_V * KT_Arrhenius ;
             # mm/d
    DEB_Lm = DEB_V / (DEB_KM * DEB_g);
             # mm
    DEB_M = pow((DEB_EHm / DEB_EHb), (1.0/3.0));
             # EHm and EHb = J

    dt(L) = (DEB_V_t / (3 * (f_cst + DEB_g))) * (f_cst * DEB_M - (L/DEB_Lm));
    BW = a_BW_L * pow((L/10)/DEB_shape), (b_BW_L));
             # BW = g; a = g/cm; L = mm --> /10 = cm

    #Volumes (mL or g) of the organs changing with the time
    V_art = sc_blood * BW * frac_art_ven * plasma; #BPA in plasma fraction
    V_ven = sc_blood * BW * (1-frac_art_ven) * plasma; #BPA in plasma fraction

    V_liver = sc_liver * BW;
    V_gonads = sc_gonads * BW;
    V viscera = sc viscera * BW;
    V_kidney = sc_kidney * BW;
    V_skin = sc_skin * BW;
    V_brain = sc_brain * BW;
    V_fat = sc_fat * BW;
    V_rp = sc_rp * BW;

```



```

V_pp = sc_pp * BW;

# Blood flow (mL/d)
F_card_g = F_card_ref * exp((TA / TR_Fcard) - (TA / TC_k)) * pow((BW/Bw_Fcard_ref),(-0.1)); # cardiac output =
mL/d/g
F_card = F_card_g * BW * plasma; # mL/d of plasma flow

# Flows to tissues corrected with the UF
F_liver = frac_liver * F_card * Unbound_fraction;
F_gonads = frac_gonads * F_card * Unbound_fraction;
F viscera = frac viscera * F_card * Unbound_fraction;
F_kidney = frac_kidney * F_card * Unbound_fraction;
F_skin = frac_skin * F_card * Unbound_fraction;
F_fat = frac_fat * F_card * Unbound_fraction;
F_brain = frac_brain * F_card * Unbound_fraction;
F_rp = frac_rp * F_card * Unbound_fraction;
F_pp = frac_pp * F_card * Unbound_fraction;

F_liver_gluco = frac_liver * F_card * Unbound_fraction_gluco;
F_gonads_gluco = frac_gonads * F_card * Unbound_fraction_gluco;
F_abdo_cavity_gluco = (frac_kidney + frac viscera) * F_card * Unbound_fraction_gluco;
F_rob_gluco = (1-(frac_liver + frac_kidney + frac_gonads + frac viscera))* F_card *
Unbound_fraction_gluco;

F_liver_sulfo = frac_liver * F_card * Unbound_fraction_sulfo;
F_gonads_sulfo = frac_gonads * F_card * Unbound_fraction_sulfo;
F_abdo_cavity_sulfo = (frac_kidney + frac viscera) * F_card * Unbound_fraction_sulfo;
F_rob_sulfo = (1-(frac_liver+ frac_kidney + frac_gonads + frac viscera))* F_card *
Unbound_fraction_sulfo;

# Effective respiratory volume (mL/d)
V_O2_g = V_O2_ref * exp((TA / TR_VO2) - (TA / TC_k)) * pow((BW/Bw_VO2_ref),(-0.1)); #mg
O2/d/g
V_O2 = V_O2_g * BW ; # mg
O2/d
C_O2_water = ((-0.24 * TC_c + 14.04) * Sat )/1000 ; # mg O2/mL
F_water = V_O2/ (O2_EE * C_O2_water) ; # mL/d
Kx = F_water ; #Kx = (tmp < F_water ? tmp : F_water) ;

##### BPA Concentrations in tissues (microg/g = microg/mL) #####
C_art = Q_art / V_art;
C_ven = Q_ven / V_ven;
C_liver = Q_liver / V_liver;
C_gonads = Q_gonads / V_gonads;
C viscera = Q viscera / V viscera;
C_kidney = Q_kidney / V_kidney;
C_fat = Q_fat / V_fat;
C_brain = Q_brain / V_brain;
C_skin = Q_skin / V_skin;
C_rp = Q_rp / V_rp;
C_pp = Q_pp / V_pp;

C_tot = ((Q_art + Q_ven + Q_liver + Q_gonads + Q_skin + Q viscera + Q_kidney + Q_brain + Q_fat + Q_rp
+ Q_pp)
/ (V_art + V_ven + V_liver + V_gonads + V_skin + V viscera +
V_kidney + V_brain + V_fat + V_rp + V_pp));

C_tot_bile = C_tot + (Q_bile/BW); # C_tot_bile with/without Q_bile/BW
C_carcass = ( Q_skin + Q_brain + Q_fat + Q_rp + Q_pp) / (V_skin + V_brain + V_fat + V_rp + V_pp);

##### BPA-g Concentrations in tissues (microg/g = microg/mL) #####
C_art_gluco = Q_art_gluco / V_art;
C_ven_gluco = Q_ven_gluco / V_ven;
C_liver_gluco = Q_liver_gluco / V_liver;
C_abdo_cavity_gluco = Q_abdo_cavity_gluco/ (V viscera + V_kidney);
C_gonads_gluco = Q_gonads_gluco / V_gonads ;
C_rob_gluco = Q_rob_gluco / (V_skin + V_brain + V_fat + V_rp + V_pp);
C_tot_gluco = ((Q_liver_gluco + Q_art_gluco + Q_ven_gluco + Q_rob_gluco +
Q_abdo_cavity_gluco + Q_gonads_gluco)
/ (V_art + V_ven + V_liver + V_gonads + V_skin
+ V viscera + V_kidney + V_brain + V_fat + V_rp + V_pp));
C_tot_bile_gluco = C_tot_gluco + (Q_bile_gluco/BW);

##### BPA-s Concentrations in tissues (microg/g = microg/mL) #####
C_art_sulfo = Q_art_sulfo / V_art;
C_ven_sulfo = Q_ven_sulfo / V_ven;
C_liver_sulfo = Q_liver_sulfo / V_liver;
C_abdo_cavity_sulfo = Q_abdo_cavity_sulfo/ (V viscera + V_kidney);
C_gonads_sulfo = Q_gonads_sulfo / V_gonads ;
C_rob_sulfo = Q_rob_sulfo / ( V_skin + V_brain + V_fat + V_rp + V_pp);
C_tot_sulfo = ((Q_liver_sulfo + Q_art_sulfo + Q_ven_sulfo + Q_rob_sulfo +
Q_abdo_cavity_sulfo + Q_gonads_sulfo )
/ (V_art + V_ven + V_liver + V_gonads + V_skin
+ V viscera + V_kidney + V_brain + V_fat + V_rp + V_pp));
C_tot_bile_sulfo = C_tot_sulfo + (Q_bile_sulfo/BW);

##### BPA and metabolite concentration in the water : exposure --> microg/g = microg/mL #####
# C_water = Q_water / V_water;
# C_water_gluco = Q_water_gluco / V_water;
# C_water_sulfo = Q_water_sulfo / V_water;

##### Scaling clearance and excretion constant#####
#Scaling Cl to blood volume
Cl_sc_plasma_gluco = Cl_plasma_gluco * V_ven * Unbound_fraction ;
Cl_sc_plasma_sulfo = Cl_plasma_sulfo * V_ven * Unbound_fraction ;

#Scaling Vmax/Cl to liver volume
Vmax_sc_gluco = Vmax_gluco * V_liver;
Vmax_sc_sulfo = Vmax_sulfo * V_liver;
#Cl_sc_liver_gluco = Cl_liver_gluco * V_liver;

```

```

#Cl_sc_liver_sulfo = Cl_liver_sulfo * V_liver;

#Temperature correction
Ke_feces_t = Ke_feces * exp((TA / TR_excretion) - (TA / TC_k));
Ke_bile_t = Ke_bile * exp((TA / TR_excretion) - (TA / TC_k));
Ke_bile_gluco_t = Ke_bile_gluco * exp((TA / TR_excretion) - (TA / TC_k));
Ke_bile_sulfo_t = Ke_bile_sulfo * exp((TA / TR_excretion) - (TA / TC_k));

##### BPA Metabolism #####

#BPA to BPA-g
dt(Q_met_liver_gluco) = (Vmax_sc_gluco *(C_liver/PC_liver) )/(Km_gluco + (C_liver/PC_liver) );
dt(Q_met_plasma_gluco) = Cl_sc_plasma_gluco * C_ven ;
#dt(Q_met_liver_gluco) = Cl_sc_liver_gluco * (C_liver/PC_liver);

#BPA to BPA-s
dt(Q_met_liver_sulfo) = (Vmax_sc_sulfo *(C_liver/PC_liver) )/(Km_sulfo + (C_liver/PC_liver) );
dt(Q_met_plasma_sulfo) = Cl_sc_plasma_sulfo * C_ven ;
#dt(Q_met_liver_sulfo) = Cl_sc_liver_gluco * (C_liver/PC_liver);

#BPA total metabolized
dt(Q_met) = dt(Q_met_liver_gluco) + dt(Q_met_plasma_gluco) + dt(Q_met_plasma_sulfo) + dt(Q_met_liver_sulfo);

##### BPA Excretion #####
dt(Q_bile) = (Ke_bile_t * Q_liver * Unbound_fraction) - event_bile * K_BG * Q_bile ;

dt(Q_excret_gills) = Kx * (Unbound_fraction * C_ven / PC_blood_water);#fixed to 0 in model 1 and 2
dt(Q_lumen_GIT) = ( - Q_lumen_GIT * Ke_feces_t + event_bile * K_BG * Q_bile );
dt(Q_excret_feces) = Q_lumen_GIT * Ke_feces_t;
dt(Q_excret) = dt(Q_excret_feces) + dt(Q_excret_gills) ;

##### BPA-G Excretion #####
dt(Q_bile_gluco) = (Ke_bile_gluco_t * Q_liver_gluco * Unbound_fraction_gluco) - event_bile *
K_BG * Q_bile_gluco ;

dt(Q_lumen_GIT_gluco) = ( - Q_lumen_GIT_gluco * Ke_feces_t + event_bile * K_BG * Q_bile_gluco );
dt(Q_excret_feces_gluco) = Q_lumen_GIT_gluco * Ke_feces_t;
dt(Q_excret_gills_gluco) = 0.0; #fixed to 0 in model 1
dt(Q_excret_gluco) = dt(Q_excret_feces_gluco)+ dt(Q_excret_gills_gluco) ;

##### BPA-S Excretion #####
dt(Q_bile_sulfo) = (Ke_bile_sulfo_t * Q_liver_sulfo * Unbound_fraction_sulfo) - event_bile *
K_BG * Q_bile_sulfo;

dt(Q_lumen_GIT_sulfo) = ( - Q_lumen_GIT_sulfo * Ke_feces_t + event_bile * K_BG * Q_bile_sulfo );
dt(Q_excret_feces_sulfo) = Q_lumen_GIT_sulfo * Ke_feces_t;
dt(Q_excret_gills_sulfo) = 0.0;#fixed to 0 in model 1
dt(Q_excret_sulfo) = dt(Q_excret_feces_sulfo)+ dt(Q_excret_gills_sulfo) ;

##### BPA absorbed : differentials in microg/d #####
dt(Q_admin_gills) = Abs_eff * Kx * C_water; ###Gills

##### BPA Blood quantity #####

dt(Q_art) = (F_card * C_ven * Unbound_fraction
- F_liver * C_art
- F_kidney * C_art
- F viscera * C_art
- F_gonads * C_art
- F_skin * C_art
- F_fat * C_art
- F_brain * C_art
- F_rp * C_art
- F_pp * C_art);

dt(Q_ven) = (F_brain * C_brain/PC_brain
+ (F_liver + F_gonads + F viscera + F_rp) * C_liver/PC_liver
+ F_fat * C_fat/PC_fat
+ (F_kidney + ((1 - a_Fpp) * F_pp)
+ ((1 - a_Fs) * F_skin) ) * (C_kidney / PC_kidney)
+ a_Fpp * F_pp * (C_pp / PC_pp)
+ a_Fs * F_skin * (C_skin / PC_skin)
- F_card * C_ven * Unbound_fraction
+ dt(Q_admin_gills)
- dt(Q_excret_gills)
- dt(Q_met_plasma_gluco)
- dt(Q_met_plasma_sulfo));

##### BPA Quantity in tissues #####

dt(Q_gonads) = F_gonads * (C_art - C_gonads/PC_gonads) ;
dt(Q_skin) = F_skin * (C_art - C_skin /PC_skin) ;
dt(Q_fat) = F_fat * (C_art - C_fat /PC_fat) ;
dt(Q_rp) = F_rp * (C_art - C_rp /PC_rp) ;
dt(Q_pp) = F_pp * (C_art - C_pp /PC_pp) ;
dt(Q_brain) = F_brain * (C_art - C_brain /PC_brain) ;

dt(Q_liver) = ( F_liver * C_art
+ F_rp *(C_rp /PC_rp )
+ F viscera *(C viscera /PC viscera )
+ F_gonads *(C_gonads /PC_gonads )
- ( F_liver + F_rp + F viscera + F_gonads ) *(C_liver /PC_liver )
- Ke_bile_t * Q_liver * Unbound_fraction
- dt(Q_met_liver_gluco)
- dt(Q_met_liver_sulfo));

dt(Q_kidney) = ( F_kidney * C_art
+ (1-a_Fpp) * F_pp * (C_pp / PC_pp )
+ (1-a_Fs) * F_skin * (C_skin / PC_skin )
- (F_kidney + (1-a_Fpp) * F_pp + (1-a_Fs) * F_skin) * (C_kidney /
PC_kidney ));

dt(Q viscera) = F viscera*(C_art - C viscera /PC viscera );

```

```

##### BPA-g Quantity in tissues #####
dt(Q_art_glucu) = ( F_card * C_ven_glucu * Unbound_fraction_glucu - F_liver_glucu * C_art_glucu - F_rob_glucu *
C_art_glucu - F_gonads_glucu * C_art_glucu - F_abdo_cavity_glucu * C_art_glucu);

dt(Q_ven_glucu) = ((F_liver_glucu + F_gonads_glucu) * (C_liver_glucu/PC_liver_glucu))
+ (F_rob_glucu * (C_rob_glucu/PC_rob_glucu))
+ (F_abdo_cavity_glucu *
(C_abdo_cavity_glucu/PC_abdo_cavity_glucu))
- F_card * C_ven_glucu * Unbound_fraction_glucu
- dt(Q_excret_gills_glucu)
+ (Conv_glucu * dt(Q_met_plasma_glucu));

dt(Q_liver_glucu) = (dt(Q_met_liver_glucu) * Conv_glucu)
+ F_liver_glucu * C_art_glucu
+ F_gonads_glucu * (C_gonads_glucu /PC_gonads_glucu )
- (F_liver_glucu + F_gonads_glucu) * (C_liver_glucu /PC_liver_glucu
)
- Ke_bile_glucu_t * Q_liver_glucu * Unbound_fraction_glucu;

dt(Q_rob_glucu) = F_rob_glucu * (C_art_glucu - (C_rob_glucu/PC_rob_glucu));
dt(Q_gonads_glucu) = F_gonads_glucu * (C_art_glucu - (C_gonads_glucu/PC_gonads_glucu));
dt(Q_abdo_cavity_glucu) = F_abdo_cavity_glucu * (C_art_glucu - (C_abdo_cavity_glucu/PC_abdo_cavity_glucu));

##### BPA-s Quantity in tissues #####
dt(Q_art_sulfo) = ( F_card * C_ven_sulfo * Unbound_fraction_sulfo - F_liver_sulfo * C_art_sulfo - F_rob_sulfo
*C_art_sulfo - F_abdo_cavity_sulfo * C_art_sulfo - F_gonads_sulfo * C_art_sulfo);

dt(Q_ven_sulfo) = ((F_liver_sulfo + F_gonads_sulfo) * (C_liver_sulfo/PC_liver_sulfo))
+ (F_rob_sulfo * (C_rob_sulfo/PC_rob_sulfo))
+ (F_abdo_cavity_sulfo *
(C_abdo_cavity_sulfo/PC_abdo_cavity_sulfo))
- F_card * C_ven_sulfo * Unbound_fraction_sulfo
- dt(Q_excret_gills_sulfo)
+ (Conv_sulfo * dt(Q_met_plasma_sulfo));

dt(Q_liver_sulfo) = (dt(Q_met_liver_sulfo) * Conv_sulfo)
+ F_liver_sulfo * C_art_sulfo
+ F_gonads_sulfo * (C_gonads_sulfo /PC_gonads_sulfo )
- (F_liver_sulfo +F_gonads_sulfo) * (C_liver_sulfo /PC_liver_sulfo
)
- Ke_bile_sulfo_t * Q_liver_sulfo * Unbound_fraction_sulfo;

dt(Q_rob_sulfo) = F_rob_sulfo * (C_art_sulfo - (C_rob_sulfo/PC_rob_sulfo));
dt(Q_gonads_sulfo) = F_gonads_sulfo * (C_art_sulfo - (C_gonads_sulfo/PC_gonads_sulfo));
dt(Q_abdo_cavity_sulfo) = F_abdo_cavity_sulfo * (C_art_sulfo - (C_abdo_cavity_sulfo/PC_abdo_cavity_sulfo));

##### Chemical kinetic in aquarium water #####
#dt(Q_water) = (dt(Q_excret) - dt(Q_elim_water) - dt(Q_admin_gills));
#dt(Q_elim_water) = Ke_water * Q_water ;
#dt(Q_water_glucu) = dt(Q_excret_glucu) ;
#dt(Q_water_sulfo) = dt(Q_excret_sulfo) ;

##### Save concentrations of BPA, BPAg and BPAs at t = 7d #####
C_tot_lind = (t == 7 ? C_tot_bile : C_tot_lind);
C_tot_glucu_lind = (t == 7 ? C_tot_bile_glucu : C_tot_glucu_lind);
C_tot_sulfo_lind = (t == 7 ? C_tot_bile_sulfo : C_tot_sulfo_lind);

} # End of Dynamics

CalcOutputs{

#calibration with log(prediction)
C_tot = (C_tot < 0 ? 1E-12 : C_tot);
C_tot_bile = (C_tot_bile < 0 ? 1E-12 : C_tot_bile);

C_tot_glucu = (C_tot_glucu < 0 ? 1E-12 : C_tot_glucu);
C_tot_bile_glucu = (C_tot_bile_glucu < 0 ? 1E-12 : C_tot_bile_glucu);

C_tot_sulfo = (C_tot_sulfo < 0 ? 1E-12 : C_tot_sulfo);
C_tot_bile_sulfo = (C_tot_bile_sulfo < 0 ? 1E-12 : C_tot_bile_sulfo);

C_brain = (C_brain < 0 ? 1E-10 : C_brain);
C_gonads = (C_gonads < 0 ? 1E-10 : C_gonads);
C_pp = (C_pp < 0 ? 1E-10 : C_pp);

C_art = (C_art < 0 ? 1E-10 : C_art);
C_liver = (C_liver < 0 ? 1E-10 : C_liver);
C_carcass = (C_carcass < 0 ? 1E-10 : C_carcass);

C_art_glucu = (C_art_glucu < 0 ? 1E-10 : C_art_glucu);
C_liver_glucu = (C_liver_glucu < 0 ? 1E-10 : C_liver_glucu);
C_rob_glucu = (C_rob_glucu < 0 ? 1E-10 : C_rob_glucu);

C_art_sulfo = (C_art_sulfo < 0 ? 1E-10 : C_art_sulfo);
C_liver_sulfo = (C_liver_sulfo < 0 ? 1E-10 : C_liver_sulfo);
C_rob_sulfo = (C_rob_sulfo < 0 ? 1E-10 : C_rob_sulfo);

#Needed to calibrate excretion in Lindholst 2003
C_tot_PC = (C_tot_lind >1E-12 ? C_tot_bile/ C_tot_lind : 1E-12);
C_tot_glucu_PC = (C_tot_glucu_lind >1E-12 ? C_tot_bile_glucu/ C_tot_glucu_lind : 1E-12);
C_tot_sulfo_PC = (C_tot_sulfo_lind >1E-12 ? C_tot_bile_sulfo/ C_tot_sulfo_lind : 1E-12);

# Mass-balance

Length = L/DEB_shape ; # physical length (mm)

```

```

    Q_Body                = (Q_art + Q_ven + Q_liver + Q_gonads + Q_brain + Q_fat + Q_skin + Q_kidney +
Q_viscera + Q_pp + Q_rp );

    Q_admin_tot          = Q_admin_gills + ivQuantity ; # amount entering body

    Q_elim_tot           = Q_excret + Q_met;

    Mass_Bal             = Q_admin_tot - Q_Body - Q_elim_tot ;
    # Mass_Bal_Sys       = (Q_admin_tot - Q_admin_gills) - Q_Body - ( Q_elim_tot - Q_excret) - Q_water ;

    Mass_Bal_gluco       = (Q_met_plasma_gluco + Q_met_liver_gluco) * Conv_gluco -
(Q_liver_gluco+Q_rob_gluco+Q_art_gluco+Q_ven_gluco + Q_lumen_GIT_gluco + Q_bile_gluco + Q_gonads_gluco + Q_abdo_cavity_gluco)
- Q_excret_gluco ;
    Mass_Bal_sulfo       = (Q_met_liver_sulfo + Q_met_plasma_sulfo) * Conv_sulfo -
(Q_liver_sulfo+Q_rob_sulfo+Q_art_sulfo+Q_ven_sulfo + Q_lumen_GIT_sulfo + Q_bile_sulfo + Q_gonads_sulfo + Q_abdo_cavity_sulfo)
- Q_excret_sulfo ;

    C_Bisphenol          = (C_tot_bile + C_tot_bile_gluco + C_tot_bile_sulfo);
} # End of CalcOutputs
End.

```

9.2. MCMC code for MCSim

```

### MCMC
### Substance : BPA

### Units:
# Quantity          microg
# Volumes:          mL
# Time:              d
# Flows:             mL/d
# Concentrations:   microg/mL
# Vmax:              microg/d/ mL Liver
# Km:                microg/mL
# Masses:            g
# Lenght:            mm
# Temperature:       Celsius
# Ventilation rate: mL/d

# Authors : Corentin Mit
# Date : 01/2022
#=====

Integrate( Lsodes, 1e-8, 1e-10, 1);

MCMC ("Stickleback_MCMC1.out", # output file
     "", # name of restart file
     "", # name of data file
     20000, 0, # iterations, print predictions flag,
     1, 20000, # printing frequency, iters to print
     578878); # random seed

# LQ_BPA_Liv = 0.005 ; #µg/g = 10E-3/2
# LQ_BPA_S_Liv = 5e-05 ; #µg/g = 0.1E-3/2
# LQ_BPA_G_Liv = 0.0015 ; #µg/g = 3E-3/2

# LQ_BPA_Blood = 0.005 ; #µg/g =10E-3/2
# LQ_BPA_S_Blood = 1E-04 ; #µg/g = 0.2E-3/2
# LQ_BPA_G_Blood = 0.0025 ; #µg/g --> 5E-3/2

# LQ_BPA_rob = 0.01 ; #µg/g =20E-3/2
# LQ_BPA_S_rob = 5E-04 ; #µg/g = 1E-3/2
# LQ_BPA_G_rob = 0.005 ; #µg/g --> 10E-3/2

Level{# global

#A priori parameter distributions
Distrib (Unbound_fraction, TruncNormal_cv, 0.035, 0.3, 1E-3, 1);
Unbound_fraction_gluco = 0.95 ; # between 0 and 1
Unbound_fraction_sulfo = 0.95 ; # between 0 and 1

# Km est en µmol/mL et Vmax en µg/jour/g de foie
Distrib (Km_gluco, TruncNormal_cv, 24.3, 0.3,1E-6, 1E6);
Distrib (Km_sulfo, TruncNormal_cv, 7.1,0.3,1E-6, 1E6);
Distrib (Ratio_Vmax_Km_gluco, TruncNormal_cv, 8.6,0.3,1E-6, 1E8);
Distrib (Ratio_Vmax_Km_sulfo, TruncNormal_cv, 17070,0.3,1E-6, 1E8);

Distrib (Cl_plasma_gluco, Uniform, 1E-6, 1E6);
Distrib (Cl_plasma_sulfo, Uniform, 1E-6, 1E6);

#Cl_plasma_gluco=0.0;
#Cl_plasma_sulfo=0.0;

Distrib (Ratio_PC_UF, TruncNormal_cv, 1681, 0.3, 1E-6, 1E6);
Distrib (PC_liver, TruncNormal_cv,2.692620,0.3,1E-6, 1E6);
Distrib (PC_gonads, TruncNormal_cv, 5.627369,0.3,1E-6, 1E6);
PC_viscera = 1.126653 ; # Partition coef viscera for BPA
Distrib (PC_fat,TruncNormal_cv,24.26,0.3,1E-6, 1E6);
PC_kidney = 4.250372 ; # Partition coef kidney for BPA
PC_skin = 1.187787 ; # Partition coef skin for BPA
PC_brain = 1.877079 ; # Partition coef skin for BPA
Distrib (PC_rp,TruncNormal_cv,1.737972,0.3,1E-6, 1E6);
Distrib (PC_pp,TruncNormal_cv,1.679407,0.3,1E-6, 1E6);

Distrib (PC_liver_gluco, TruncNormal_cv, 3.5, 0.3, 1E-10, 1E6);
Distrib (PC_rob_gluco, TruncNormal_cv, 6.3, 0.3, 1E-10, 1E6);
PC_abdo_cavity_gluco = 6.89;

```

```

PC_gonads_gluco = 6.92;
Distrib (Ke_bile_gluco, Uniform, 1E-6, 1E6);

Distrib (PC_liver_sulfo, TruncNormal_cv, 3.8, 0.3, 1E-10, 1E6);
Distrib (PC_rob_sulfo, TruncNormal_cv, 7.0, 0.3, 1E-10, 1E6);
PC_abdo_cavity_sulfo = 7.46;
PC_gonads_sulfo = 7.28;
Distrib (Ke_bile_sulfo, Uniform, 1E-6, 1E6);

K_BG = 1E10 ; # Excreted flow from biliary vesicle to faeces (1/d)
Ke_bile = 1E-12 ; # Excreted flow of BPA from liver to biliary vesicle (1/d)

Abs_eff = 1.0;
plasma = 0.55 ; # Stickleback https://doi.org/10.1242/jeb.065425
#water_content_blood = 0.839 ; # Bertelsen 1998 in trout

# Calcul des vraisemblances
Likelihood (C_art, LogNormal, Prediction(C_art), 2.0);
Likelihood (C_liver, LogNormal, Prediction(C_liver), 2.0);
Likelihood (C_carcass, LogNormal, Prediction(C_carcass), 2.0);

Likelihood (C_art_gluco, LogNormal, Prediction(C_art_gluco), 2.0);
Likelihood (C_liver_gluco, LogNormal, Prediction(C_liver_gluco), 2.0);
Likelihood (C_rob_gluco, LogNormal, Prediction(C_rob_gluco), 2.0);

Likelihood (C_art_sulfo, LogNormal, Prediction(C_art_sulfo), 2.0);
Likelihood (C_liver_sulfo, LogNormal, Prediction(C_liver_sulfo), 2.0);
Likelihood (C_rob_sulfo, LogNormal, Prediction(C_rob_sulfo), 2.0);

Level { # individual

Simulation { #Stickleback male at 10 ug/L (nominal concentration)

# Physiological parameters
Bw_Fcard_ref= 0.294 ; # Body weight of reference for F_card from Ekstrom, 2016 (Perch value)
Bw_VO2_ref = 0.97 ; # Body weight of reference for VO2 from Brafield, 1976 and Walkey, 1970
DEB_V = 1.26 ; # Energy conductance (mm/d) (DEB model parameter)
DEB_g = 0.7398 ; # Energy investment ratio (SU) (DEB model parameter)
DEB_KM = 0.122 ; # Somatic maintenance rate coefficient (1/d) (DEB model parameter)
DEB_EHm = 1 ; # Energy at State of maturity at metamorphosis (J)
DEB_EHb = 1 ; # Energy at State of maturity at birth (J)
DEB_shape = 0.247 ;
a_BW_L = 0.01543825; # = (0.249^3), # Bw= a*TL^b parameter (mg/mm)
b_BW_L = 3.0 ; # b relation BW(mg)=F(L(mm)) --> SU

# Environmental condition
TA = 6130 ; # Arrhenius temperature in Kelvin
TR_DEB = 293.65; # (Kelvin)
TR_Fcard = 289.15; # (Kelvin) -> temperature oprimal : 16 C
TR_VO2 = 283.15; # (Kelvin)
TR_excretion = 289.15; # (Kelvin)

# Effective respiratory volume & cardiac output
F_card_ref = 62.96969 ; # = Qb_ref_perch * (Bw_ref^(0.75)) / Bw_ref # (mL/d/g) = 46.368 *
(0.294^(0.75)) / 0.294 --> allometric scaling function from Ekstrom, 2016
V_O2_ref = 4.03 ; # reference oxygen consumption rate (mg O2/g/d) --> from Brafield, 1976
O2_EE = 0.71 ; # Oxygen extraction efficiency of 71% proposed by Erickson, 1990
Sat = 0.90 ; # dissolved oxygen saturation of 90% proposed by Erickson, 1990

# volume scaling factor : fraction of BW (%)
sc_blood = 0.009 ;
sc_gonads = 0.00781598 ;
sc_brain = 0.012 ;
sc_liver = 0.053860073 ;
sc_fat = 0.0168;
sc_skin = 0.036 ;
sc viscera= 0.055 ;
sc_kidney = 0.011725124 ;
sc_rp = 0.032 ;

# Fraction of arterial blood flow
frac_gonads = 0.0054 ;
frac_brain = 0.0392 ;
frac_liver = 0.0529 ;
frac_fat = 0.0095 ;
frac_skin = 0.0186 ;
frac viscera= 0.0886 ;
frac_kidney = 0.114 ;
frac_rp = 0.1074 ;

#inputs
Bw_i = 1.67; #Mean mass of fish
Temperature = 16;
f_cst = 0.82;
V_water = 1E+12 ; #mL
ivQuantity = 0.0;
event_bile = 1;

C_water= NDoses( 171 ,

0.00025,0.000849747474747475,0.00144949494949495,0.002049242424242424,0.0026489898989899,0.00324873737373737,0.003848
48484848485,0.00444823232323232,0.00500099502487562,0.0050134328358209,0.00502587064676617,0.00503830845771144,0.005050746268
65672,0.00506318407960199,0.00507562189054726,0.00508805970149254,0.00510049751243781,0.00511293532338308,0.00512537313432836
,0.00513781094527363,0.00515024875621891,0.00516268656716418,0.00517512437810945,0.00518756218905473,0.0052,0.005220833333333
3,0.00524166666666667,0.0052625,0.00528333333333333,0.00530416666666667,0.005325,0.00534583333333333,0.00536666666666667,0.0
053875,0.00540833333333333,0.00542916666666667,0.00545,0.00547083333333333,0.00549166666666667,0.0055125,0.00553333333333333,
0.00555416666666667,0.005575,0.00559583333333333,0.00561666666666667,0.0056375,0.00565833333333333,0.00567916666666667,0.0057
,0.00570208333333333,0.00570416666666667,0.00570625,0.00570833333333333,0.00571041666666667,0.0057125,0.00571458333333333,0.0
057166666666667,0.00571875,0.00572083333333333,0.00572291666666667,0.005725,0.00572708333333333,0.00572916666666667,0.005731
25,0.00573333333333333,0.00573541666666667,0.0057375,0.00573958333333333,0.00574166666666667,0.00574375,0.00574583333333333,0.0
057479166666667,0.00575,0.00575208333333333,0.00575416666666667,0.00575625,0.00575833333333333,0.00576041666666667,0.00576
25,0.00576458333333333,0.00576666666666667,0.00576875,0.00577083333333333,0.00577291666666667,0.005775,0.00577708333333333,0.

```



```

sc_liver = 0.056462165 ;
sc_fat = 0.0168;
sc_skin = 0.036 ;
sc_viscera = 0.055 ;
sc_kidney = 0.012830141 ;
sc_rp = 0.032 ;

# Fraction of arterial blood flow
frac_gonads =0.0053 ;
frac_brain =0.0386 ;
frac_liver =0.0546 ;
frac_fat =0.0094 ;
frac_skin =0.0184;
frac_viscera =0.087 ;
frac_kidney =0.123 ;
frac_rp =0.106 ;

#inputs
Bw_i = 1.67 ; # Mean mass of fish
Temperature = 16 ; # water temperature°C
f_cst = 0.82 ; # food
V_water = 1E+12 ; # Aquarium water volume (mL)
ivQuantity = 0.0 ;
event_bile = 1 ;

C_water= NDoses( 171 ,

0.00025,0.003765625,0.008333333333333333,0.025,0.0319512195121951,0.0389024390243902,0.0458536585365854,0.05280487804
87805,0.0592007984031936,0.0592107784431138,0.0592207584830339,0.0592307385229541,0.0592407185628743,0.0592506986027944,0.059
2606786427146,0.0592706586826347,0.0592806387225549,0.0592906187624751,0.0593005988023952,0.0593105788423154,0.05932055888223
55,0.0593305389221557,0.0593405189620759,0.059350499001996,0.0593604790419162,0.0593704590818363,0.0593804391217565,0.0593904
191616767,0.0594003992015968,0.059410379241517,0.0594203592814371,0.0594303393213573,0.0594403193612774,0.05945022994011976,0.
0594602794411178,0.0594702594810379,0.0594802395209581,0.0594902195608782,0.0595001996007984,0.0595101796407186,0.05952015968
06387,0.0595301397205589,0.059540119760479,0.0595500998003992,0.0595600798403194,0.0595700598802395,0.0595800399201597,0.0595
900199600798,0.0596,0.05970625,0.0598125,0.05991875,0.060025,0.06013125,0.0602375,0.06034375,0.06045,0.06055625,0.0606625,0.0
6076875,0.060875,0.06098125,0.0610875,0.06119375,0.0613,0.06140625,0.0615125,0.06161875,0.061725,0.06183125,0.0619375,0.06204
375,0.06215,0.06225625,0.0623625,0.06246875,0.062575,0.06268125,0.0627875,0.06289375,0.063,0.06310625,0.0632125,0.06331875,0.
063425,0.06353125,0.0636375,0.06374375,0.06385,0.06395625,0.0640625,0.06416875,0.064275,0.06438125,0.0644875,0.06459375,0.0647
7,0.064875,0.064975,0.065075,0.065175,0.065275,0.065375,0.065475,0.065575,0.065675,0.065775,0.065875,0.065975,0.066075,0.066175,
0.066275,0.066375,0.066475,0.066575,0.066675,0.066775,0.066875,0.066975,0.067075,0.067175,0.067275,0.067375,0.067475,0.067575,
0.067675,0.067775,0.067875,0.067975,0.068075,0.068175,0.068275,0.068375,0.068475,0.068575,0.068675,0.068775,0.068875,0.068975,
0.069075,0.069175,0.069275,0.069375,0.069475,0.069575,0.069675,0.069775,0.069875,0.069975,0.07,0.070075,0.070175,0.070275,0.070375,
0.070475,0.070575,0.070675,0.070775,0.070875,0.070975,0.071075,0.071175,0.071275,0.071375,0.071475,0.071575,0.071675,0.071775,
0.071875,0.071975,0.072075,0.072175,0.072275,0.072375,0.072475,0.072575,0.072675,0.072775,0.072875,0.072975,0.073075,0.073175,
0.073275,0.073375,0.073475,0.073575,0.073675,0.073775,0.073875,0.073975,0.074075,0.074175,0.074275,0.074375,0.074475,0.074575,
0.074675,0.074775,0.074875,0.074975,0.075075,0.075175,0.075275,0.075375,0.075475,0.075575,0.075675,0.075775,0.075875,0.075975,0.076075,
0.076175,0.076275,0.076375,0.076475,0.076575,0.076675,0.076775,0.076875,0.076975,0.077075,0.077175,0.077275,0.077375,0.077475,
0.077575,0.077675,0.077775,0.077875,0.077975,0.078075,0.078175,0.078275,0.078375,0.078475,0.078575,0.078675,0.078775,0.078875,
0.078975,0.079075,0.079175,0.079275,0.079375,0.079475,0.079575,0.079675,0.079775,0.079875,0.079975,0.08,0.080075,0.080175,0.080275,
0.080375,0.080475,0.080575,0.080675,0.080775,0.080875,0.080975,0.081075,0.081175,0.081275,0.081375,0.081475,0.081575,0.081675,
0.081775,0.081875,0.081975,0.082075,0.082175,0.082275,0.082375,0.082475,0.082575,0.082675,0.082775,0.082875,0.082975,0.083075,0.083175,
0.083275,0.083375,0.083475,0.083575,0.083675,0.083775,0.083875,0.083975,0.084075,0.084175,0.084275,0.084375,0.084475,0.084575,0.084675,
0.084775,0.084875,0.084975,0.085075,0.085175,0.085275,0.085375,0.085475,0.085575,0.085675,0.085775,0.085875,0.085975,0.086075,0.086175,
0.086275,0.086375,0.086475,0.086575,0.086675,0.086775,0.086875,0.086975,0.087075,0.087175,0.087275,0.087375,0.087475,0.087575,0.087675,
0.087775,0.087875,0.087975,0.088075,0.088175,0.088275,0.088375,0.088475,0.088575,0.088675,0.088775,0.088875,0.088975,0.089075,0.089175,
0.089275,0.089375,0.089475,0.089575,0.089675,0.089775,0.089875,0.089975,0.09,0.090075,0.090175,0.090275,0.090375,0.090475,0.090575,
0.090675,0.090775,0.090875,0.090975,0.091075,0.091175,0.091275,0.091375,0.091475,0.091575,0.091675,0.091775,0.091875,0.091975,0.092075,
0.092175,0.092275,0.092375,0.092475,0.092575,0.092675,0.092775,0.092875,0.092975,0.093075,0.093175,0.093275,0.093375,0.093475,0.093575,
0.093675,0.093775,0.093875,0.093975,0.094075,0.094175,0.094275,0.094375,0.094475,0.094575,0.094675,0.094775,0.094875,0.094975,0.095075,
0.095175,0.095275,0.095375,0.095475,0.095575,0.095675,0.095775,0.095875,0.095975,0.096075,0.096175,0.096275,0.096375,0.096475,0.096575,
0.096675,0.096775,0.096875,0.096975,0.097075,0.097175,0.097275,0.097375,0.097475,0.097575,0.097675,0.097775,0.097875,0.097975,0.098075,
0.098175,0.098275,0.098375,0.098475,0.098575,0.098675,0.098775,0.098875,0.098975,0.099075,0.099175,0.099275,0.099375,0.099475,0.099575,
0.099675,0.099775,0.099875,0.099975,1,1.000075,1.000175,1.000275,1.000375,1.000475,1.000575,1.000675,1.000775,1.000875,1.000975,1.001075,
1.001175,1.001275,1.001375,1.001475,1.001575,1.001675,1.001775,1.001875,1.001975,1.002075,1.002175,1.002275,1.002375,1.002475,1.002575,
1.002675,1.002775,1.002875,1.002975,1.003075,1.003175,1.003275,1.003375,1.003475,1.003575,1.003675,1.003775,1.003875,1.003975,1.004075,
1.004175,1.004275,1.004375,1.004475,1.004575,1.004675,1.004775,1.004875,1.004975,1.005075,1.005175,1.005275,1.005375,1.005475,1.005575,
1.005675,1.005775,1.005875,1.005975,1.006075,1.006175,1.006275,1.006375,1.006475,1.006575,1.006675,1.006775,1.006875,1.006975,1.007075,
1.007175,1.007275,1.007375,1.007475,1.007575,1.007675,1.007775,1.007875,1.007975,1.008075,1.008175,1.008275,1.008375,1.008475,1.008575,
1.008675,1.008775,1.008875,1.008975,1.009075,1.009175,1.009275,1.009375,1.009475,1.009575,1.009675,1.009775,1.009875,1.009975,1.01,1.010075,
1.010175,1.010275,1.010375,1.010475,1.010575,1.010675,1.010775,1.010875,1.010975,1.011075,1.011175,1.011275,1.011375,1.011475,1.011575,
1.011675,1.011775,1.011875,1.011975,1.012075,1.012175,1.012275,1.012375,1.012475,1.012575,1.012675,1.012775,1.012875,1.012975,1.013075,
1.013175,1.013275,1.013375,1.013475,1.013575,1.013675,1.013775,1.013875,1.013975,1.014075,1.014175,1.014275,1.014375,1.014475,1.014575,
1.014675,1.014775,1.014875,1.014975,1.015075,1.015175,1.015275,1.015375,1.015475,1.015575,1.015675,1.015775,1.015875,1.015975,1.016075,
1.016175,1.016275,1.016375,1.016475,1.016575,1.016675,1.016775,1.016875,1.016975,1.017075,1.017175,1.017275,1.017375,1.017475,1.017575,
1.017675,1.017775,1.017875,1.017975,1.018075,1.018175,1.018275,1.018375,1.018475,1.018575,1.018675,1.018775,1.018875,1.018975,1.019075,
1.019175,1.019275,1.019375,1.019475,1.019575,1.019675,1.019775,1.019875,1.019975,1.02,1.020075,1.020175,1.020275,1.020375,1.020475,1.020575,
1.020675,1.020775,1.020875,1.020975,1.021075,1.021175,1.021275,1.021375,1.021475,1.021575,1.021675,1.021775,1.021875,1.021975,1.022075,
1.022175,1.022275,1.022375,1.022475,1.022575,1.022675,1.022775,1.022875,1.022975,1.023075,1.023175,1.023275,1.023375,1.023475,1.023575,
1.023675,1.023775,1.023875,1.023975,1.024075,1.024175,1.024275,1.024375,1.024475,1.024575,1.024675,1.024775,1.024875,1.024975,1.025075,
1.025175,1.025275,1.025375,1.025475,1.025575,1.025675,1.025775,1.025875,1.025975,1.026075,1.026175,1.026275,1.026375,1.026475,1.026575,
1.026675,1.026775,1.026875,1.026975,1.027075,1.027175,1.027275,1.027375,1.027475,1.027575,1.027675,1.027775,1.027875,1.027975,1.028075,
1.028175,1.028275,1.028375,1.028475,1.028575,1.028675,1.028775,1.028875,1.028975,1.029075,1.029175,1.029275,1.029375,1.029475,1.029575,
1.029675,1.029775,1.029875,1.029975,1.03,1.030075,1.030175,1.030275,1.030375,1.030475,1.030575,1.030675,1.030775,1.030875,1.030975,1.031075,
1.031175,1.031275,1.031375,1.031475,1.031575,1.031675,1.031775,1.031875,1.031975,1.032075,1.032175,1.032275,1.032375,1.032475,1.032575,
1.032675,1.032775,1.032875,1.032975,1.033075,1.033175,1.033275,1.033375,1.033475,1.033575,1.033675,1.033775,1.033875,1.033975,1.034075,
1.034175,1.034275,1.034375,1.034475,1.034575,1.034675,1.034775,1.034875,1.034975,1.035075,1.035175,1.035275,1.035375,1.035475,1.035575,
1.035675,1.035775,1.035875,1.035975,1.036075,1.036175,1.036275,1.036375,1.036475,1.036575,1.036675,1.036775,1.036875,1.036975,1.037075,
1.037175,1.037275,1.037375,1.037475,1.037575,1.037675,1.037775,1.037875,1.037975,1.038075,1.038175,1.038275,1.038375,1.038475,1.038575,
1.038675,1.038775,1.038875,1.038975,1.039075,1.039175,1.039275,1.039375,1.039475,1.039575,1.039675,1.039775,1.039875,1.039975,1.04,1.040075,
1.040175,1.040275,1.040375,1.040475,1.040575,1.040675,1.040775,1.040875,1.040975,1.041075,1.041175,1.041275,1.041375,1.041475,1.041575,
1.041675,1.041775,1.041875,1.041975,1.042075,1.042175,1.042275,1.042375,1.042475,1.042575,1.042675,1.042775,1.042875,1.042975,1.043075,
1.043175,1.043275,1.043375,1.043475,1.043575,1.043675,1.043775,1.043875,1.043975,1.044075,1.044175,1.044275,1.044375,1.044475,1.044575,
1.044675,1.044775,1.044875,1.044975,1.045075,1.045175,1.045275,1.045375,1.045475,1.045575,1.045675,1.045775,1.045875,1.045975,1.046075,
1.046175,1.046275,1.046375,1.046475,1.046575,1.046675,1.046775,1.046875,1.046975,1.047075,1.047175,1.047275,1.047375,1.047475,1.047575,
1.047675,1.047775,1.047875,1.047975,1.048075,1.048175,1.048275,1.048375,1.048475,1.048575,1.048675,1.048775,1.048875,1.048975,1.049075,
1.049175,1.049275,1.049375,1.049475,1.049575,1.049675,1.049775,1.049875,1.049975,1.05,1.050075,1.050175,1.050275,1.050375,1.050475,1.050575,
1.050675,1.050775,1.050875,1.050975,1.051075,1.051175,1.051275,1.051375,1.051475,1.051575,1.051675,1.051775,1.051875,1.051975,1.052075,
1.052175,1.052275,1.052375,1.052475,1.052575,1.052675,1.052775,1.052875,1.052975,1.053075,1.053175,1.053275,1.053375,1.053475,1.053575,
1.053675,1.053775,1.053875,1.053975,1.054075,1.054175,1.054275,1.054375,1.054475,1.054575,1.054675,1.054775,1.054875,1.054975,1.055075,
1.055175,1.055275,1.055375,1.055475,1.055575,1.055675,1.055775,1.055875,1.055975,1.056075,1.056175,1.056275,1.056375,1.056475,1.056575,
1.056675,1.056775,1.056875,1.056975,1.057075,1.057175,1.057275,1.057375,1.057475,1.057575,1.057675,1.057775,1.057875,1.057975,1.058075,
1.058175,1.058275,1.058375,1.058475,1.058575,1.058675,1.058775,1.058875,1.058975,1.059075,1.059175,1.059275,1.059375,1.059475,1.059575,
1.059675,1.059775,1.059875,1.059975,1.06,1.060075,1.060175,1.060275,1.060375,1.060475,1.060575,1.060675,1.060775,1.060875,1.060975,1.061075,
1.061175,1.061275,1.061375,1.061475,1.061575,1.061675,1.061775,1.061875,1.061975,1.062075,1.062175,1.062275,1.062375,1.062475,1.062575,
1.062675,1.062775,1.062875,1.062975,1.063075,1.063175,1.063275,1.063375,1.063475,1.063575,1.063675,1.063775,1.063875,1.063975,1.064075,
1.064175,1.064275,1.064375,1.064475,1.064575,1.064675,1.064775,1.064875,1.064975,1.065075,1.065175,1.065275,1.065375,1.065475,1.065575,
1.065675,1.065775,1.065875,1.065975,1.066075,1.066175,1.066275,1.066375,1.066475,1.066575,1.066675,1.066775,1.066875,1.066975,1.067075,
1.067175,1.067275,1.067375,1.067475,1.067575,1.067675,1.067775,1.067875,1.067975,1.068075,1.068175,1.068275,1.068375,1.068475,1.068575,
1.068675,1.068775,1.068875,1.068975,1.069075,1.069175,1.069275,1.069375,1.069475,1.069575,1.069675,1.069775,1.069875,1.069975,1.07,1.070075,
1.070175,1.070275,1.070375,1.070475,1.070575,1.070675,1.070775,1.070875,1.070975,1.071075,1.071175,1.071275,1.071375,1.071475,1.071575,
1.071675,1.071775,1.071875,1.071975,1.072075,1.072175,1.072275,1.072375,1.072475,1.072575,1.072675,1.072775,1.072875,1.072975,1.073075,
1.073175,1.073275,1.073375,1.073475,1.073575,1.073675,1.073775,1.073875,1.073975,1.074075,1.074175,1.074275,1.074375,1.074475,1.074575,
1.074675,1.074775,1.074875,1.074975,1.075075,1.075175,1.075275,1.075375,1.075475,1.075575,1.075675,1.075775,1.075875,1.075975,1.076075,
1.076175,1.076275,1.076375,1.076475,1.076575,1.076675,1.076775,1.076875,1.076975,1.077075,1.077175,1.077275,1.077375,1.077475,1.077575,
1.077675,1.077775,1.077875,1.077975,1.078075,1.078175,1.078275,1.078375,1.078475,1.078575,1.078675,1.078775,1.078875,1.078975,1.079075,
1.079175,1.079275,1.079375,1.079475,1.079575,1.079675,1.079775,1.079875,1.079975,1.08,1.080075,1.080175,1.080275,1.080375,1.080475,1.080575,
1.080675,1.080775,1.080875,1.080975,1.081075,1.081175,1.081275,1.081375,1.081475,1.081575,1.081675,1.081775,1.081875,1.081975,1.082075,
```

}

Simulation { #Stickleback female at 10 µg/L (nominal concentration)

Physiological parameters

Bw_Fcard_ref= 0.294 ; # Body weight of reference for F_card from Ekstrom, 2016 (Perch value)
Bw_VO2_ref = 0.97 ; # Body weight of reference for VO2 from Brafield, 1976 and Walkey, 1970
DEB_V = 1.26 ; # Energy conductance (mm/d) (DEB model parameter)
DEB_g = 0.662 ; # Energy investment ratio (SU) (DEB model parameter)
DEB_KM = 0.122 ; # Somatic maintenance rate coefficient (1/d) (DEB model parameter)
DEB_EHm = 1 ; # Energy at State of maturity at metamorphosis (J)
DEB_EHb = 1 ; # Energy at State of maturity at birth (J)
DEB_shape = 0.247 ;
a_BW_L = 0.01543825; # = (0.249^3), # Bw= a*TL^b parameter (mg/mm)
b_BW_L = 3.0 ; # b relation BW(mg)=F(L(mm)) --> SU

Environmental condition

TA = 6130 ; # Arrhenius temperature in Kelvin
TR_DEB = 293.65; # (Kelvin)
TR_Fcard = 289.15; # (Kelvin) -> temperature optimal : 16 C
TR_VO2 = 283.15; # (Kelvin)
TR_excretion = 289.15; # (Kelvin)

Effective respiratory volume & cardiac output

F_card_ref = 62.96969 ; # = Qb_ref_perch * (Bw_ref^(0.75)) / Bw_ref # (mL/d/g) = 46.368 * (0.294^(0.75))
/ 0.294 --> allometric scaling function from Ekstrom, 2016

V_O2_ref = 4.03; # reference oxygen consumption rate (mg O2/g/d) --> from Brafield, 1976
O2_EE = 0.71 ; # Oxygen extraction efficiency of 71% proposed by Erickson, 1990
Sat = 0.90 ; # dissolved oxygen saturation of 90% proposed by Erickson, 1990

volume scaling factor : fraction of BW (%)

sc_blood = 0.011 ;
sc_gonads = 0.025975868 ;
sc_brain = 0.010 ;
sc_liver = 0.070052019 ;
sc_fat = 0.0168 ;
sc_skin = 0.061 ;
sc viscera= 0.066 ;
sc_kidney = 0.007569314 ;
sc_rp = 0.025 ;

Fraction of arterial blood flow

frac_gonads =0.0016 ;
frac_brain =0.0251;
frac_liver =0.06;
frac_fat =0.0073;
frac_skin =0.0242;
frac viscera=0.0816;
frac_kidney =0.0728;
frac_rp =0.1033;

#inputs

Bw_i = 1.85 ; #Mean fish mass
Temperature = 16 ;
f_cst = 0.83 ;
V_water = 1E+12 ;#mL
ivQuantity = 0.0 ;
event_bile = 1 ;

C_water= NDoses(171 ,

0.00025,0.000786616161616161,0.00132323232323232,0.00185984848484848,0.00239646464646465,0.00293308080808081,0.00346
969696969697,0.00400631313131313,0.00450319361277445,0.00454311377245509,0.00458303393213573,0.00462295409181637,0.0046628742
5149701,0.00470279441117764,0.00474271457085828,0.00478263473053892,0.00482255489021956,0.0048624750499002,0.0049023952095808
4,0.00494231536926148,0.0049822352894212,0.00502215568862275,0.00506207584830339,0.00510199600798403,0.00514191616766467,0.0
0518183632734531,0.00522175648702595,0.00526167664670659,0.00530159680638723,0.00534151696606786,0.0053814371257485,0.0054213
5728542914,0.00546127744510978,0.00550119760479042,0.00554111776447106,0.0055810379241517,0.00562095808383234,0.0056608782435
1297,0.00570079840319361,0.00574071856287425,0.00578063872255489,0.00582055888223553,0.00586047904191617,0.00590039920159681,
0.00594031936127744,0.00598023952095808,0.00602015968063872,0.00606007984031936,0.0061,0.00610625,0.0061125,0.00611875,0.0061
25,0.00613125,0.0061375,0.00614375,0.00615,0.00615625,0.0061625,0.00616875,0.006175,0.00618125,0.0061875,0.00619375,0.0062,0
00620625,0.0062125,0.00621875,0.006225,0.00623125,0.0062375,0.00624375,0.00625,0.00625625,0.0062625,0.00626875,0.006275,0.006
28125,0.0062875,0.00629375,0.0063,0.00630625,0.0063125,0.00631875,0.006325,0.00633125,0.0063375,0.00634375,0.00635,0.00635625
,0.0063625,0.00636875,0.006375,0.00638125,0.0063875,0.00639375,0.0064,0.00643833333333333,0.006466666666667,0.006475,0.0064
33333333333,0.0064916666666667,0.0065,0.00651083333333333,0.0065416666666667,0.006575,0.0066,0.006625,0.00665833333333333,0.006697,0.0067
66667,0.0068,0.00683333333333333,0.00686666666667,0.0069,0.00693333333333333,0.00696666666667,0.007,0.00706666666667,0.0071,0.00713333333333333,
0.00716666666667,0.0072,0.00723333333333333,0.00726666666667,0.0073,0.00733333333333333,0.00736666666667,0.0074,0.00743333333333333,
0.00746666666667,0.0075,0.00753333333333333,0.00756666666667,0.0076,0.00763333333333333,0.00766666666667,0.0077,0.00773333333333333,
0.00776666666667,0.0078,0.00783333333333333,0.00786666666667,0.0079,0.00793333333333333,0.00796666666667,0.008,0.00806666666667,0.0081,
0.00813333333333333,0.00816666666667,0.0082,0.00823333333333333,0.00826666666667,0.0083,0.00833333333333333,0.00836666666667,0.0084,
0.00843333333333333,0.00846666666667,0.0085,0.00853333333333333,0.00856666666667,0.0086,0.00863333333333333,0.00866666666667,0.0087,
0.00873333333333333,0.00876666666667,0.0088,0.00883333333333333,0.00886666666667,0.0089,0.00893333333333333,0.00896666666667,0.009,
0.00906666666667,0.0091,0.00913333333333333,0.00916666666667,0.0092,0.00923333333333333,0.00926666666667,0.0093,0.00933333333333333,
0.00936666666667,0.0094,0.00943333333333333,0.00946666666667,0.0095,0.00953333333333333,0.00956666666667,0.0096,0.00963333333333333,
0.00966666666667,0.0097,0.00973333333333333,0.00976666666667,0.0098,0.00983333333333333,0.00986666666667,0.0099,0.00993333333333333,
0.00996666666667,0.01,0.01006666666667,0.0101,0.01013333333333333,0.01016666666667,0.0102,0.01023333333333333,0.01026666666667,0.0103,
0.01033333333333333,0.01036666666667,0.0104,0.01043333333333333,0.01046666666667,0.0105,0.01053333333333333,0.01056666666667,0.0106,
0.01063333333333333,0.01066666666667,0.0107,0.01073333333333333,0.01076666666667,0.0108,0.01083333333333333,0.01086666666667,0.0109,
0.01093333333333333,0.01096666666667,0.011,0.01106666666667,0.0111,0.01113333333333333,0.01116666666667,0.0112,0.01123333333333333,
0.01126666666667,0.0113,0.01133333333333333,0.01136666666667,0.0114,0.01143333333333333,0.01146666666667,0.0115,0.01153333333333333,
0.01156666666667,0.0116,0.01163333333333333,0.01166666666667,0.0117,0.01173333333333333,0.01176666666667,0.0118,0.01183333333333333,
0.01186666666667,0.0119,0.01193333333333333,0.01196666666667,0.012,0.01206666666667,0.0121,0.01213333333333333,0.01216666666667,0.0122,
0.01223333333333333,0.01226666666667,0.0123,0.01233333333333333,0.01236666666667,0.0124,0.01243333333333333,0.01246666666667,0.0125,
0.01253333333333333,0.01256666666667,0.0126,0.01263333333333333,0.01266666666667,0.0127,0.01273333333333333,0.01276666666667,0.0128,
0.01283333333333333,0.01286666666667,0.0129,0.01293333333333333,0.01296666666667,0.013,0.01306666666667,0.0131,0.01313333333333333,
0.01316666666667,0.0132,0.01323333333333333,0.01326666666667,0.0133,0.01333333333333333,0.01336666666667,0.0134,0.01343333333333333,
0.01346666666667,0.0135,0.01353333333333333,0.01356666666667,0.0136,0.01363333333333333,0.01366666666667,0.0137,0.01373333333333333,
0.01376666666667,0.0138,0.01383333333333333,0.01386666666667,0.0139,0.01393333333333333,0.01396666666667,0.014,0.01406666666667,0.0141,
0.01413333333333333,0.01416666666667,0.0142,0.01423333333333333,0.01426666666667,0.0143,0.01433333333333333,0.01436666666667,0.0144,
0.01443333333333333,0.01446666666667,0.0145,0.01453333333333333,0.01456666666667,0.0146,0.01463333333333333,0.01466666666667,0.0147,
0.01473333333333333,0.01476666666667,0.0148,0.01483333333333333,0.01486666666667,0.0149,0.01493333333333333,0.01496666666667,0.015,
0.01506666666667,0.0151,0.01513333333333333,0.01516666666667,0.0152,0.01523333333333333,0.01526666666667,0.0153,0.01533333333333333,
0.01536666666667,0.0154,0.01543333333333333,0.01546666666667,0.0155,0.01553333333333333,0.01556666666667,0.0156,0.01563333333333333,
0.01566666666667,0.0157,0.01573333333333333,0.01576666666667,0.0158,0.01583333333333333,0.01586666666667,0.0159,0.01593333333333333,
0.01596666666667,0.016,0.01606666666667,0.0161,0.01613333333333333,0.01616666666667,0.0162,0.01623333333333333,0.01626666666667,0.0163,
0.01633333333333333,0.01636666666667,0.0164,0.01643333333333333,0.01646666666667,0.0165,0.01653333333333333,0.01656666666667,0.0166,
0.01663333333333333,0.01666666666667,0.0167,0.01673333333333333,0.01676666666667,0.0168,0.01683333333333333,0.01686666666667,0.0169,
0.01693333333333333,0.01696666666667,0.017,0.01706666666667,0.0171,0.01713333333333333,0.01716666666667,0.0172,0.01723333333333333,
0.01726666666667,0.0173,0.01733333333333333,0.01736666666667,0.0174,0.01743333333333333,0.01746666666667,0.0175,0.01753333333333333,
0.01756666666667,0.0176,0.01763333333333333,0.01766666666667,0.0177,0.01773333333333333,0.01776666666667,0.0178,0.01783333333333333,
0.01786666666667,0.0179,0.01793333333333333,0.01796666666667,0.018,0.01806666666667,0.0181,0.01813333333333333,0.01816666666667,0.0182,
0.01823333333333333,0.01826666666667,0.0183,0.01833333333333333,0.01836666666667,0.0184,0.01843333333333333,0.01846666666667,0.0185,
0.01853333333333333,0.01856666666667,0.0186,0.01863333333333333,0.01866666666667,0.0187,0.01873333333333333,0.01876666666667,0.0188,
0.01883333333333333,0.01886666666667,0.0189,0.01893333333333333,0.01896666666667,0.019,0.01906666666667,0.0191,0.01913333333333333,
0.01916666666667,0.0192,0.01923333333333333,0.01926666666667,0.0193,0.01933333333333333,0.01936666666667,0.0194,0.01943333333333333,
0.01946666666667,0.0195,0.01953333333333333,0.01956666666667,0.0196,0.01963333333333333,0.01966666666667,0.0197,0.01973333333333333,
0.01976666666667,0.0198,0.01983333333333333,0.01986666666667,0.0199,0.01993333333333333,0.01996666666667,0.02,0.02006666666667,0.0201,
0.02013333333333333,0.02016666666667,0.0202,0.02023333333333333,0.02026666666667,0.0203,0.02033333333333333,0.02036666666667,0.0204,
0.02043333333333333,0.02046666666667,0.0205,0.02053333333333333,0.02056666666667,0.0206,0.02063333333333333,0.02066666666667,0.0207,
0.02073333333333333,0.02076666666667,0.0208,0.02083333333333333,0.02086666666667,0.0209,0.02093333333333333,0.02096666666667,0.021,
0.02106666666667,0.0211,0.02113333333333333,0.02116666666667,0.0212,0.02123333333333333,0.02126666666667,0.0213,0.02133333333333333,
0.02136666666667,0.0214,0.02143333333333333,0.02146666666667,0.0215,0.02153333333333333,0.02156666666667,0.0216,0.02163333333333333,
0.02166666666667,0.0217,0.02173333333333333,0.02176666666667,0.0218,0.02183333333333333,0.02186666666667,0.0219,0.02193333333333333,
0.02196666666667,0.022,0.02206666666667,0.0221,0.02213333333333333,0.02216666666667,0.0222,0.02223333333333333,0.02226666666667,0.0223,
0.02233333333333333,0.02236666666667,0.0224,0.02243333333333333,0.02246666666667,0.0225,0.02253333333333333,0.02256666666667,0.0226,
0.02263333333333333,0.02266666666667,0.0227,0.02273333333333333,0.02276666666667,0.0228,0.02283333333333333,0.02286666666667,0.0229,
0.02293333333333333,0.02296666666667,0.023,0.02306666666667,0.0231,0.02313333333333333,0.02316666666667,0.0232,0.02323333333333333,
0.02326666666667,0.0233,0.02333333333333333,0.02336666666667,0.0234,0.02343333333333333,0.02346666666667,0.0235,0.02353333333333333,
0.02356666666667,0.0236,0.02363333333333333,0.02366666666667,0.0237,0.02373333333333333,0.02376666666667,0.0238,0.02383333333333333,
0.02386666666667,0.0239,0.02393333333333333,0.02396666666667,0.024,0.02406666666667,0.0241,0.02413333333333333,0.02416666666667,0.0242,
0.02423333333333333,0.02426666666667,0.0243,0.02433333333333333,0.02436666666667,0.0244,0.02443333333333333,0.02446666666667,0.0245,
0.02453333333333333,0.02456666666667,0.0246,0.02463333333333333,0.02466666666667,0.0247,0.02473333333333333,0.02476666666667,0.0248,
0.02483333333333333,0.02486666666667,0.0249,0.02493333333333333,0.02496666666667,0.025,0.02506666666667,0.0251,0.02513333333333333,
0.02516666666667,0.0252,0.02523333333333333,0.02526666666667,0.0253,0.02533333333333333,0.02536666666667,0.0254,0.02543333333333333,
0.02546666666667,0.0255,0.02553333333333333,0.02556666666667,0.0256,0.02563333333333333,0.02566666666667,0.0257,0.02573333333333333,
0.02576666666667,0.0258,0.02583333333333333,0.02586666666667,0.0259,0.02593333333333333,0.02596666666667,0.026,0.02606666666667,0.0261,
0.02613333333333333,0.02616666666667,0.0262,0.02623333333333333,0.02626666666667,0.0263,0.02633333333333333,0.02636666666667,0.0264,
0.02643333333333333,0.02646666666667,0.0265,0.02653333333333333,0.02656666666667,0.0266,0.02663333333333333,0.02666666666667,0.0267,
0.02673333333333333,0.02676666666667,0.0268,0.02683333333333333,0.02686666666667,0.0269,0.02693333333333333,0.02696666666667,0.027,
0.02706666666667,0.0271,0.02713333333333333,0.02716666666667,0.0272,0.02723333333333333,0.02726666666667,0.0273,0.02733333333333333,
0.02736666666667,0.0274,0.02743333333333333,0.02746666666667,0.0275,0.02753333333333333,0.02756666666667,0.0276,0.02763333333333333,
0.02766666666667,0.0277,0.02773333333333333,0.02776666666667,0.0278,0.02783333333333333,0.02786666666667,0.0279,0.02793333333333333,
0.02796666666667,0.028,0.02806666666667,0.0281,0.02813333333333333,0.02816666666667,0.0282,0.02823333333333333,0.02826666666667,0.0283,
0.02833333333333333,0.02836666666667,0.0284,0.02843333333333333,0.02846666666667,0.0285,0.


```

# Experimental data
# LQ_BPA/2 24.7 27.1 26.0 LQ_BPA/2 LQ_BPA/2
Data(C_art, -1, 24.7E-3, 27.1E-3, 27.1E-3, 27.1E-3, 27.1E-3, 26.0E-3, 26.0E-3, 26.0E-3, 26.0E-3, 5.0E-3, -1);
Print(C_art, 0.25, 1.02, 4.02, 4.0201, 4.0202, 4.0203, 4.0204, 7.04, 7.0401, 7.0402, 7.0403, 7.0404, 8, 14);

# 11.3, !356.5!, 100.4, 41.7, LQ_BPA/2, LQ_BPA/2 ### 3.6x à 8.6x valeur à 4 et 7jours ###
Data(C_liver, 11.3E-3, -1, 100.4E-3, 41.7E-3, 5.0E-3, -1 );
Print(C_liver, 0.25, 1.02, 4.02, 7.04, 8, 14);

# LQ_BPA/2 10.0 10.9 12.7 LQ_BPA/2 LQ_BPA/2
Data(C_carcass, -1, 10.0E-3, 10.9E-3, 12.7E-3, 2.5E-3, -1 );
Print(C_carcass, 0.25, 1.02, 4.02, 7.04, 8, 14);

# 44.0 170.363 243.5 185.6 LQ_BPA_G/2 LQ_BPA_G/2
Data(C_art_gluco, 44.0E-3, 170.4E-3, 243.5E-3, 185.6E-3, 9.1E-3, -1);
Print(C_art_gluco, 0.25, 1.02, 4.02, 7.04, 8, 14);

# 19.8 !405.3! 73.5 152.2 LQ_BPA_G/2 LQ_BPA_G/2 ### 5.5x à 2.6x valeur à 4 et 7jours ###
Data(C_liver_gluco, 19.8E-3, -1, 73.5E-3, 152.2E-3, 1.5E-3, -1 );
Print(C_liver_gluco, 0.25, 1.02, 4.02, 7.04, 8, 14);

# 8.1 63.0 71.8 48.4 8.9 5.7
Data(C_rob_gluco, 8.1E-3, 63.0E-3, 71.8E-3, 48.4E-3, 8.9E-3, 5.7E-3);
Print(C_rob_gluco, 0.25, 1.02, 4.02, 7.04, 8, 14);

# LQ_BPA_S/2 1.3 1.1 LQ_BPA_S/2 LQ_BPA_S/2 LQ_BPA_S/2
Data(C_art_sulfo, -1, 1.3E-3, 1.1E-3, 0.9E-3, -1, -1);
Print(C_art_sulfo, 0.25, 1.02, 4.02, 7.04, 8, 14);

# LQ_BPA_S/2, 3.8, 1.4, 1.0, LQ_BPA_S/2, LQ_BPA_S/2
Data(C_liver_sulfo, -1, 3.8E-3, 1.4E-3, 1.0E-3, 0.05E-03, -1 );
Print(C_liver_sulfo, 0.25, 1.02, 4.02, 7.04, 8, 14);

# 0.27 0.77 0.37 0.62 LQ_BPA_S/2 LQ_BPA_S/2
Data(C_rob_sulfo, 2.7E-4, 7.7E-4, 3.7E-4, 6.2E-4, 1.3E-04, -1);
Print(C_rob_sulfo, 0.25, 1.02, 4.02, 7.04, 8, 14);
}

Simulation { #Stickleback female at 100 µg/L (nominal concentration)

# Physiological parameters
Bw_Fcard_ref= 0.294 ; # Body weight of reference for F_card from Ekstrom, 2016 (Perch value)
Bw_VO2_ref = 0.97 ; # Body weight of reference for VO2 from Brafield, 1976 and Walkey, 1970
DEB_V = 1.26 ; # Energy conductance (mm/d) (DEB model parameter)
DEB_g = 0.662 ; # Energy investment ratio (SU) (DEB model parameter)
DEB_KM = 0.122 ; # Somatic maintenance rate coefficient (1/d) (DEB model parameter)
DEB_EHm = 1 ; # Energy at State of maturity at metamorphosis (J)
DEB_EHb = 1 ; # Energy at State of maturity at birth (J)
DEB_shape = 0.247 ;
a_BW_L = 0.01543825; # = (0.249^3), # Bw= a*TL^b parameter (mg/mm)
b_BW_L = 3.0 ; # b relation BW(mg)=F(L(mm)) --> SU

# Environmental condition
TA = 6130 ; # Arrhenius temperature in Kelvin
TR_DEB = 293.65; # (Kelvin)
TR_Fcard = 289.15; # (Kelvin) -> temperature oprimal : 16 C
TR_VO2 = 283.15; # (Kelvin)
TR_excretion = 289.15; # (Kelvin)

# Effective respiratory volume & cardiac output
F_card_ref = 62.96969 ; # = Qb_ref_perch * (Bw_ref^(0.75)) / Bw_ref # (mL/d/g) = 46.368 * (0.294^(0.75))
/ 0.294 --> allometric scaling function from Ekstrom, 2016
V_O2_ref = 4.03; # reference oxygen consumption rate (mg O2/g/d) --> from Brafield, 1976
O2_EE = 0.71 ; # Oxygen extraction efficiency of 71% proposed by Erickson, 1990
Sat = 0.90 ; # dissolved oxygen saturation of 90% proposed by Erickson, 1990

# volume scaling factor : fraction of BW (%)
sc_blood = 0.011 ;
sc_gonads = 0.029681373 ;
sc_brain = 0.010 ;
sc_liver = 0.056965414;
sc_fat = 0.0168;
sc_skin = 0.061 ;
sc viscera= 0.066 ;
sc_kidney = 0.007957133 ;
sc_rp = 0.025 ;

# Fraction of arterial blood flow
frac_gonads =0.0018 ;
frac_brain =0.0251;
frac_liver =0.0488;
frac_fat =0.0073;
frac_skin =0.0242;
frac viscera=0.0816;
frac_kidney =0.0765;
frac_rp =0.1033;

#inputs
Bw_i = 1.85; #Mean mass of fish (g)
Temperature = 16;
f_cst = 0.83;
V_water = 1E+12 ;#mL
iyQuantity = 0.0;
event_bile = 1;

C_water= NDoses( 171 ,

0.00025,0.00913020833333333,0.0177296296296296,0.0231,0.0301731707317073,0.0372463414634146,0.044319512195122,0.0513
926829268293,0.0579388059701493,0.0584238805970149,0.0589089552238806,0.0593940298507463,0.0598791044776119,0.060364179104477
6,0.0608492537313433,0.061334328358209,0.0618194029850746,0.0623044776119403,0.062789552238806,0.0632746268656716,0.063759701

```


10. References

- Bertelsen, S.L., Hoffman, A.D., Gallinat, C.A., Elonen, C.M. & Nichols, J.W. (1998). Evaluation of log K_{ow} and tissue lipid content as predictors of chemical partitioning to fish tissues. *Environ. Toxicol. Chem.*, 17, 1447-1455.
- Bois, F.Y. (2009). GNU MCSim: Bayesian statistical inference for SBML-coded systems biology models. *Bioinformatics*, 25, 1453-1454.
- Brey, T., Müller-Wiegmann, C., Zittier, Z.M.C. & Hagen, W. (2010). Body composition in aquatic organisms — A global data bank of relationships between mass, elemental composition and energy content. *Journal of Sea Research*, 64, 334-340.
- Dalziel, A.C., Ou, M. & Schulte, P.M. (2012). Mechanisms underlying parallel reductions in aerobic capacity in non-migratory threespine stickleback (*Gasterosteus aculeatus*) populations. *Journal of Experimental Biology*, 215, 746-759.
- Grech, A., Tebby, C., Brochot, C., Bois, F.Y., Bado-Nilles, A., Dorne, J.L. *et al.* (2019). Generic physiologically-based toxicokinetic modelling for fish: Integration of environmental factors and species variability. *Science of the Total Environment*, 651, 516-531.
- Lindholm, C., Pedersen, S.N. & Bjerregaard, P. (2001). Uptake, metabolism and excretion of bisphenol A in the rainbow trout (*Oncorhynchus mykiss*). *Aquatic Toxicology*, 55, 75-84.
- R Core Team (2019). R: A Language and Environment for Statistical Computing. R Foundation for Statistical Computing Vienna, Austria.
- Saltelli, A., Chan, K. & Scott, E.M. (2008). *Sensitivity Analysis*. John Wiley & Sons, Ltd edn, New York.
- Sobol, I.M., Tarantola, S., Gatelli, D., Kucherenko, S.S. & Mauntz, W. (2007). Estimating the approximation errors when fixing unessential factors in global sensitivity analysis. *Reliability Engineering & System Safety*, 92, 957-960.